

T-2742

A SEISMIC STUDY OF THE LOWER CRETACEOUS
MUDDY SANDSTONE, SOUTHEAST BIG HORN BASIN,
WYOMING

ARTHUR LAKES LIBRARY
COLORADO SCHOOL of MINES
GOLDEN, COLORADO 80401

by
Steve E. Milligan

ProQuest Number: 10782462

All rights reserved

INFORMATION TO ALL USERS

The quality of this reproduction is dependent upon the quality of the copy submitted.

In the unlikely event that the author did not send a complete manuscript and there are missing pages, these will be noted. Also, if material had to be removed, a note will indicate the deletion.



ProQuest 10782462

Published by ProQuest LLC (2018). Copyright of the Dissertation is held by the Author.

All rights reserved.

This work is protected against unauthorized copying under Title 17, United States Code
Microform Edition © ProQuest LLC.

ProQuest LLC.
789 East Eisenhower Parkway
P.O. Box 1346
Ann Arbor, MI 48106 – 1346

T-2742

A thesis submitted to the Faculty and the Board of Trustees of the Colorado School of Mines in partial fulfillment of the requirements for the degree of Master of Science (Geophysics).

Golden, Colorado

Date April 21/83

Signed: Steve E. Milligan
Steve E. Milligan

Approved: Thomas L. Davis
Thomas L. Davis
Thesis Advisor

Golden, Colorado

Date April 21/83

George V. Keller
George V. Keller
Head of Department
Department of Geophysics

ABSTRACT

Well data from southeast Big Horn basin was used to design a geologic model for the lower Cretaceous Muddy interval. Laterally continuous valley-fill sandstone occurs unconformably on top of the Thermopolis shale over a regressive sandstone. An uppermost sandstone was deposited as offshore marine bars during late Muddy time. This sandstone forms discontinuous elongate features that all trend northeast. Early Muddy regressive sandstone deposits and marine bar sandstones tend to occur together at localities that were topographically high in Muddy time, while thicker valley-fill deposits reside in paleotopographic lows which occurred during a sea level drop during mid-Muddy time. In the study area, predominant northwest and northeast depositional trends in the lower Cretaceous strata are believed to be related to regional structural control.

Synthetic seismic models indicate that the basal sandstone (regressive and valley-fill sandstones combined) thickness can be measured from vertical peak-to-trough differences from high resolution (90 Hz) wavelet-processed seismic data. Marine bar sandstones over 15 ft thick that are at least 15 ft above the valley-fill sandstone will be

detectable on this data. Lower resolution (35 Hz) wavelet-processed data may be used to determine major changes in total Muddy thickness by measuring amplitude variations. Conventionally processed seismic data from the study area was used to substantiate and detail the Muddy interval geologic model. A thickening basal sandstone results in an increased amplitude response in the actual data. Presence of Muddy marine bar sandstone is denoted by an extremely low amplitude, low frequency seismic signature.

The Muddy geologic model may be used in conjunction with seismic data to locate and differentiate between valley-fill sediments and upper marine bar sandstones. This may be a valuable aid to the explorationist because both sandstones represent possible hydrocarbon reservoirs in southeast Big Horn basin.

TABLE OF CONTENTS

	Page
ABSTRACT *	iii
LIST OF FIGURES	vi
LIST OF PLATES	xi
ACKNOWLEDGEMENTSxii
INTRODUCTION	1
LOWER CRETACEOUS GEOLOGY	3
Stratigraphy in Big Horn basin.	5
Clovery	5
Thermopolis	7
Muddy	9
Shell Creek	10
Mowry	11
Regional Muddy Equivalents.	11
Depositional History of the Muddy	12
Previous Theories	12
Well Log Analysis	31
Structure Maps.	33
Isopachs.	40
Qualitative Aspects	48
Facies Assignments.	49
SEISMIC MODELING	55
Procedures.	55
Limitations of Seismic Modeling	58
Results	61
Factors Affecting Modeling Results.	79
Gradational Boundaries.	79
Porosity.	81
Depth of Burial	84
Gas Effects	88
Rock Fractures.	89
SEISMIC DATA ANALYSIS AND INTERPRETATION	90
Acquisition and Processing Parameters	90
Wavelet Extraction.	90
Muddy Seismic Signature Recognition and Interpretation.	94

	page
FUTURE WORK.	115
CONCLUSIONS.	117
REFERENCES CITED	120
APPENDIX OF ONE-DIMENSIONAL MODELS	122

LIST OF FIGURES

Figure		Page
1.	Relationship between the Big Horn basin and regional structural elements.	4
2.	Lower Cretaceous nomenclature in the Big Horn basin.	6
3.	Stratigraphic relationship between the lower Cretaceous units in Wyoming and western South Dakota.	13
4.	Distribution of the Muddy and its equivalents in Wyoming from Haun and Barlow (1962).	14
5.	Boreal sea transgressed from the north during early Cretaceous time	17
6.	Muddy facies distribution in the Big Horn basin as defined by Paull (1957).	22
7.	Examples of bar facies and alternating continental, littoral, and marine facies in the Big Horn basin as defined by Paull (1957).	25
8.	Examples of deltaic, neritic, and back-bar facies in the Big Horn basin as defined by Paull (1957).	26
9.	Four zones of the Muddy from a well in the Kitty field of the Powder River basin. Modified from Larberg (1981)	27
10.	Location of the eighty wells used in the log analysis.	32
11.	Depth to top of Muddy relative to sea level	34
12.	Depth to top of Muddy relative to land surface	36
13.	Paleotopography during early Muddy time based on a marker bed above Muddy	38

Figure	Page
14. Paleotopography during early Muddy time based on a marker bed below Muddy.	39
15. Isopach of entire Muddy interval	41
16. Typical well in study area containing basal and upper Muddy sandstones	43
17. Isopach of Muddy basal sandstone	44
18. Isopach of Muddy upper sandstone	45
19. Isopach over a portion of the Shell Creek shale.	46
20. Isopach of a portion of the Thermopolis shale.	47
21. A thin sheet of sandstone was deposited over the Thermopolis shale when the lower Cretaceous sea regressed.	52
22. Valleys were cut into the Thermopolis shale as the area was uplifted.	52
23. Influx of clastic sediments filled in eroded valleys as sea began to transgress	53
24. After the sea inundated the area, marine bars were deposited on paleotopographic highs	53
25. Comparison of a high frequency one-dimensional model made using only the sonic log and a model made using sonic and density logs.	56
26. The three wavelets used in the seismic modeling	59
27. Laterally thickening two-dimensional single sandstone velocity model	64
28. High resolution vertical incidence seismic response for the single-sandstone model.	65
29. Low resolution vertical incidence seismic response for the single-sandstone model.	66

Figure	Page
30. Vertical incidence seismic response for the single-sandstone model utilizing the extracted wavelet67
31. Two-dimensional velocity model consisting of a laterally thickening basal sandstone overlain by a thin upper sandstone73
32. High resolution vertical incidence seismic response for the two-sandstone model.74
33. Low resolution vertical incidence seismic response for the two-sandstone model.76
34. Vertical incidence seismic response for the two-sandstone model utilizing the extracted wavelet77
35. Contour map of interval transit time taken from the Muddy basal sandstone sonic log response.82
36. Contour map of variation in the ratio of Muddy velocity to Shell Creek shale velocity.86
37. Contour map of variation in the ratio of Muddy velocity to Thermopolis shale velocity.87
38. Location of the three Grant Geophysical seismic lines91
39. Processing sequence used for the three seismic lines92
40. Grant Geophysical seismic data over the Muddy interval.93
41. Comparison of a model utilizing the extracted wavelet, a model utilizing a phase-rotated Ricker wavelet, and an actual seismic data trace95
42. Comparison between actual data and three seismic models that each contain the Muddy basal sandstone, but not the upper sandstone97

Figure	Page
43. Comparison between actual data and three seismic models that each contain the Muddy basal sandstone, but not the upper sandstone.98
44. Comparison between actual data and two seismic models that each contain the Muddy basal and upper sandstones.99
45. Isopach of Muddy basal sandstone utilizing well control and seismic data.	101
46. Isopach of Muddy upper sandstone utilizing well control and seismic data.	103
47. Change in Muddy seismic response due to presence of upper bar sandstone.	105
48. Seismic response due to alternating facies in the Muddy.	106
49. Change in Muddy seismic response due to a gradational change from basal sandstone only to a basal and upper bar sandstone	107
50. Map of study area showing general locations of the three example seismic sections from Grant Geophysical seismic data.	108
51. The extent of the three Muddy sandstones interpreted from the seismic and well data	110
52. Isochron map of an interval above the Muddy. Map produced from Grant Geophysical seismic data.	112
53. Isochron map of an interval below the Muddy. Map produced from Grant Geophysical seismic data.	113

LIST OF PLATES

(located in pocket in back of thesis)

- I. Gamma ray responses from wells in the study area.
- II. Geologic cross section and synthetic seismic responses of the Muddy interval from five wells in the study area.
- III. Muddy response from the three seismic lines in the study area.

ACKNOWLEDGEMENTS

I wish to thank my thesis committee members, Dr. Jim Applegate, Dr. Harry Kent, and especially my thesis advisor, Dr. Tom Davis, for their valuable comments and support throughout this project.

I am grateful to Tenneco Oil for the thesis topic and the necessary financial aid. I also wish to thank Grant Geophysical Corporation for use of their seismic data, Conoco Oil for the seismic check shot survey, and Sohio Petroleum for use of their well logs files and their Denver Computer Center. Special appreciation is extended to Monte Naylor at Sohio for his technical advice in regard to the seismic modeling. My gratitude is also extended to Earl Jaynes at Sohio for his interest and desire in seeing the completion of this project. I am especially thankful to my wife, Lisa, for the drafting, typing, and ideas concerning the geologic model for this thesis.

INTRODUCTION

The lower Cretaceous age Muddy has long been a target for oil and gas exploration in the Rocky Mountain basins. Within the Big Horn basin of Wyoming, most of the Muddy structural traps with oil and gas potential have been exploited. However, the extreme lateral variation in Muddy thickness presents many possible stratigraphic oil and gas traps that have not been explored. The purpose of this thesis is to evaluate the use of the seismic reflection method as an exploration tool for locating stratigraphic anomalies in the Muddy. Data for the study were collected over a portion of the southeast Big Horn basin that includes Wyoming townships 43N to 46N and ranges 89W to 93W.

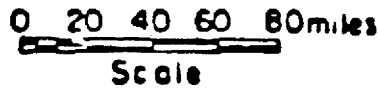
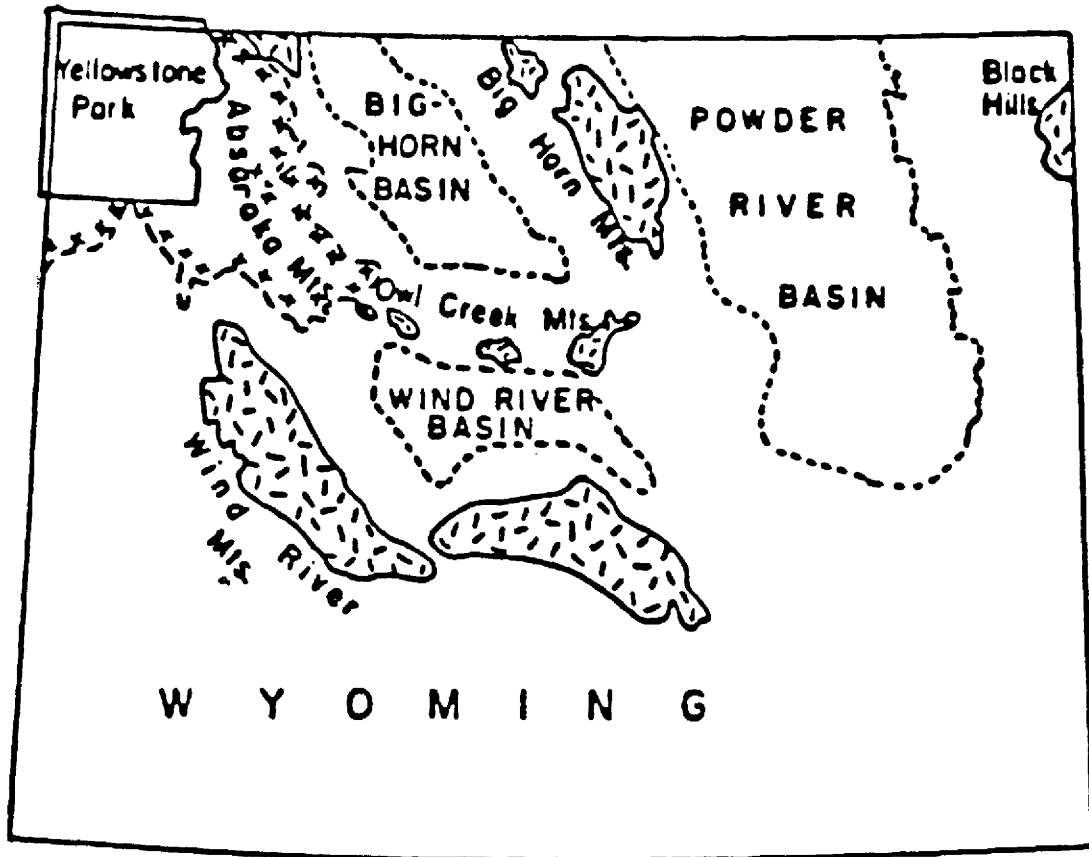
Three primary objectives of this thesis are: first, to establish a generalized geologic model for Muddy deposition in the study area; second, to examine through use of synthetic seismic models the capability of the seismic method to detect changes in thickness for the entire Muddy and for individual sandstone facies within the unit; and third, to determine if variations in sandstone porosity, gas saturation, depth of burial, acoustic boundaries, and rock fractures significantly change the signature of the Muddy.

Synthetic seismic models and borehole logs were used to work with the objectives listed above. Seismic data is used along with the seismic models to further the geologic model developed.

LOWER CRETACEOUS GEOLOGY

The Big Horn basin is a large structural basin bordered on all but the north by large mountain ranges (Fig. 1). The southern border is formed by the low-lying Owl Creek mountains, while to the west lie the Absaroka and the Beartooth mountains. The eastern portion of the Big Horn basin is separated from the Powder River basin by the Big Horn mountains. The northern margin of the basin is vaguely defined by an anticlinal trend extending from the Beartooth mountains eastward to the Pryor mountains (Wilson, 1936).

Structural deformation that formed the Big Horn basin is a result of the Laramide Orogeny, that began in late Cretaceous time. In late Jurassic and early Cretaceous time, prior to the Laramide Orogeny, the site of the present day Big Horn basin was not a structural or sedimentary basin (Paull, 1957). Instead, it was part of a much larger area covered by a shallow sea that extended throughout much of the western continental interior region. Lower Cretaceous strata consist of sandstones and shales deposited as this vast sea transgressed across the western plains area.



LEGEND




-  Limits of Absaroka Volcanics.
-  Outcrop area of Pre-C rocks.
-  Outline of present structural basins.

Figure 1. Relationship between the Big Horn basin and regional structural elements. Modified from Paull, 1957.

STRATIGRAPHY

The stratigraphic column for the lower Cretaceous of the Big Horn basin is shown in Figure 2. The physical rock descriptions listed below are from work done by Paull (1957) and Eicher (1962). The descriptions generally apply to lower Cretaceous strata throughout the basin, however selective rock sample descriptions from near the study area in the extreme southeast portion of the basin have been included in this study.

Cloverly

The base of the Cloverly is usually found to include the Pryor conglomerate. This unit is highly variable in thickness, ranging from 80 ft in some places to being completely non-existent in other locations. The Pryor consists of chert and quartz pebble conglomerate, conglomeratic sandstone, sandstone with interbedded siltstone and vari-colored shale (Paull, 1957). The Fuson, also called the Middle shale member, lies above the Pryor conglomerate. This unit is predominately shales, gray, red and purple in color. Occasional irregularly bedded sandstones and siltstones one ft to five ft thick may be found. The Fuson varies from 10 ft to 40 ft thick and contains moderate amounts of carbonaceous material and

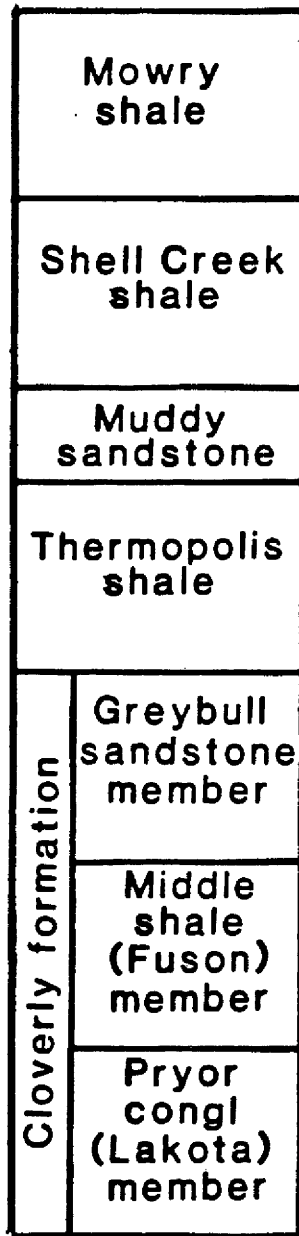


Figure 2. Lower Cretaceous nomenclature in the Big Horn basin.

plant imprints. The uppermost member of the Cloverly is the Greybull sandstone. This member usually consists of three to ten ft beds of silty- to fine-grained quartz sandstone commonly iron stained, ripple-marked, and calcareous. Gray and black shale stringers are occasionally interbedded with the sandstone. Quartz grains of the sandstone have well developed secondary crystal faces. The total thickness of the Greybull member ranges from 10 ft to 40 ft.

Thermopolis

This predominately shale formation includes the approximate 300 ft interval between the Cloverly formation and Muddy. The Thermopolis can be seen in outcrop to contain four easily distinguishable members. The basal 100 ft of the Thermopolis is termed the Rusty Beds member. This member is characterized by very thinly interbedded siltstones and gray shales. Abundant ironstone concretions found in the Rusty Beds result in a weathered rust rubble surface in outcrop. In the basal portion of the Rusty Beds member, thick brown-weathered sandstone beds often occur that have very short lateral extents. The contact between the basal Thermopolis and the underlying Greybull member of the Cloverly formation

is often difficult to distinguish. The major portion of the Rusty Beds member is composed of thinly interbedded dark shales and siltstones rich in carbonaceous material. Thin beds of sandy limestone, cross-bedded sandstone, and ironstone can be identified that are extremely widespread and laterally persistent.

Above the Rusty Beds lies a thicker shale called the Lower shale by Eicher (1962). This dark gray fissile shale is commonly around 90 ft thick and contains only a few very thin sandstone, sandy limestone, and ironstone beds. Also a few rare, greenish, half-foot bentonite beds appear near the top of the Lower shale member. The bulk of the shale is slightly silty, resulting in gray crusty weathered surface.

The third member of the Thermopolis is the Middle Silty shale. This 30 ft member contains gray and tan silty shale interbedded with thin siltstones and sandy limestone. The beds are laterally persistent over a large area and have an appearance similar to the Rusty Beds member.

The top portion of the Thermopolis consists of about 30 ft of black fissile shale with very little silt content. The contact between this nearly homogeneous shale and the Middle Silty shale below is very abrupt. Near the

top of this shale exists one of two very thin bentonite beds.

Muddy

The Muddy is situated above the thick black shales of the Thermopolis and below the black shales of the Shell Creek. The Muddy in the southeast Big Horn basin is characterized as a highly variable unit composed of sandstone, siltstone, shale, bentonite beds, coals, and local chert pebble conglomerate. The rapid degree of lateral variability within the Muddy is not demonstrated by any of the other lower Cretaceous units of the Big Horn basin. While in some localities the Muddy contains no sandstones, in other places 20 miles away, the Muddy contains well over 100 ft of massive sandstone. Therefore, it is a distinctive and yet variable unit encased between two uniform and persistent shale units. Although the Muddy may only be a silty shale in some places, it still persists and is easily identifiable. The contact of the Muddy with the underlying Thermopolis is also variable. At many localities, the massive sandstone forms an abrupt contact with the black Thermopolis shale indicating a possible surface of nonconformity. However, at other places the contact is so gradational that there appears to be no break in sedi-

mentation between the Thermopolis and the Muddy (Eicher, 1962). The sandstones of the Muddy exhibit great lithologic variability in that they may be calcareous, bentonitic, or very clean quartzose sandstones (Paull, 1957). The quartz grain size of the Muddy is more consistent and almost always found to be fine to very fine sized.

Shell Creek

The thick black fissile shale between the Muddy and the Mowry is named the Shell Creek shale by Eicher while others call this unit the Upper Thermopolis. The Shell Creek ranges in thickness from 300 ft to 200 ft, thinning toward the south. The bentonite beds, which are much more substantial in this unit than below it, average two- to three-ft thick. However, the substantial bentonite beds may be as thick as nine ft (Eicher, 1962). Since bentonite beds are the result of regional volcanism, they are usually laterally persistent over extremely large areas. However, some of the thinner bentonite beds may have portions eroded away by water currents after deposition. This eroded bentonitic material was then mixed with other clastic sediments. Thin occasional beds of ironstone are also present in the Shell Creek, although

they can be considered somewhat of a rarity in this shale unit.

Mowry

The Mowry forms the uppermost portion of the lower Cretaceous. This formation is composed of siliceous, silty dark shale interbedded with siltstone and bentonite. The shales of the Mowry are harder and more siliceous than those of the underlying Shell Creek. These silica-rich shales have the same chemical composition as a silicified bentonite. There is a fairly rapid change from the soft Shell Creek shale to the harder silica-rich Mowry shale. The thickness of the Mowry is around 340 ft to 370 ft (Moberly, 1962).

REGIONAL MUDDY EQUIVALENTS

Early drillers in the Big Horn basin devised the term 'Muddy Sandstone' to describe the sandy unit found within the Thermopolis shale. Hintze (1915) was the first to publish a description of what he termed the Muddy found near the Greybull area.

Today, the lateral persistence of the Muddy and its equivalents in the Rocky Mountain basins are well documented (Eicher, 1962). In the western portion of

the adjoining Powder River basin, the Muddy is called the same, while in the east, it is called the Newcastle sandstone. In the southern Williston basin and in the Denver basin, the Muddy is equivalent to portions of the 'J' sandstone. In Figure 3, Haun and Barlow (1962) show that the Muddy is actually equivalent to the basal portion of the Newcastle and the 'J' sandstone. South of the Big Horn basin, the Muddy was studied in the Wind River basin by Whitford (1959), Dresser (1974) and Gopinath (1978). In Figure 4, Haun and Barlow (1962) show the distribution of the Muddy equivalents throughout the state of Wyoming.

DEPOSITIONAL HISTORY OF THE MUDDY

Previous Theories

The depositional history of the Muddy and its equivalents has been studied quite extensively throughout many of the Rocky Mountain basins. In particular, many more recent studies have been focused on the Denver and the Powder River basins where the Muddy has been a prolific producer of oil and gas. However, within the Big Horn basin, very little if any recent work has been directed toward the Muddy. Collier (1922) was one of the first to speculate on the

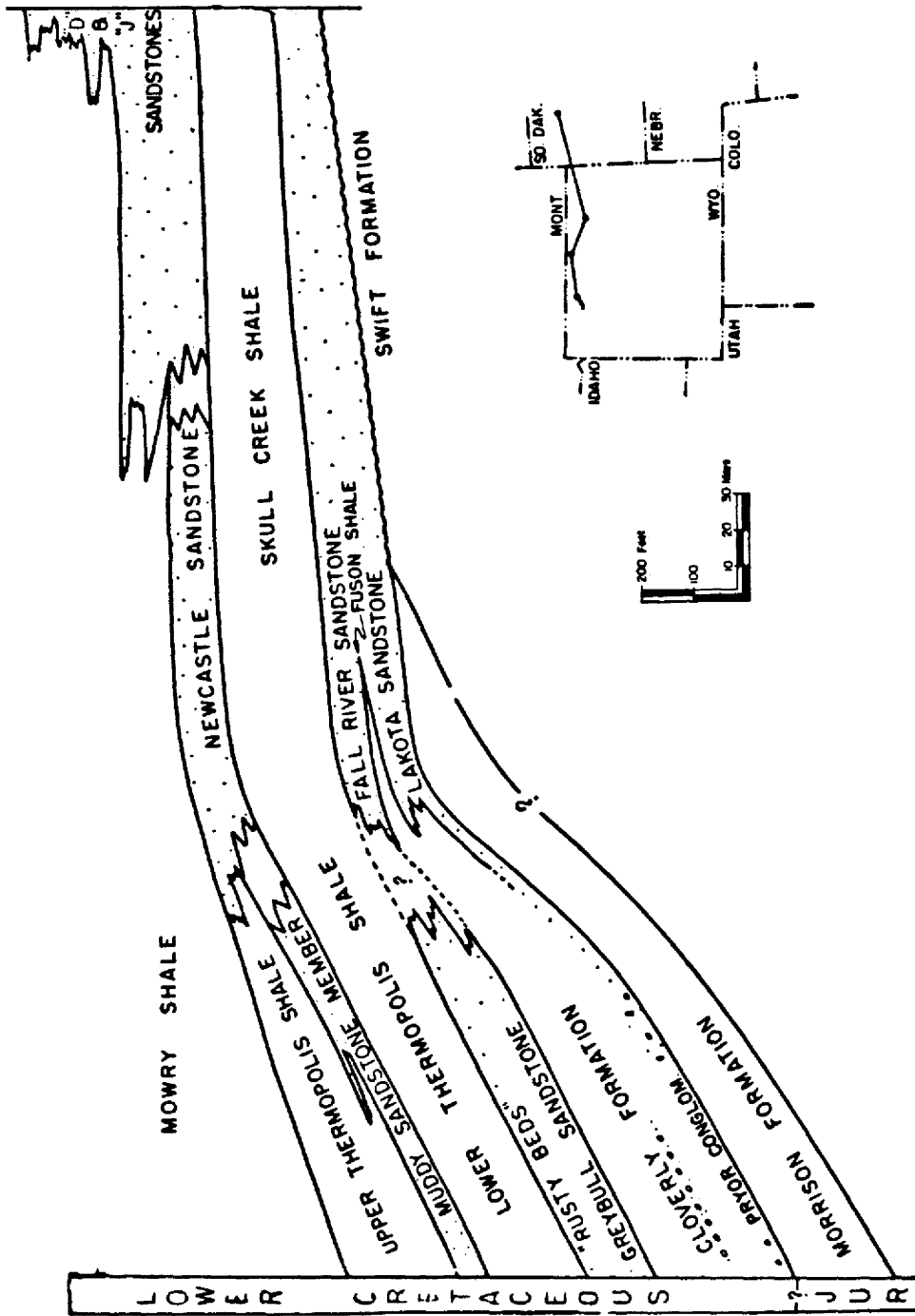


Figure 3. Stratigraphic relationship between the lower Cretaceous units in Wyoming and western South Dakota. Haun and Barlow, 1962.

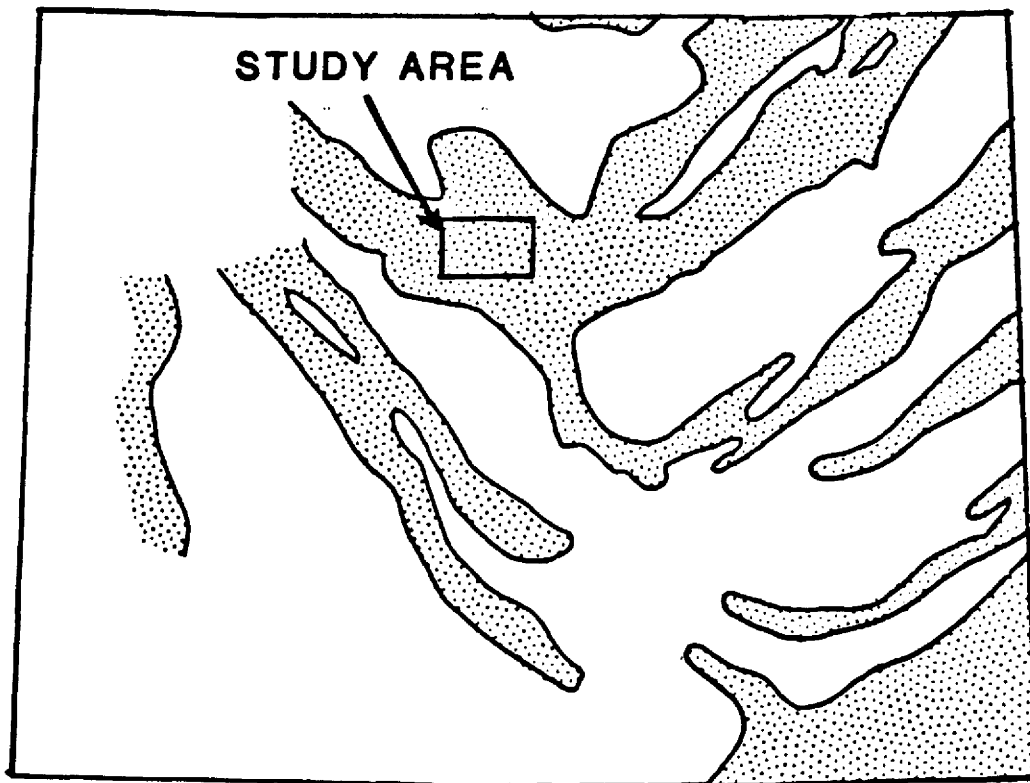


Figure 4. Distribution of the Muddy and its equivalents in Wyoming. Modified from Haun and Barlow, 1962.

depositional history of the Muddy or equivalent sandstones in a study of the Osage oil field in Weston County, Wyoming. He noted that while the Newcastle contained fragments of coal and petrified wood, other portions of the sandstone not far away deposited as a sandy mud, exhibit characteristics of deeper water marine deposition. He concluded that the Newcastle sandstone was not deposited entirely under marine conditions as previously thought.

In a study of the Wyoming lower Cretaceous fauna, Curry (1962) found that while the Shell Creek and the Thermopolis shales contain only marine fossils, the Muddy contained nonmarine as well as marine fossils. The nonmarine fossils are restricted to the base of the Muddy in a particular facies of irregular claystones and siltstones. The nonmarine varieties include dogfish amia, beetle wings, and a few delicate fern leaves. Curry points out that while some nonmarine fossils are found in a particular basal Muddy facies, the vast majority of fossils found throughout the Muddy are marine. Curry drew a correlation between the occurrence of the nonmarine Muddy facies and sandstone deposition on paleotopographic highs such as islands.

Eicher (1962) believed that throughout Thermopolis

deposition, the interior Cretaceous sea transgressed from the north giving way to continually deepening marine conditions. This sea was part of the Boreal sea that opened up northward into the Arctic ocean (Fig. 5) Eicher gives paleontological evidence that the Boreal sea which extended into Wyoming was not connected with the Gulf sea until late in Thermopolis time.

When the Gulf sea transgressed northward over the former drainage divide south of Kansas to join the Boreal sea, an abrupt change in deposition occurred that marks the Upper shale's base in the Thermopolis. At the close of the Thermopolis, the seas regressed, leaving an "extremely uniform, low-relief sediment surface formed over a large part of the western interior." Eicher attributes the sudden lateral facies changes and various fossil assemblages of the Muddy to a variety of local shallow-water environments. Within the Big Horn basin, he assigns the thick Muddy bodies primarily to bar deposition. However, at some Big Horn localities near the basin margin, he did note extensive local erosion of the Thermopolis Upper shale, indicating possible Muddy channeling. Eicher also recognized that the Muddy and Shell Creek shale are rich in bentonite while the Thermopolis shale is not. He relates the

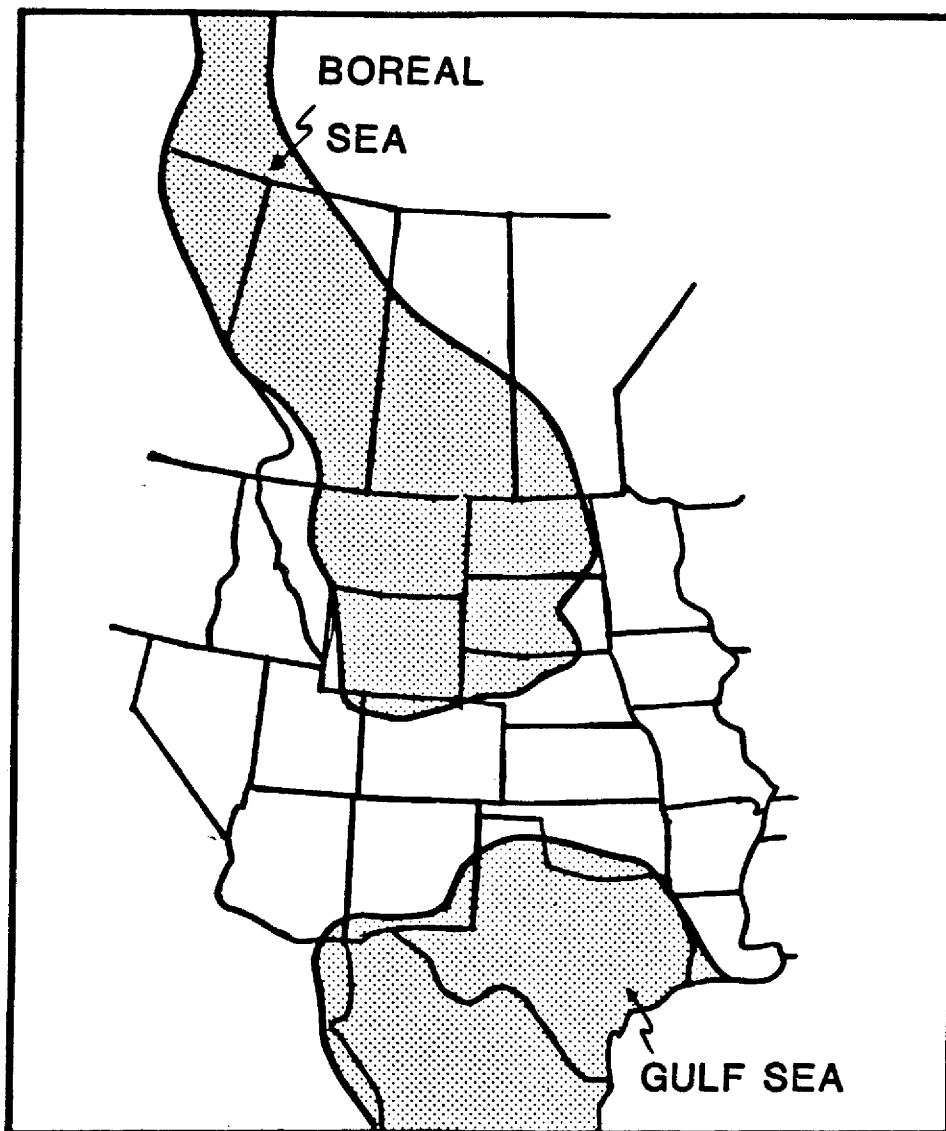


Figure 5. Boreal sea transgressed from the north during early Thermopalis time. Modified from Wulf, 1962.

bentonite content to an "important outburst of volcanic activity apparently coincident with the uplift of the depositional basin and the influx of coarser Muddy sediments." Eicher believed that the gradational contact between the Muddy and the Shell Creek shale was the result of continuous deposition in a deepening Boreal sea that transgressed from the north. As the sea became deeper, shale deposition occurred in conditions similar to those of Thermopolis time.

In a study of Newcastle outcrops in Weston County, Wyoming, Baker (1962) suggests that the lower portion of the Muddy was deposited as a nonmarine (alluvial) plain. Baker summarized the events for this Muddy depositional model as follows:

- 1) Very fast regression of lower Cretaceous sea leading to an abrupt termination of the Skull Creek shale (Thermopolis equivalent)
- 2) Subaerial exposure of the Skull Creek shale results in valley-like erosional topography,
- 3) Lower Newcastle deposition occurs as an influx of nonmarine sediments fills in the valley-like erosional depressions and continues to build up as alluvial plain deposits,

- 4) Rise in the Cretaceous sea level results in deposition of the upper portion of the Newcastle as a marine transgressive sheet sandstone,
- 5) Return to marine shale deposition (Nefsy shale, equivalent to Shell Creek shale) as sea level continued to rise.

Baker gives the following evidence in favor of a nonmarine alluvial origin for the Newcastle in his particular study area:

- 1) The Newcastle formation has a 'sharp, non-transitional, erosional contact with the underlying Skull Creek shale',
- 2) The over-all shape of the sandstone is lenticular in cross-section and elongate in a southwest direction, similar in appearance to a sand-filled erosional valley,
- 3) Presence of many typically non-marine facies such as carbonaceous mud rocks and sandstone, coal seams, and channel-fill sandstones that contain many terrestrial plant remains but no marine fossils,
- 4) The extreme lateral variability in depositional patterns and evidence of channeling and bed truncation are more indicative of a non-marine

than a marine environment,

- 5) Presence of typically non-marine sedimentary structures such as mudcracks, slump structures, roots, and in-place plants.

Baker observed that the thickest and best developed Newcastle deposits occur where the pre-Newcastle erosion cut deepest into the Skull Creek shale. He went on to suggest that the deeper erosional valley-like features occurred along pre-existing topographic lows such as areas of major drainage. Baker does not attempt to extend the Newcastle non-marine alluvial plain facies westward to include the Big Horn basin. Instead he speculates that there may be a westward lateral transition to margin marine (delta plain deposits), and possibly completely marine deposits in Wyoming. Baker's observations of the Newcastle (Muddy) differ from those of Eicher on two points. First, Baker found only sharp contacts between the Newcastle and the underlying Skull Creek while Eicher observed both sharp and gradational contacts at the base of the Muddy. Second, Eicher claimed to find both marine and non-marine fossils in the Muddy while Baker only found non-marine fossils. These two points of discrepancy are probably related to the fact that Baker's study was confined to his area in eastern Powder River

basin while Eicher's work concerned almost all of Wyoming with special emphasis on Northern Big Horn basin.

The most extensive work that concerned the Muddy in the Big Horn basin was that of Richard Paull in 1957. Paull mapped in detail the lithology, sedimentary structures, and mineralogy for the Thermopolis, Muddy, and Shell Creek interval at 35 outcrop locations along the outer edge of the Big Horn basin. He believed that the Muddy and its equivalents in the Rocky Mountain basins are the result of a tectonic disturbance of the sediment source area. This tectonic pulsation caused the Muddy source area to shed large amounts of coarser grained sediments into the shallow Cretaceous seaway. As the influx of sediment filled the shallow sea, subsidence occurred at a rate sufficient to allow for the sorting, winnowing and distribution of the sediments over a very large area. Paull claims that this situation set the stage for a large variety of sedimentary environments to prevail within a close proximity to one another. In fact, Paull asserts that there are five different depositional environments responsible for the Muddy in the Big Horn basin (Fig. 6). He believed that the initial influx of the Muddy clastic material into the Big Horn basin was deposited in a

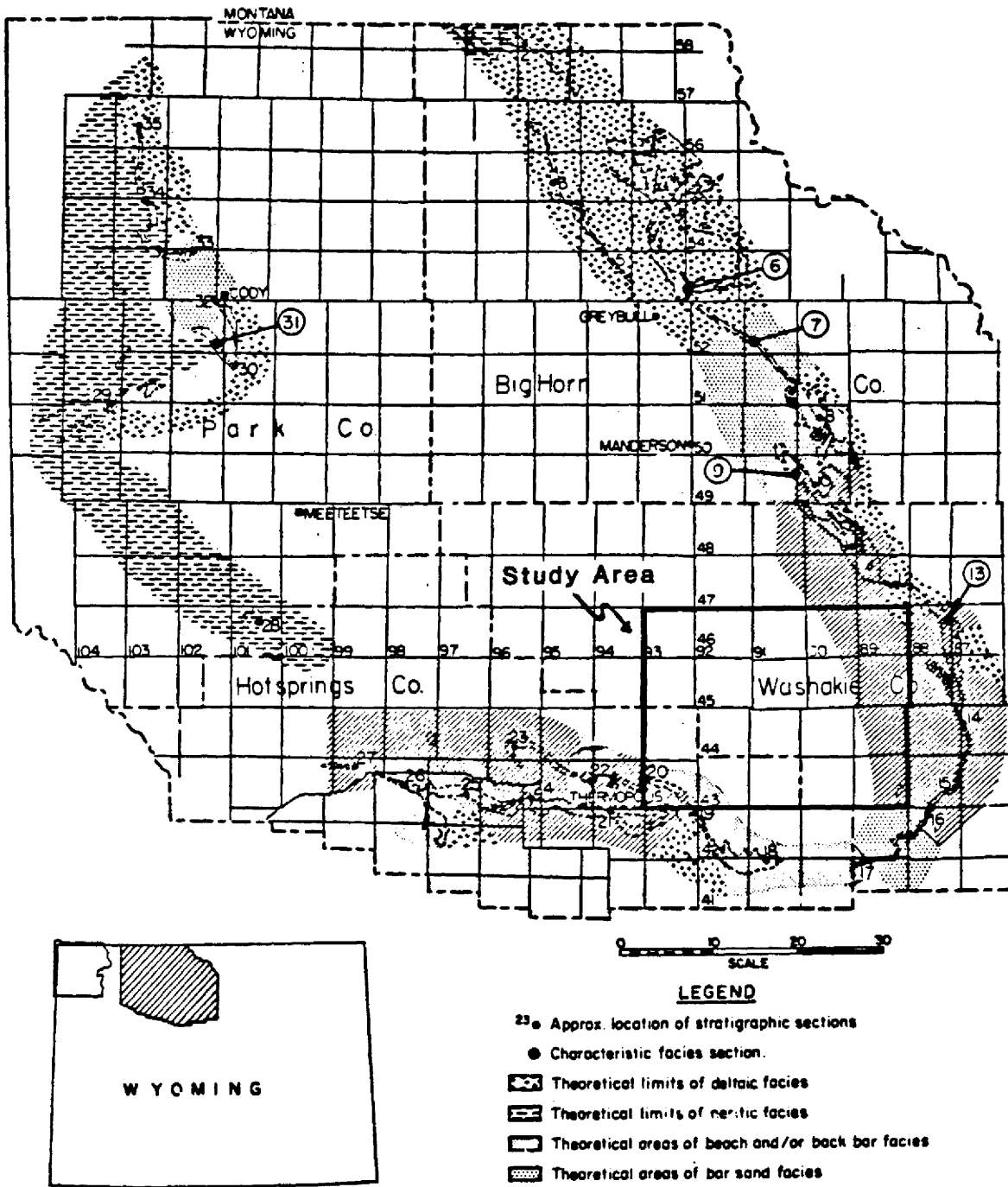


Figure 6. Muddy facies distribution in the Big Horn basin determined from outcrop. Modified from Paull, 1957.

deltaic environment. This facies is characterized by fine quartz sand floating in a matrix of bentonite. The massive beds of salt and pepper sandstone are occasionally separated by very thin shale layers and conglomeratic or coarse-grained lenses. This facies averaged 25-30 ft thick and is almost always void of any true bedding implying a very rapid type of deposition. Contrary to Baker's finding, Paull observed both gradational and sharp contacts between the base of the Muddy and the Thermopolis shale, although the abrupt contacts are more common for the deltaic facies. Paull believed that the other four designated facies: 1) bar facies, 2) back-bar and beach, 3) cyclic-alternating continental, littoral, and marine facies, and 4) neritic facies were all deposited after the occurrence of the deltaic facies and resulted from the reworking of deltaic sediments. Therefore, the deltaic facies "controls and determines the location and depositional environments of all other facies types", claims Paull. He gives two types of evidence to support his statement. First, the deltaic sediments are less mature than those of the other four facies. The deltaic facies contain more feldspar, a slightly larger grain size, and much more bentonite and biotite than the other four facies. Secondly, the deltaic facies almost

always is located at the base of the Muddy section, stratigraphically below other facies, if it occurs at all. At many locations, Paull claims that the thicker deltaic sediments were deposited in scours, or channels eroded into the Thermopolis shale.

Lithologic columns of the deltaic facies as well as the four other facies that Paull claims to observe in the Big Horn basin are shown in Figures 7 and 8. Each of the example columns represent only a single facies. However, as Paull points out, often a single outcrop will exhibit a combination of facies with the deltaic deposits comprising the basal portion of the Muddy and one of more of the other facies forming the remainder of the Muddy section.

In one of the more recent studies of the Muddy, Larberg (1981) examined cores and logs from wells near Kitty field in the Powder River basin of Wyoming. He was able to define four separate and recognizable zones within the Muddy interval. Figure 9 shows Larberg's four Muddy zones interpreted from a well log in Kitty Field. He believed that the entire Muddy interval represents an overall transgression of the lower Cretaceous sea. The lowermost zone (four) is interpreted as fluvial channel sandstones deposited in narrow sinuous belts. These

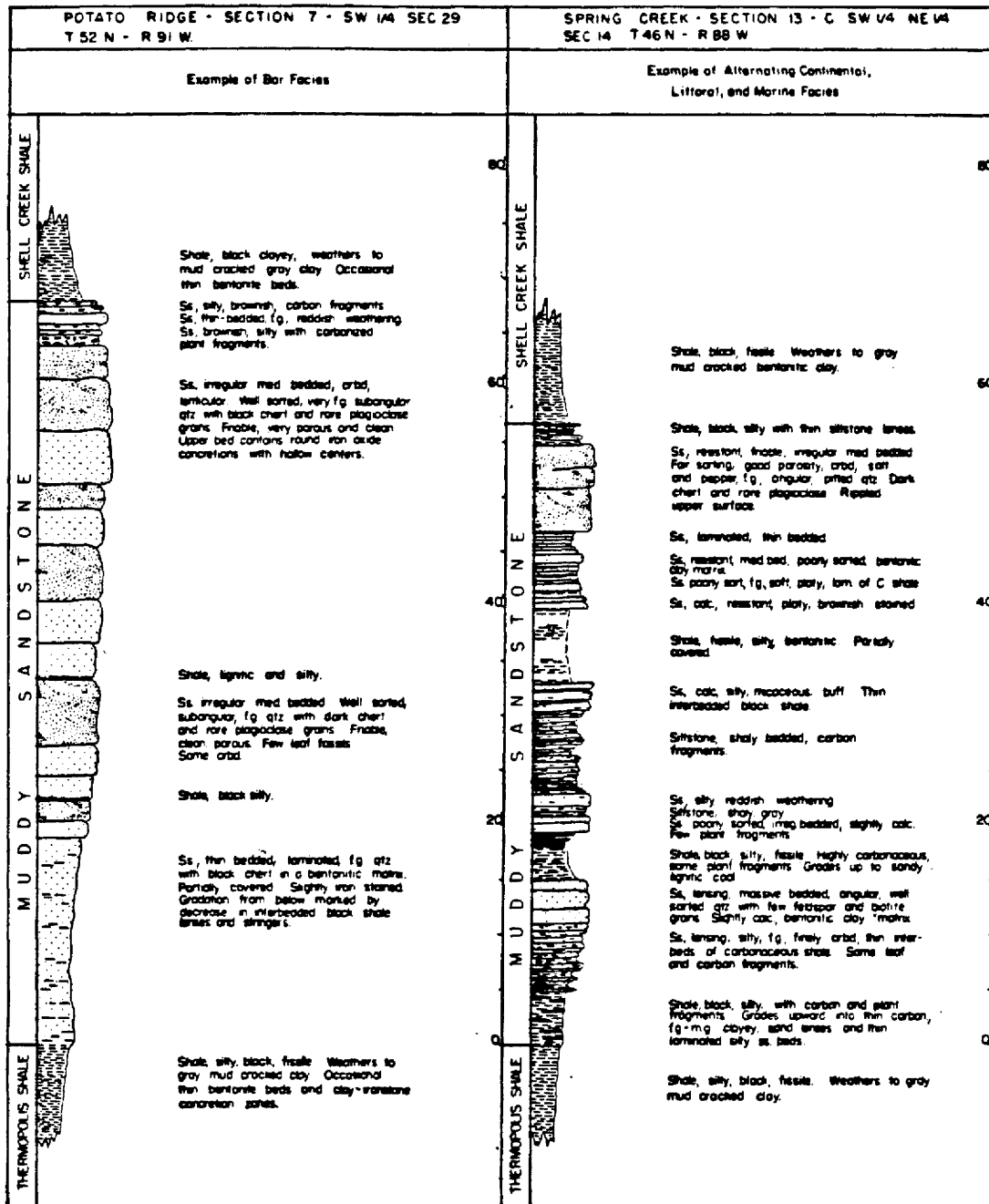


Figure 7. Examples of bar facies and alternating continental, littoral, and marine facies in the Big Horn basin as defined by Paull, 1957.

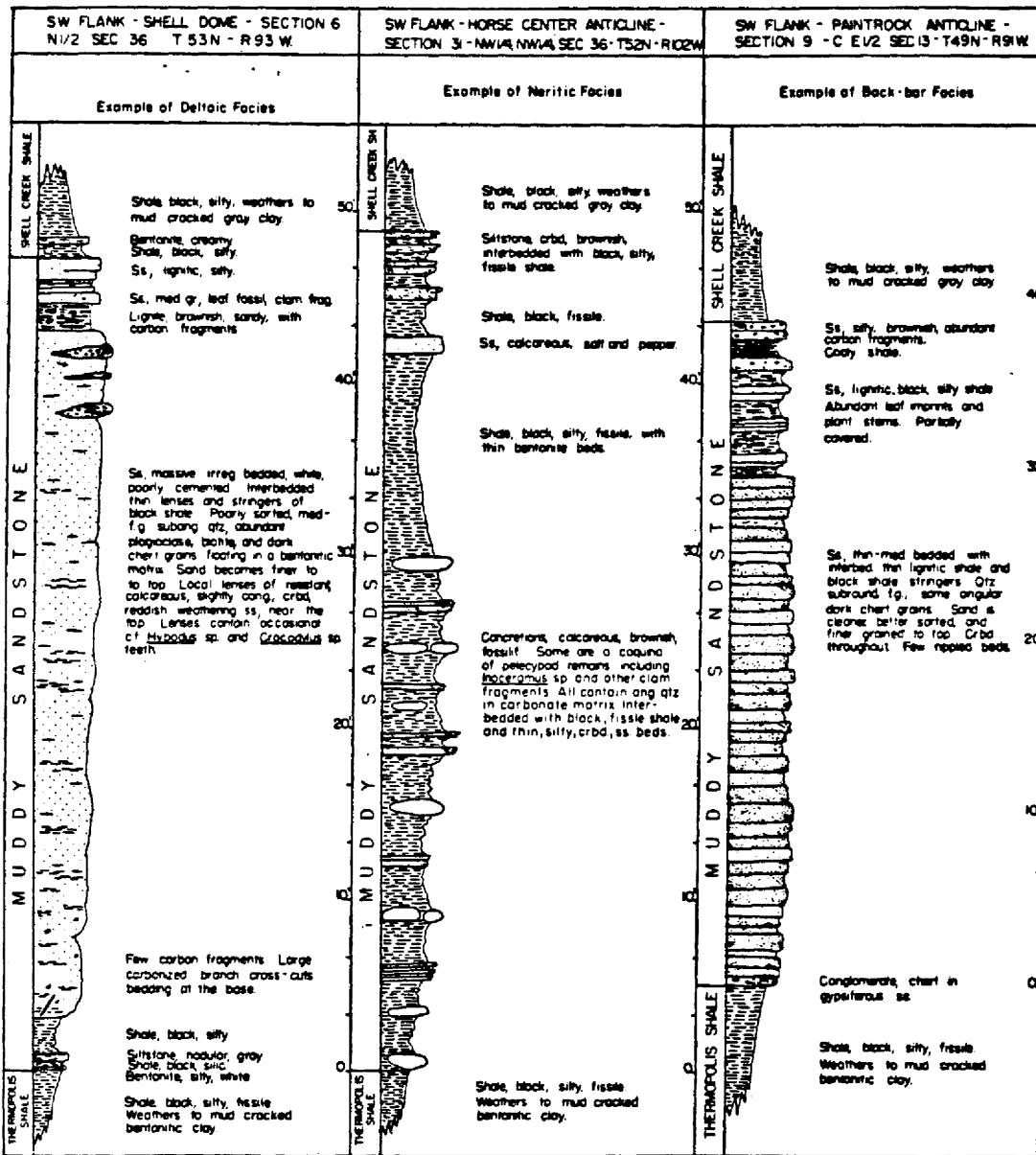


Figure 8. Examples of deltaic, neritic, and back-bar facies in the Big Horn basin as defined by Paull, 1957.

**Chevron #7 Simpson
33 T51N R73W**

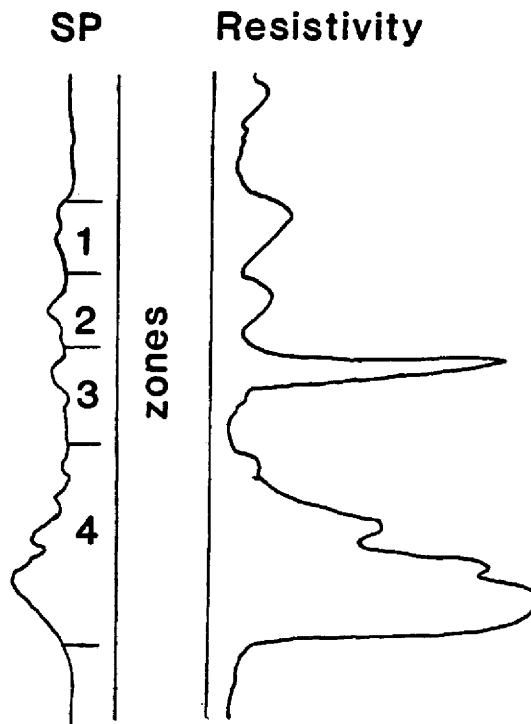


Figure 9. Four zones of the Muddy from a well in the Kitty field of the Powder River basin. Modified from Larberg, 1981.

sandstones were deposited in topographic lows atop the unconformable Skull Creek surface. Zones two and three are interpreted as strand line deposits that were continually reworked by the transgressing sea. Zone one, which consists of siltstones and mudstones, is believed to represent slightly deeper water deposits beyond the strand plain just prior to an abrupt transgressive surge that started deep-water shale deposition. Although Larberg's depositional model is constructed for a small and specific area, it does present a very plausible scenario to explain regional deposition of the Muddy interval.

While many people in the past have noticed that thicker basal Muddy deposits seem to occur or fill-in paleotopographic lows in the underlying Skull Creek shale, until recently very little has been written concerning the cause of these topographic features on a typically low relief marine shale surface. Weimer and Sonnenberg (1982) related changes in the 'J' sandstone thickness to basement block movement in the Denver basin. Their geologic model for the 'J' sandstone can be summarized as follows: A regression of the early Cretaceous sea that marked the beginning of Muddy time is responsible for shoreline and shallow marine sandstone deposition. These early Muddy deposits have a conformable

and gradational contact with the Skull Creek shale. These regressive sandstones are also very fine- to fine- grained and interpreted to be delta front, shoreline, and marine bar sandstones. Weimer and Sonnenberg believe that slight movements of basement block faults in Cretaceous time influenced the Muddy sedimentation such that rivers and associated deltas of the lower Muddy were positioned in topographic lows or grabens. Topographic highs, situated over basement horst structures, received Muddy sediments from delta margin and interdeltaic environments. The resulting regressive sediments were laterally variable, yet persistent. At this point, a further drop in sea level caused all or most of the existing deposition basin to be exposed and drained. Erosion occurred along the topographic lows (i.e., structural grabens) where rivers existed, resulting in deep valley incisement into portions of the regressive Muddy and even into the underlying Skull Creek shale. Weimer and Sonnenberg relate this lowering of the early Cretaceous sea to a worldwide sea level drop reported by Vail (1977) occurring approximately 97 million years before the present. Next, a rise in sea level occurred, causing the incised valleys to be modified and filled with fluvial and estuarine sediments. These valley-fill deposits are characterized as

fine- to medium-grained, cross-stratified, and well-sorted. According to Weimer and Sonnenberg, the origin of these sediments varies from alluvial plain to transitional deposits. A continued rise in sea level coupled with renewed fault block movement resulted in erosion of strata from the top of the horst block and deposition of a thin widespread conglomerate transgressive lag positioned over the horst block on the unconformable surface. Later, marine siltstone and shale deposition predominated throughout the area as sea level continued to rise, bringing Muddy deposition to a close.

There are two major differences between this geologic model and those models previously discussed. First, this model relates the Muddy depositional patterns to deep basement block faulting. Second, in this model, the first sandstone deposited (regressive sandstone) is finer-grained and influenced more by marine conditions than the later valley-fill sandstones. However, it should be noted that the valley-fill sandstones may locally be stratigraphically lower than the earlier marine sandstones since the valleys were incised into Skull Creek shale in some of the topographically lower locations.

In a more recent article by Weimer et al. (1983), evidence indicates the presence of valley-fill sandstones

and marginal marine deposits in the Newcastle formation of eastern Powder River basin. Isopach data for lower Cretaceous time stratigraphic intervals indicates that recurrent movement of basement fault blocks influenced the positioning and thickness of these sedimentary facies within the Newcastle. This paper also reveals that seismic response amplitude can be used to identify net sandstone content within the Newcastle formation.

Well Log Analysis

The study area in southeast Big Horn basin contains numerous oil and gas wells that penetrate the lower Cretaceous interval. Eighty of the wells that were logged through the Muddy interval were used to examine its stratigraphic and structural properties. The locations of these wells are shown in Figure 10. While no single type of log was run throughout all 80 wells, combinations of gamma ray, S.P., and resistivity logs were deemed adequate to provide consistent and accurate measurements for use in most of this study.

The primary purpose of this well log analysis was to determine certain properties of the Muddy within the study area. The quantitative measurements were thickness, velocity, and depth below surface. The qualitative

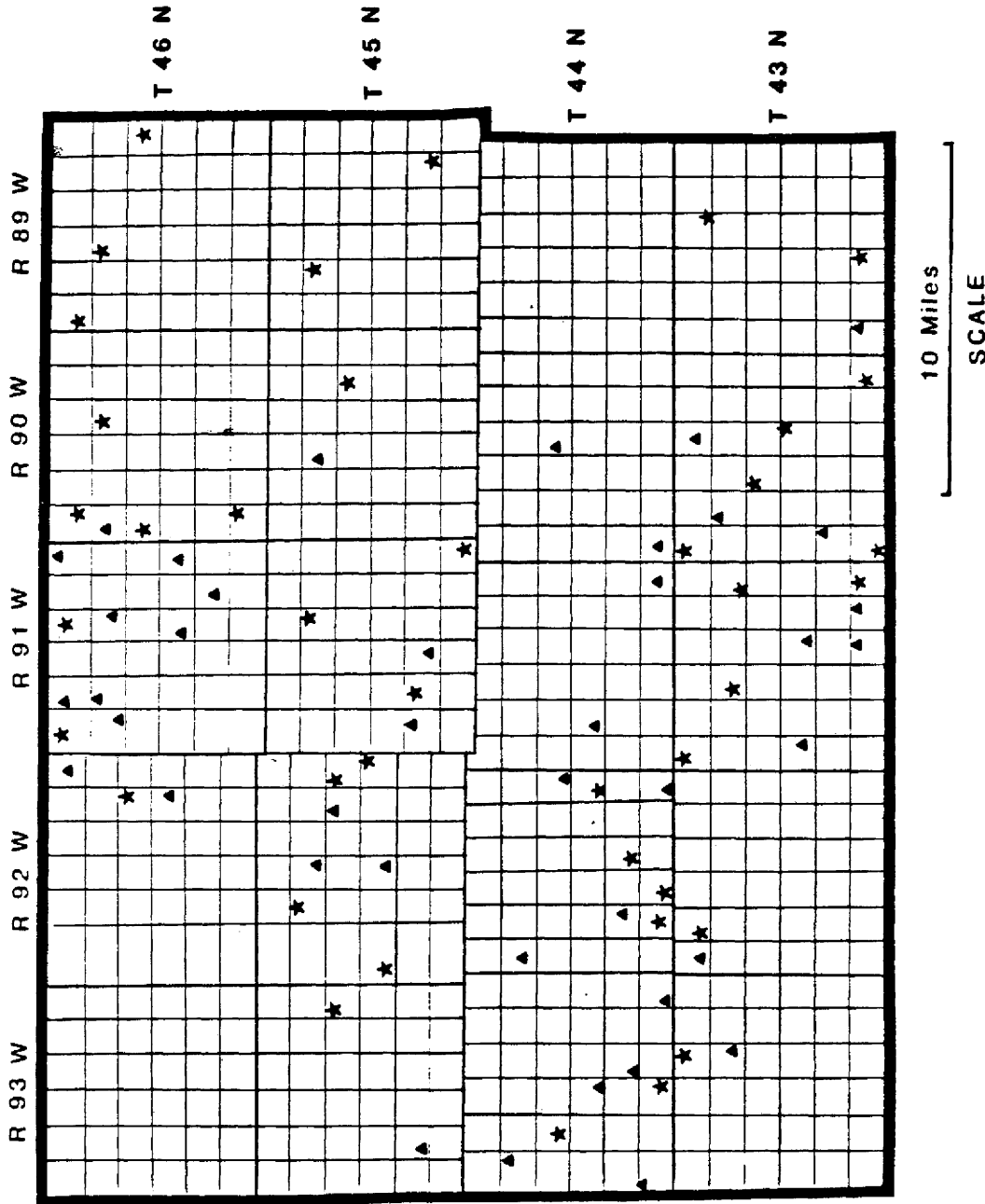


Figure 10. Location of the eighty wells used in the log analysis. Wells denoted by a star were used for seismic modeling.

properties of the Muddy that were studied include the type of bedding (thin versus massive) and the conditions of the upper and lower contacts. The data from the well logs were used in conjunction with the one-dimensional synthetic seismic models to determine how variations in geology affect the Muddy's seismic response.

A secondary purpose for the well log analysis was to extract information from the logs for use in defining depositional patterns within the Muddy. For this purpose, the paleotopography of the Muddy was examined, the Muddy was subdivided into genetic units, and each of these genetic units was isopached. Only the gamma ray logs were used to subdivide the Muddy into differing sandstones and correlate these sandstones from well to well. The S.P. and resistivity logs were not consistent enough to be used for this task.

Structure. The present day structure of the Muddy was calculated using the base of the Muddy as a reference. Figure 11 is a contoured map for depth of the Muddy relative to sea level. The largest structural gradient found for the Muddy is in the extreme west of the study area where the structural dip is approximately 14 degrees. It was important to define the greatest

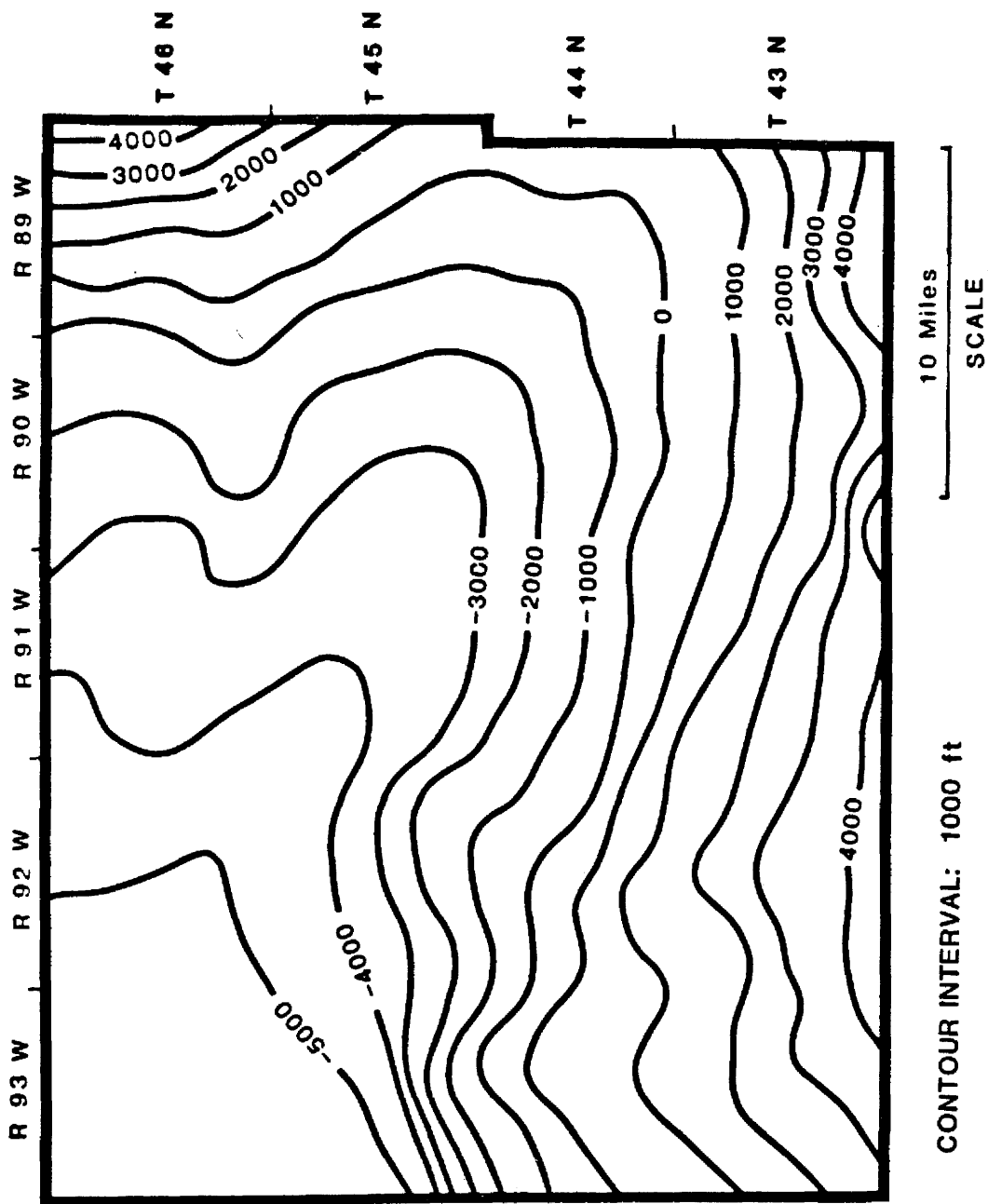


Figure 11. Depth to top of Muddy relative to sea level.

structural dip for the Muddy so that it could be judged if the amount of distortion in the isopach maps is significant. If the 14 degree slope in the Muddy is the largest in the study area, then isopach values from the wells should be in error no more than 3%. This logic assumes that the boreholes are vertical.

In Figure 12, the contours represent the vertical distance from the land surface to the base of the Muddy. Therefore, the map shows the thickness of the sedimentary rocks on top of the Muddy. This map is important to the seismic modeling work presented later in this paper.

A map for the paleo-structure, or better termed, paleotopography was also made. This map should represent the surface topography during time of deposition of lowermost beds of the Muddy. The values for the map were calculated by measuring the distance between the base of the Muddy and a reference marker bed that is believed to be very consistent and a time stratigraphic marker. A good choice for such a marker bed is a very thin, possibly bentonitic sandstone deposited within one of the thick marine shales that are found above and below the Muddy.

In order to check this method, two marker beds were chosen, one above the Muddy, and one below. Neither of the marker beds is more than 100 ft above or below the

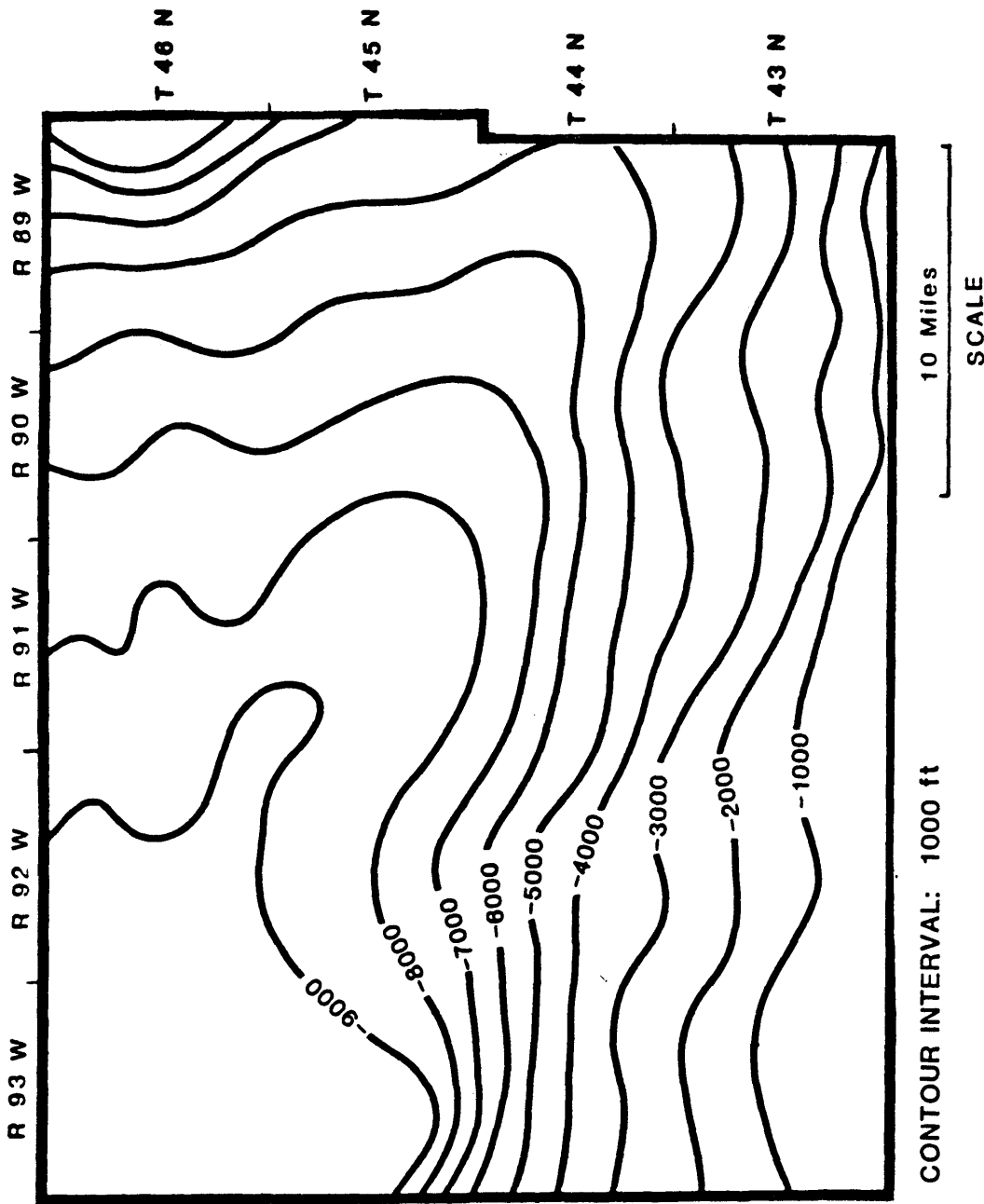


Figure 12. Depth to top of Muddy relative to land surface.

Muddy The Muddy paleotopographic maps made using the marker beds above and below the Muddy are shown in Figures 13 and 14, respectively. In Figure 13, paleotopographic lows are represented by larger isopach values, while in Figure 14, paleotopographic lows are represented by smaller isopach values. Dashed lines denote drainage patterns in early Muddy time on both paleotopography maps. In comparing the two paleotopographic maps, we see that while there are numerous minor differences between the maps, they are very similar on a more regional scale. The high degree of similarity between the two paleotopographic maps indicates that the maps are a good approximation of the Muddy depositional surface. It should be noted that these paleotopographic maps may include features created not only before but during Muddy deposition, such as scouring or channeling into the underlying Thermopolis shale. The predominant features on the Muddy paleotopography include the large linear north trending depression or valley with numerous smaller depressions branching off in a northwest direction from the larger feature and a few such features branching off in a northeast trend. Most of these topographic features tend to extend linearly over a long distance without being segmented or abruptly stopped.

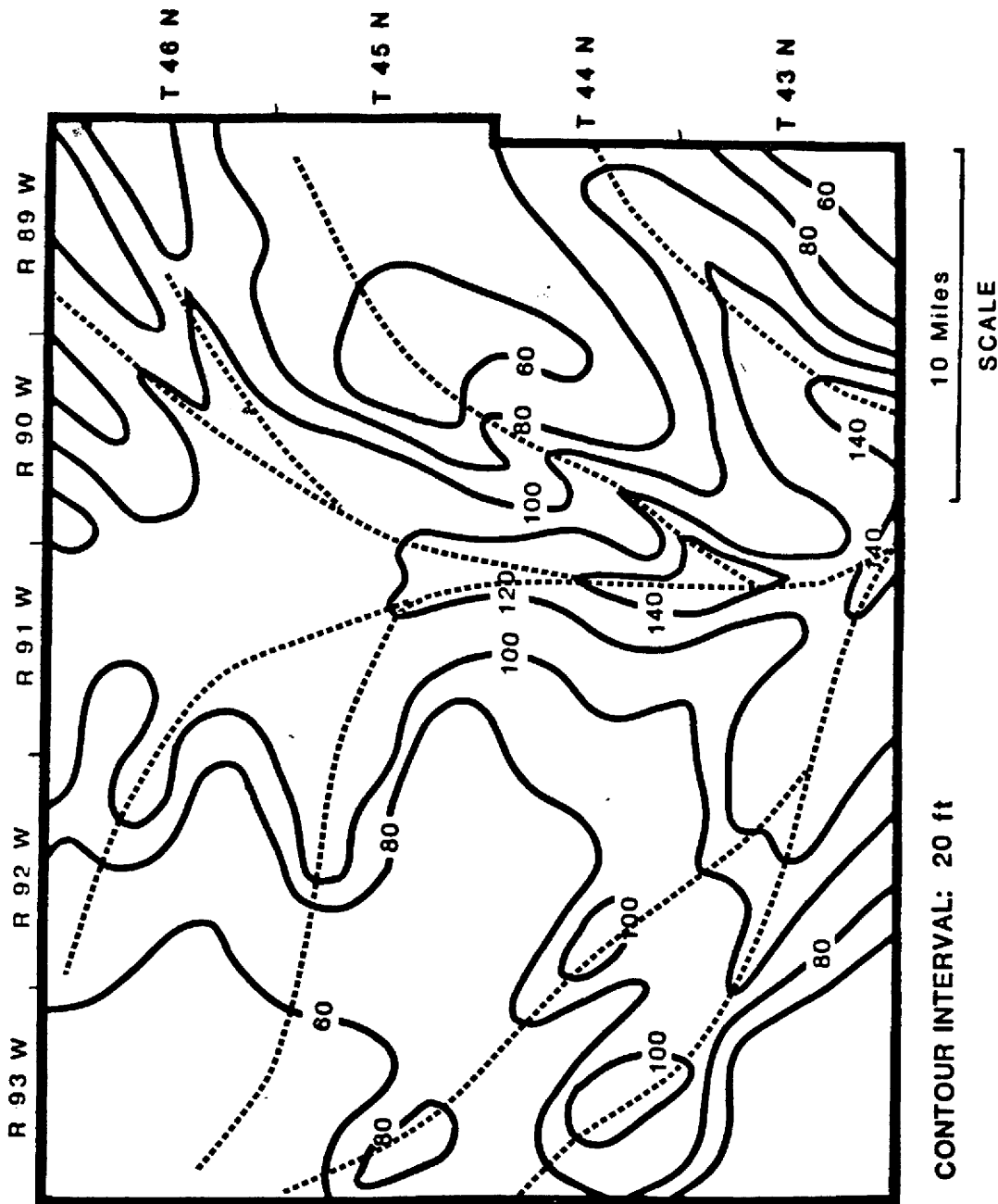


Figure 13. Paleotopography during early Muddy time based on a marker bed above Muddy.

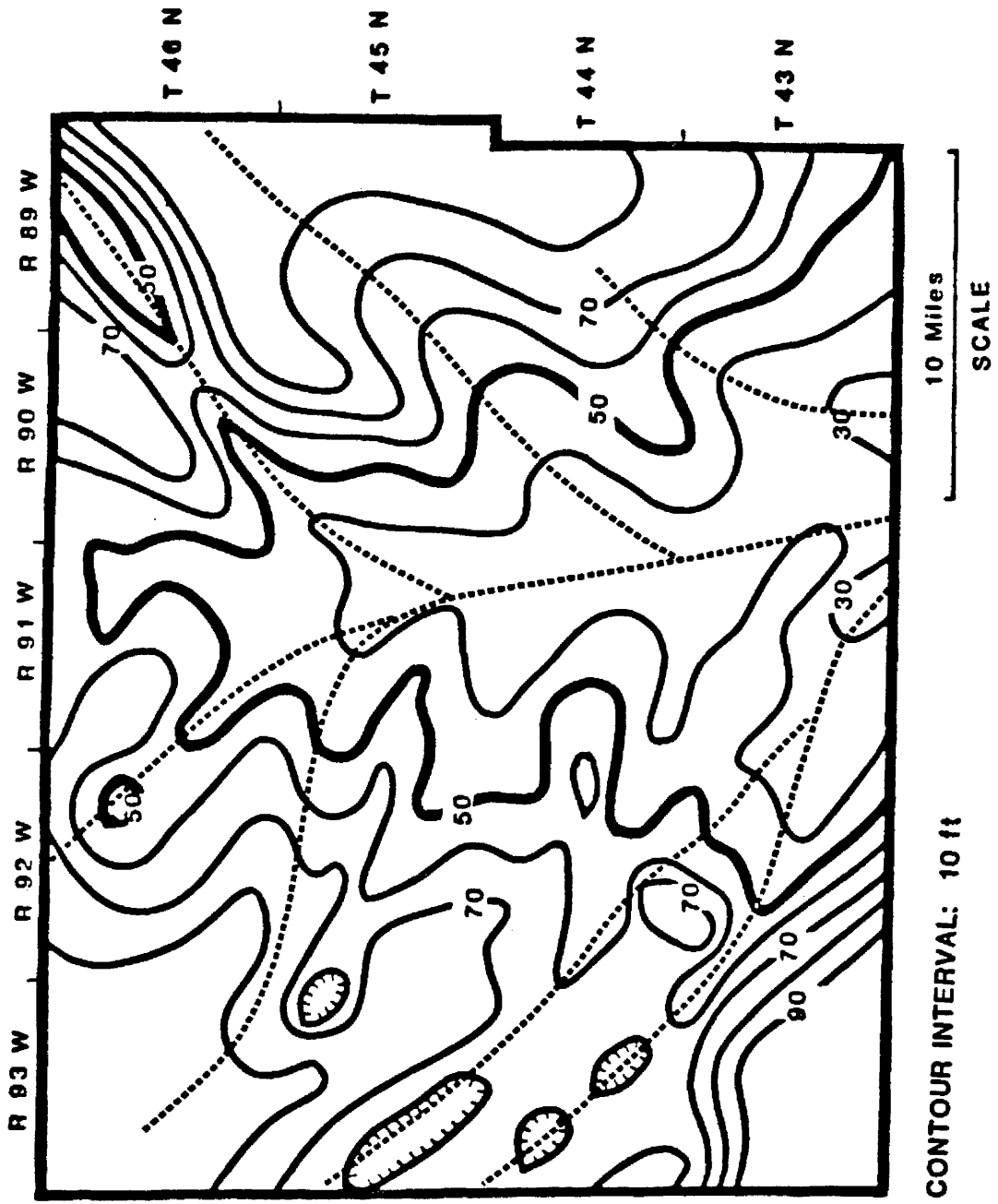


Figure 14. Paleotopography during early Muddy time based on a marker bed below Muddy.

This topography is indicative of an erosional surface where the linear low features were caused by channeling or valley incisement. These channels or valleys branch out from the main feature in a northwest and northeast direction. This indicates that the topography sloped to the south, toward the Cretaceous seaway.

Isopachs. The top and the base of the Muddy were determined on all of the eighty wells using combinations of the gamma ray, resistivity, and S.P. logs. Both top and basal contacts of the Muddy were easy to locate because of the thick marine shales that encase it. An isopach map of the entire Muddy unit within the study area is shown in Figure 15. It should be noted that this isopach map includes both sandstones and shales found within the Muddy.

The primary features of this map include the north trending linear thick that extends across the middle of the study area. Smaller northwest and northeast trending linear Muddy thicks branch off from the larger north trending thick. This thickness represents the total interval of interest over which the Muddy's seismic response is later analysed. However, for the purpose of seismic analysis, the Muddy should not be treated as

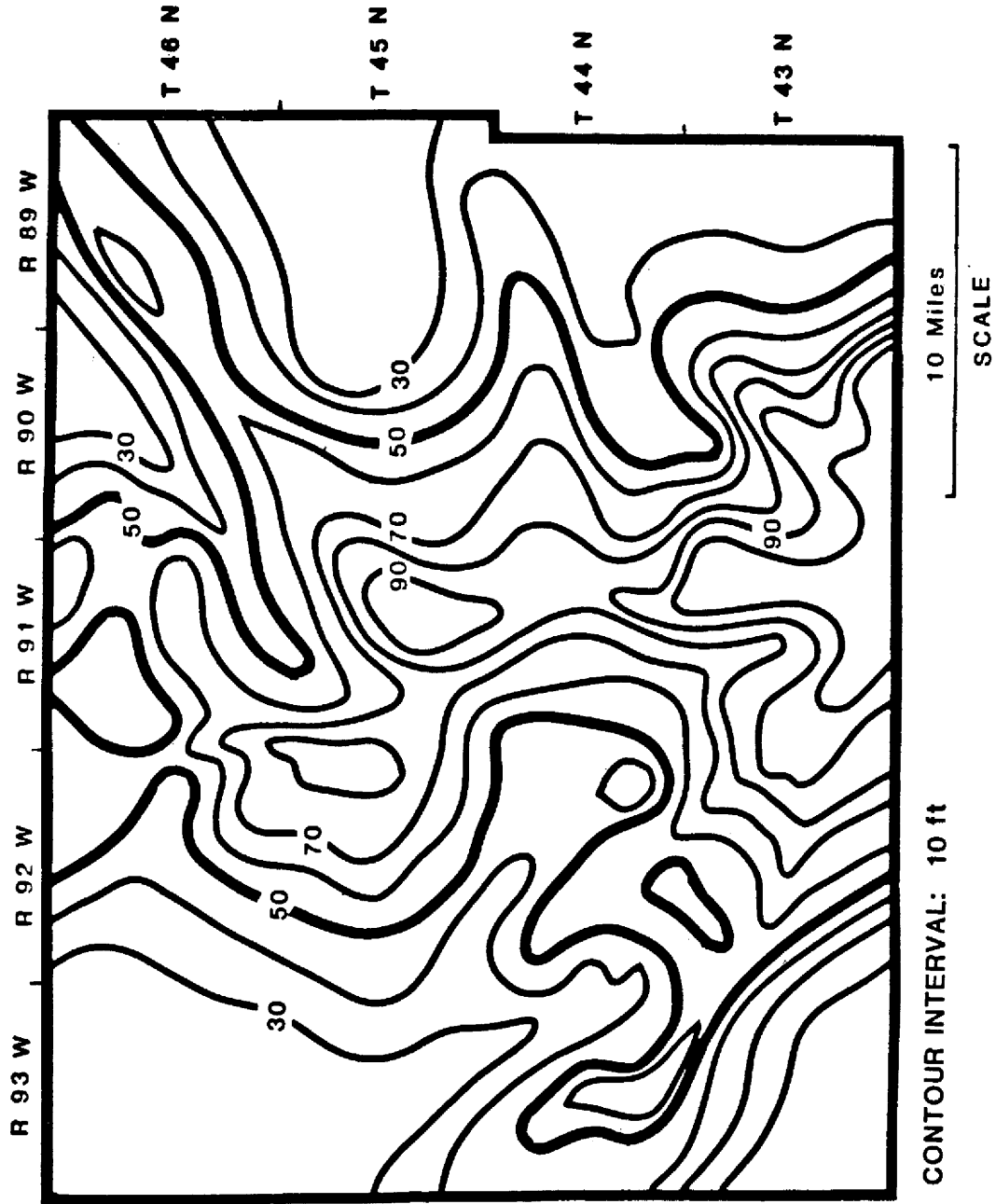


Figure 15. Isopach of entire Muddy interval.

single homogeneous unit.

Lithologically, the Muddy can be divided into a massive basal sandstone with a shale and a second less massive sandstone usually found at the top. Figure 16 shows how the two sandstones appear in a typical well in the study area. Isopach maps of the basal and the upper sandstones are shown in Figures 17 and 18, respectively. Only those wells that had gamma ray logs in the study area were used to subdivide the Muddy into the basal and upper sandstones for the isopach maps. While Figure 17 shows that the basal sandstone thickness pattern is very similar to that of the total Muddy isopach, the upper sandstone isopach in Figure 18 shows a series of elongate parallel bodies trending northeast with no similarity to the basal sandstone thickness configuration. Most of the bodies of the upper sandstone lie perpendicular to and intersect the thicker sandstone trends of the basal unit.

Intervals above the Muddy in the Shell Creek shale and below the Muddy in the Thermopolis were also isopached (Figures 19 and 20). Laterally continuous bentonitic layers were used as markers for the measurement of the intervals. These intervals were isopached to see if patterns in the Muddy deposition can be found in other depositional units. If similar depositional patterns exist over long

TENNECO #1 TUFFY FEDERAL
sec 13 T45N R92W

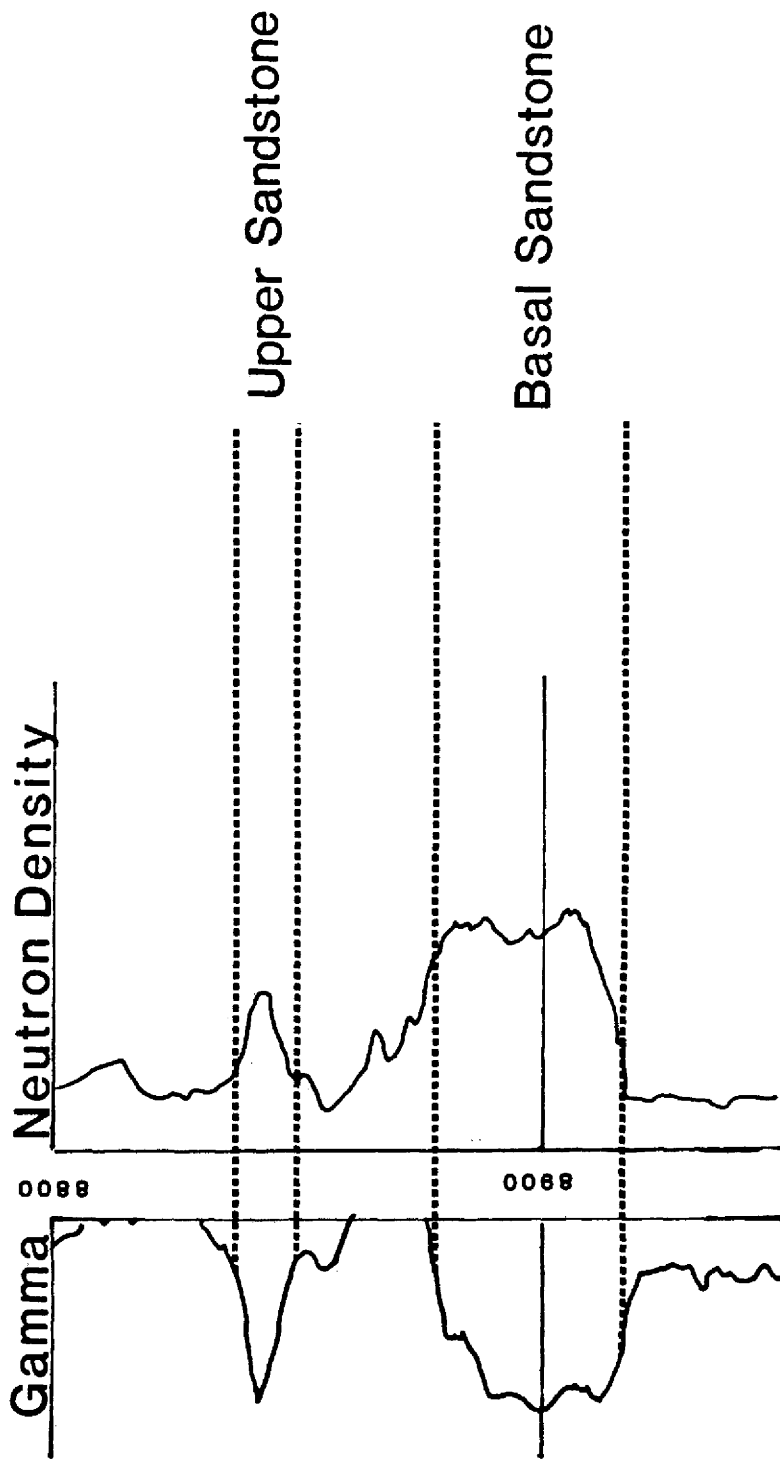


Figure 16. Typical well in study area containing basal and upper Muddy sandstones.

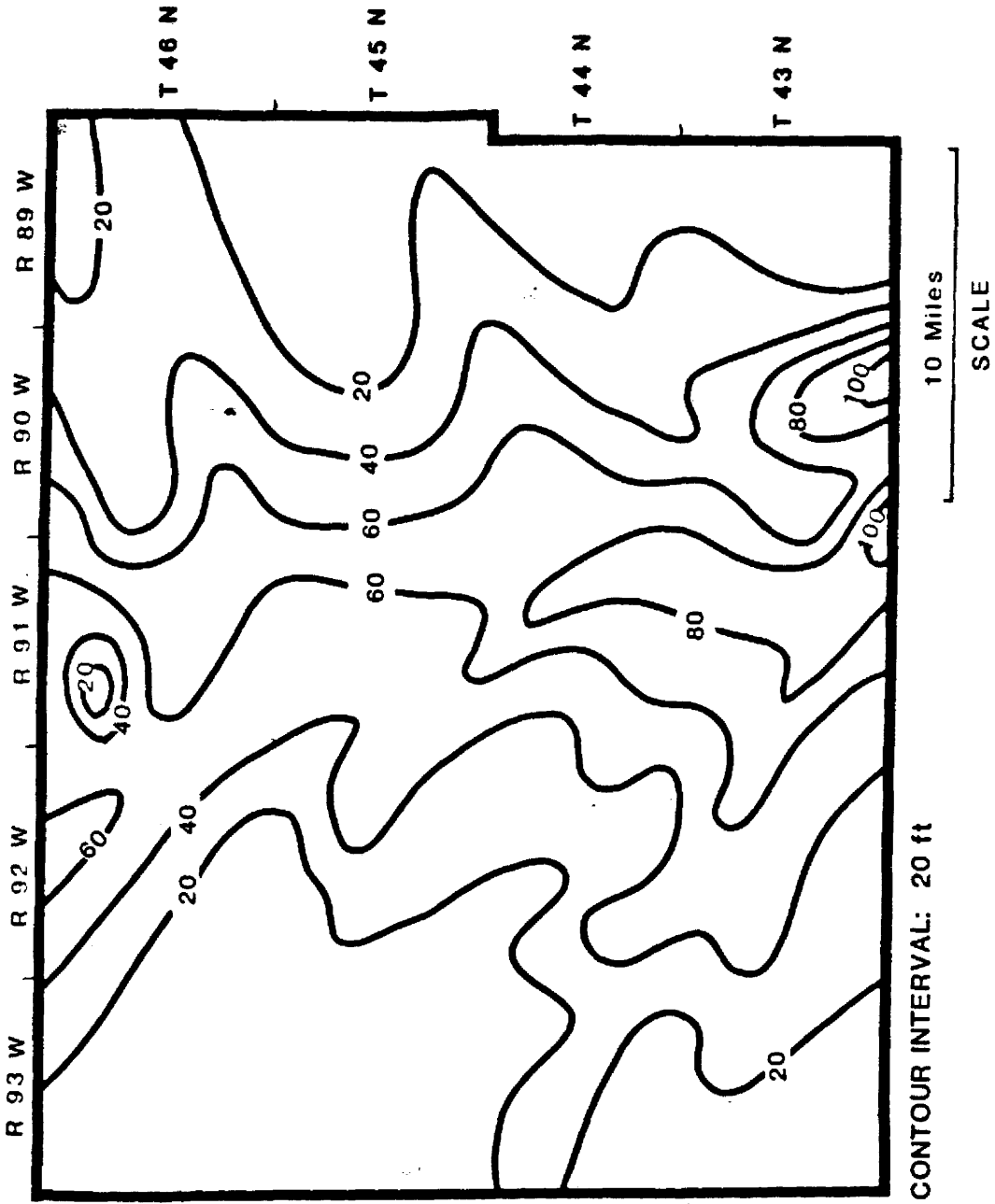


Figure 17. Isopach of basal Muddy sandstone.

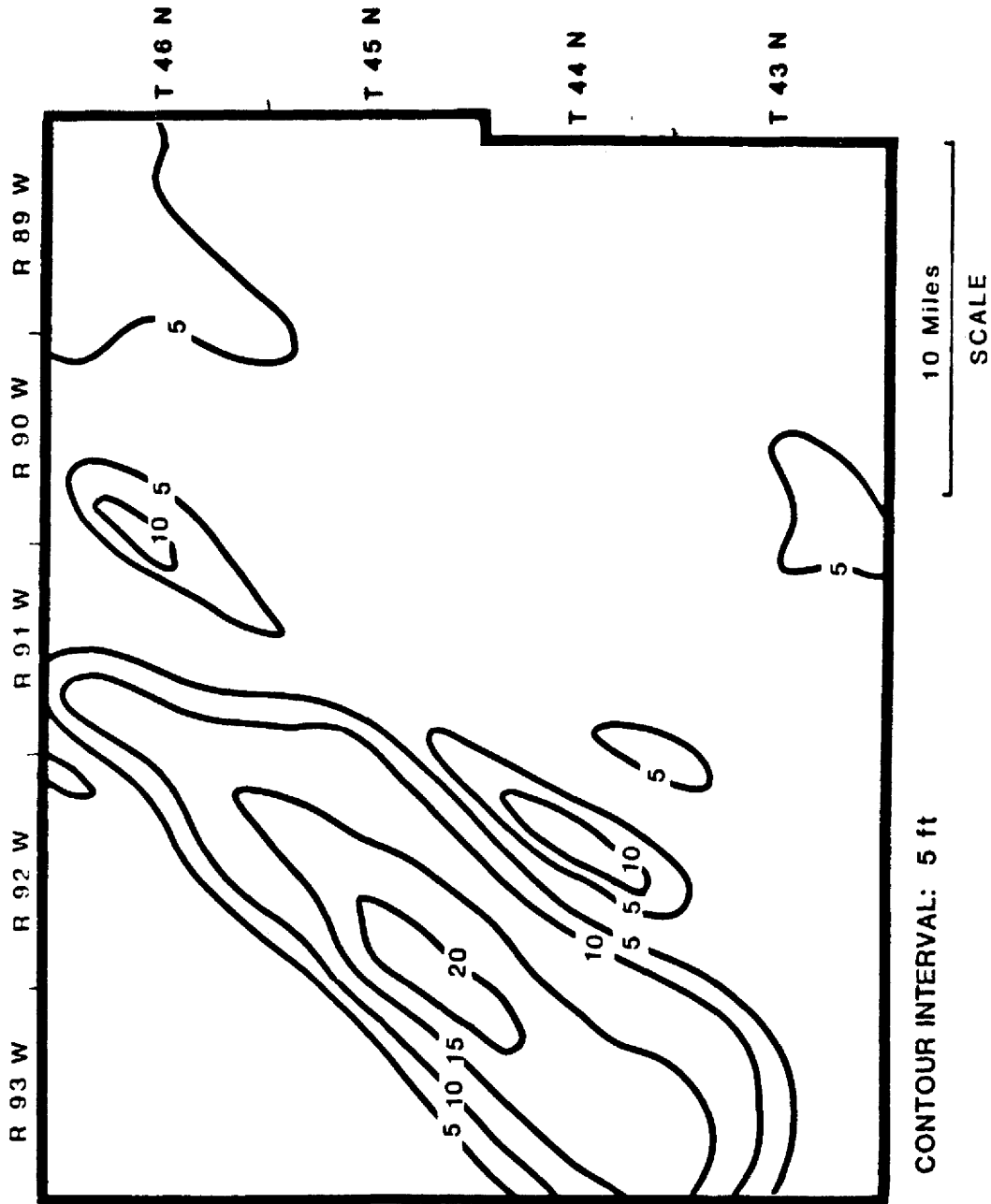


Figure 18. Isopach of upper Muddy sandstone.

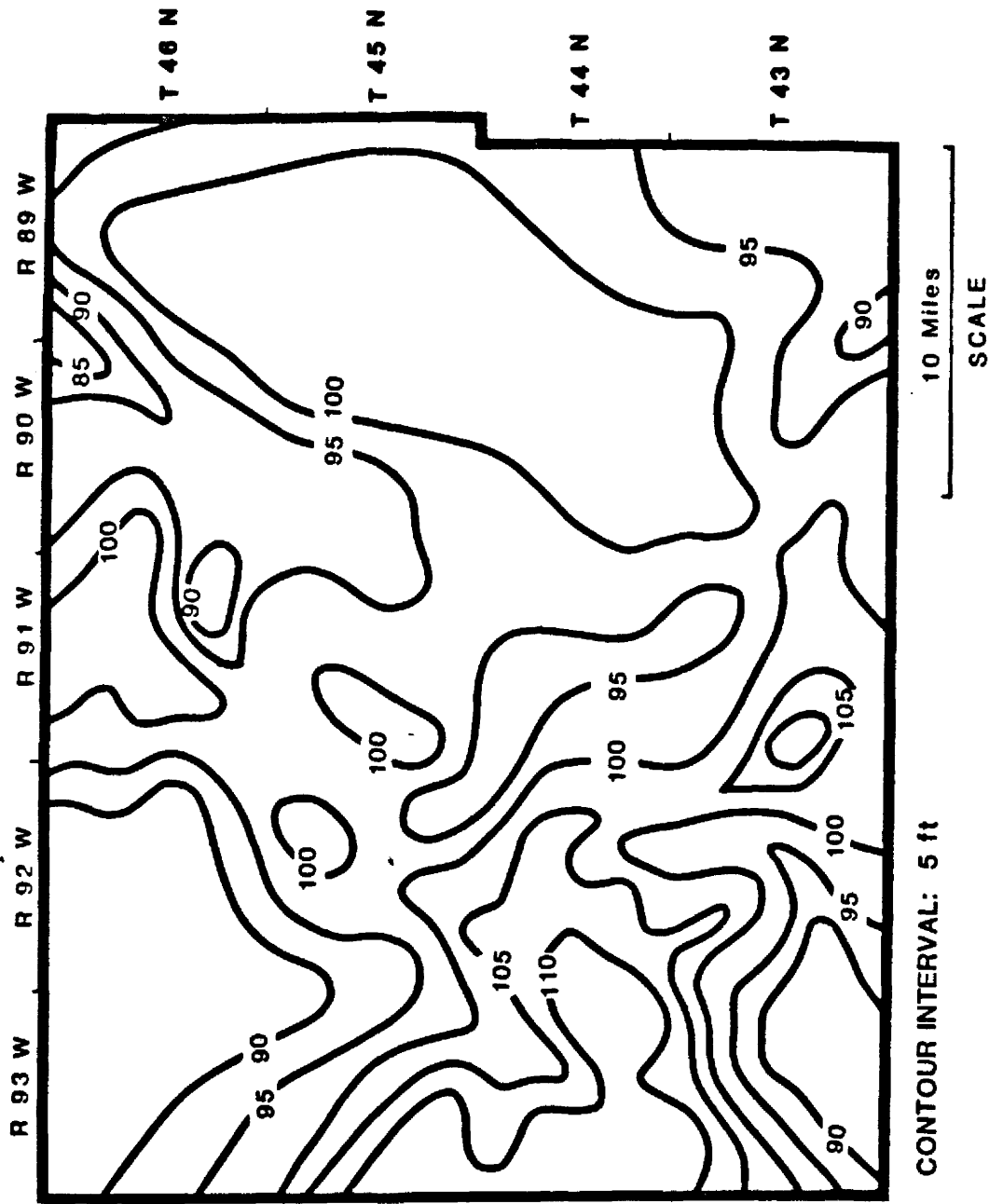


Figure 19. Isopach over a portion of the Shell Creek shale.

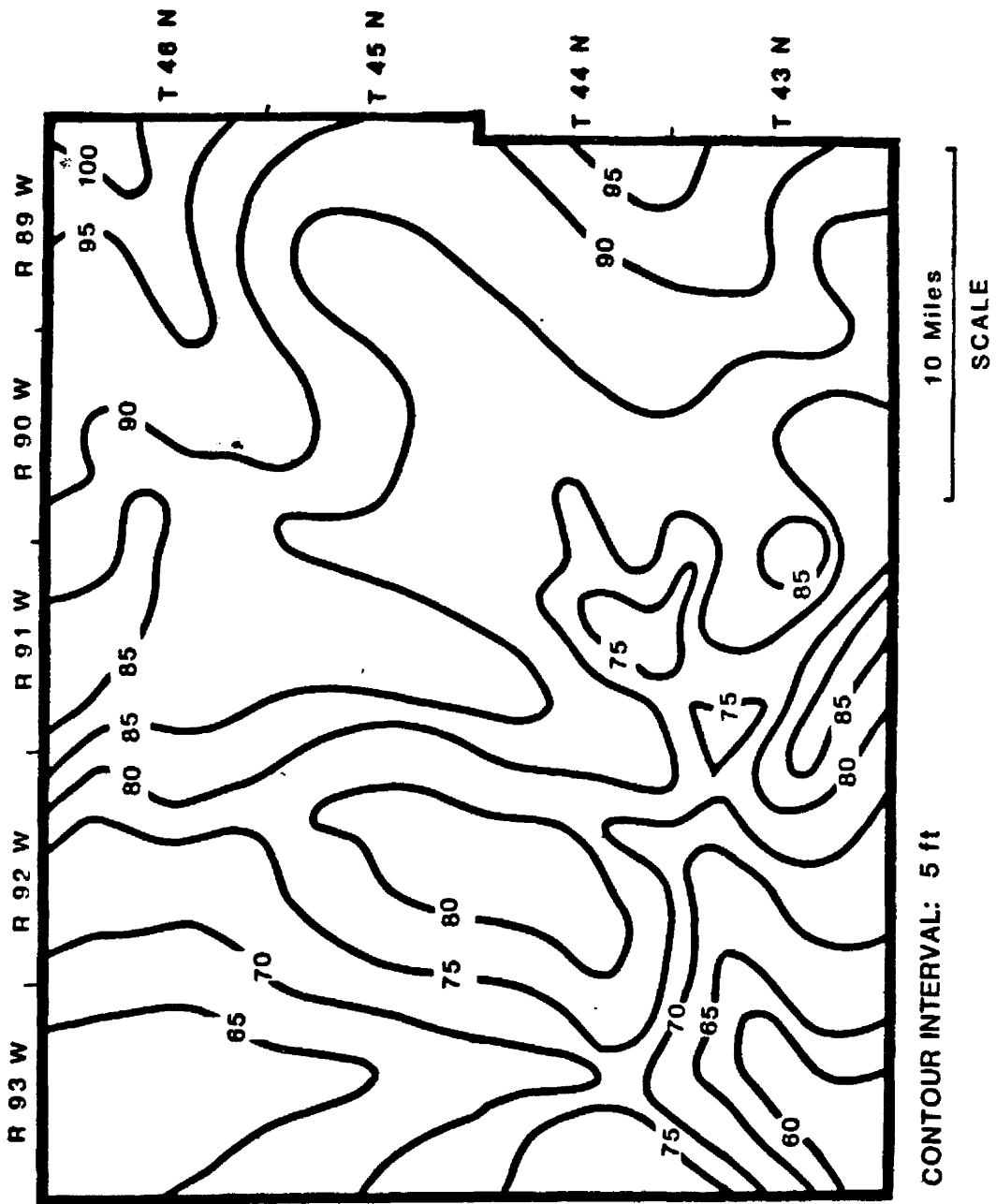


Figure 20. Isopach of a portion of the Thermopolis shale.

periods of geologic time, deep seated structural movement may be influencing sediment deposition. Both isopach maps do show sediment thickness configurations trending northwest and northeast, similar to trends found in basal Muddy deposits and in Muddy paleotopography. The similarity found among these maps does provide strong evidence of persistent northeast-northwest sedimentological and structural trends in lower Cretaceous time.

Qualitative Aspects. The well logs also reveal more qualitative aspects of the Muddy such as the type of bedding, amount of sandstone versus shale, and the condition of the sandstone-shale contacts. The important qualitative parameters not only aid in determining depositional facies within the Muddy, but also must be considered as key variables in understanding the seismic response of the Muddy. However, due to the difficulty of assigning exact values to the qualitative parameters, no type of precise maps could be made that depicted such aspects of the Muddy as bedding or type of sandstone-shale contacts. Therefore, a single map of the available gamma ray responses over the Muddy from the wells used in the study was produced (Plate I).

Facies Assignments. The division of the Muddy into lower and an upper sandstone was based primarily on the physical boundaries within the unit. However, it is believed that these two sandstones also represent separate depositional facies. If we compare the isopach of Muddy basal sandstone to paleotopography, there is a very strong correlation between position of basal sandstone thicks and paleotopographic lows. The size and configuration of the early Muddy paleotopographic features are indicative of an erosional surface with large depressions resulting from valley incisement. Therefore the basal Muddy is probably a valley-fill facies. The mixed marine and non-marine fossil assemblage found in the lower Muddy is evidence that a transitional environment was responsible for depositing the valley-fill sediments.

In most cases, the basal sandstone has a sharp lower contact with the erosional surface of the Thermopolis shale below. However, many times the lower Muddy has a gradational base in areas where the paleotopography was a relative high. I believe this to be evidence of a regressive sandstone deposit situated between the Thermopolis shale and valley-fill deposits of the Muddy, similar to the lower 'J' sandstone deposits reported by Weimer and Sonnenberg (1982) in the Denver basin. The basal sand-

stone of the Muddy that appears as a single sandstone body on the well logs may actually be two sandstones separated by an unconformity.

Only remnants of the regressive sandstone deposits remain in the study area. At these localities the basal sandstone of the Muddy appears to grade conformably into the Thermopolis shale when actually there may exist an unconformity in the middle of the sandstone unit. Mapping all regressive sandstone deposits in the study area is difficult due to the obscure log response.

The upper sandstone deposits of the Muddy may be the result of marine deposition as only marine fossils have been found in this sandstone. Upper and lower contacts of this sandstone with the surrounding shale are variable although they tend to be more gradational than abrupt.

The isopach of the upper sandstone shows one large linear body with a few smaller sandstone bodies, all trending near parallel to an ancient shoreline. The size of the larger feature may be the result of a prograding barrier island complex, although a series of en echelon marine bars may appear as a single unit because of the sparse well control.

The possible sequence of events that lead to the deposition of the Muddy interval are illustrated in

Figures 21-24. While Figures 21-24 probably represent a gross simplification of the actual Muddy depositional process, they do summarize the major events responsible for the various Muddy facies.

Muddy deposition began as the Cretaceous sea receded from the study area in a southeast direction, leaving a sheet-like regressive sandstone deposit behind over the marine Thermopolis shale (Fig. 21). Uplift of the area resulted in a continued regression of the sea. Drainage patterns developed that cut large northeast and northwest trending valleys into the regressive deposits. Valley incisement cut completely through the regressive sandstone and deep into the underlying Thermopolis shale, leaving isolated remnants of the sandstone between the valleys (Fig. 22). The overall lateral extent of regressive sandstone is difficult to determine.

After this erosional period, the Cretaceous sea began to transgress back over the area depositing the valley-fill sandstone unconformably over the eroded surface (Fig. 23). Nearshore marine siltstone and mudstone was deposited over the thick transgressive sandstones as the sea continued to deepen. Next, numerous offshore bars developed parallel to the coast on areas that had remained topographically high throughout Muddy

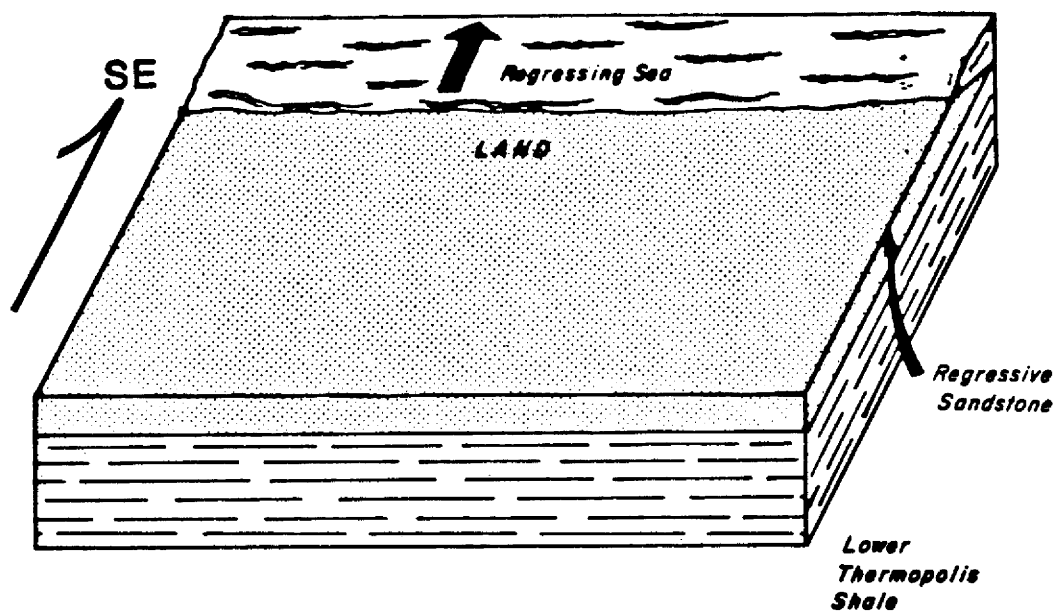


Figure 21. A thin sheet of sandstone was deposited over the Thermopolis shale when the early Cretaceous sea regressed.

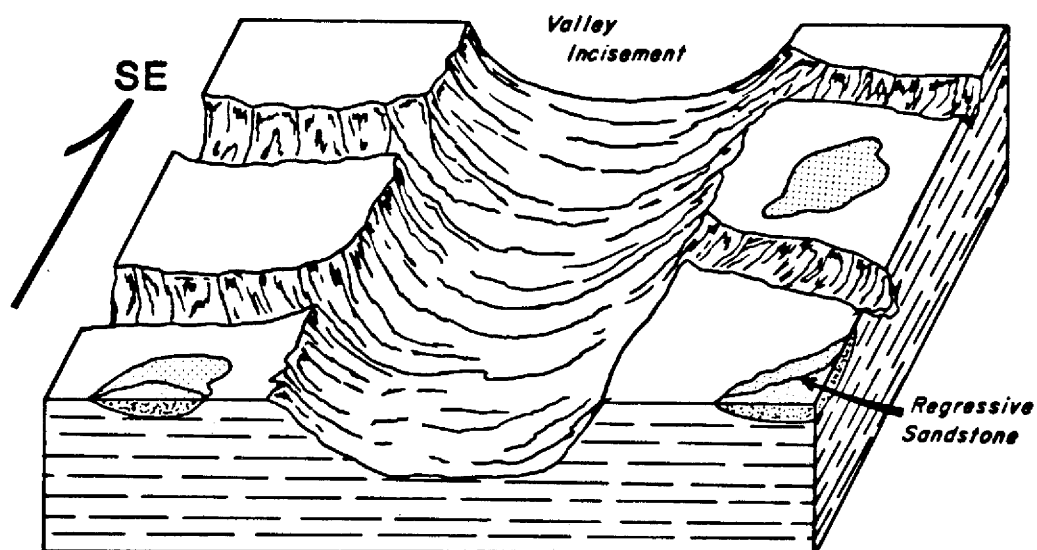


Figure 22. Valleys were cut into the Thermopolis shale as the area was uplifted.

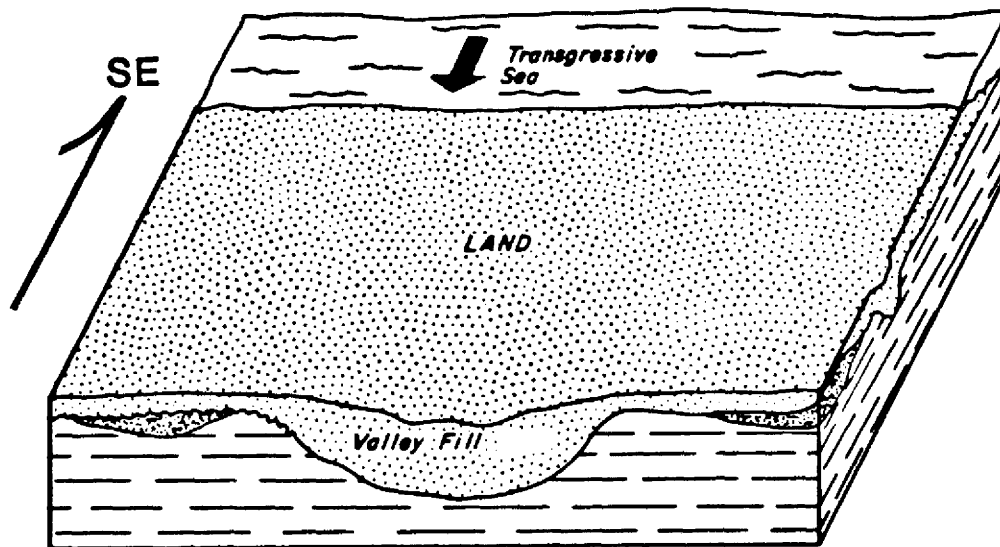


Figure 23. Influx of clastic sediments filled in eroded valleys as sea began to transgress.

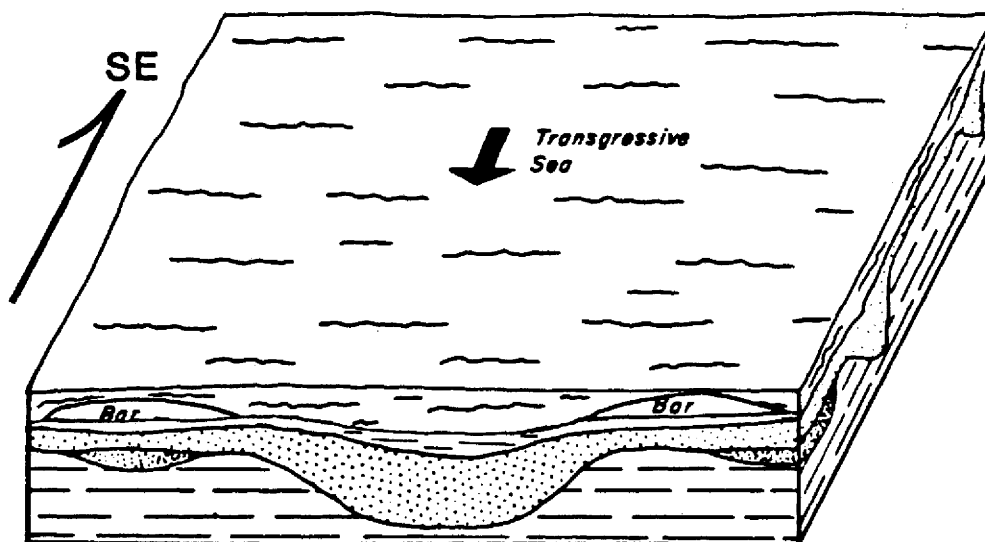


Figure 24. After the sea inundated the area, marine bars were deposited on paleotopographic highs.

deposition (Fig. 24). Large amounts of marine clastic material were supplied to the bars by means of longshore currents. After extensive bar development, the transgressing sea finally covered the bars with Shell Creek shale deposits. The marine bars, which represent the upper Muddy range between five and twenty ft thick.

The valley-fill sandstone is believed to account for most of the basal unit thickness. The contact between the regressive sandstone and valley-fill deposits cannot be exactly determined from logs, hence it is difficult to assess the exact extent and thickness of these two basal sandstones.

SEISMIC MODELING

Procedures

One-dimensional seismic models, more commonly known as synthetic seismograms, were made for 40 of the 80 wells in the study area. Less than 10% of the 40 wells used in the modeling had density logs. Several tests were made to compare a model made using both velocity and density information with a model made using only velocity data. The comparison in Figure 25, which is typical of the test results, indicates that the additional density information produces only very subtle changes in the response amplitude. Therefore, the models were made using velocity data as the geologic input while the density was kept constant. Sonic log data were collected from 500 ft above the top of the Muddy interval to 500 ft below the base giving approximately 1100 ft of data for each model. Sonic logs were edited to delete erroneous spikes. The Shell Creek shale above the Muddy caused extensive cycle skipping in many of the logs. Usually, the resistivity and the gamma ray logs could be used to edit the sonic log over the poor data zones. A few of the sonic logs were missing portions within the 1100 ft zone to be modeled. The missing zone was always a portion of the Shell Creek shale or Thermopolis, but never the Muddy interval it-

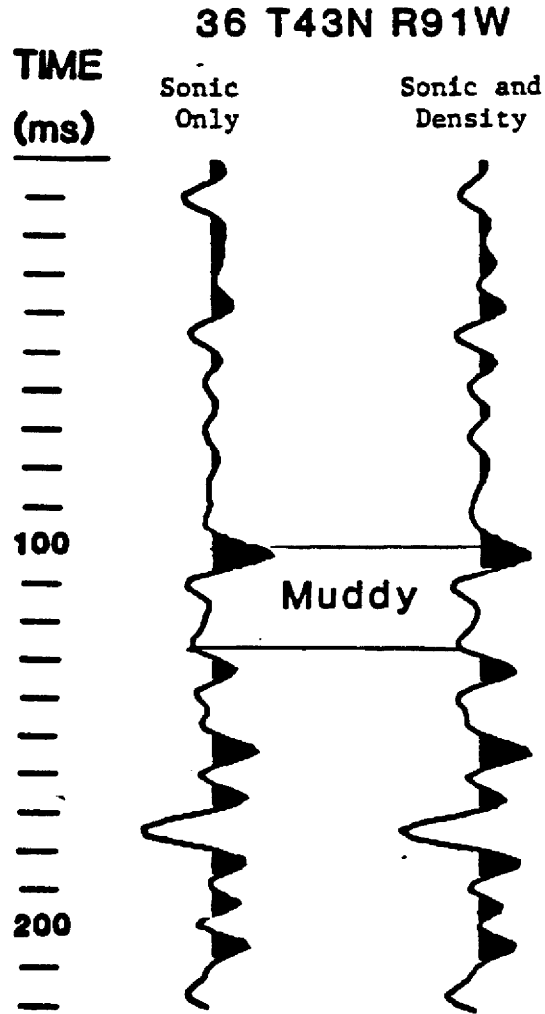


Figure 25. Comparison of a high frequency one-dimensional model made using only the sonic log and a model made using sonic and density logs.

self. For these cases, the resistivity log was used in conjunction with a nearby complete sonic log to synthesize the missing portion of the sonic log.

The edited sonic log was digitized at a two ft sample interval and input into the Compagnie Generale de Geophysique (C.G.G.) synthetic (Diglog) seismogram routine on a Cyber computer. Although a one ft sample interval may have added more stratigraphic detail to the models, the two ft interval was used for reasons of economy. The C.G.G. program integrates the sonic log so that the velocity data is transformed into a function of time instead of depth. An acoustic impedance curve is calculated using the time converted sonic log and assumes a constant density. Next reflection coefficients are derived from the acoustic impedance curve. A wavelet defined by the user is then convolved with the reflection coefficient series to produce the synthetic seismic trace. Three different wavelets were used for the models in this study. The wavelets are: 1) a relatively high resolution Butterworth wavelet with the lowest frequency at 10 Hz with a 12 dB/octave ramp and a high frequency of 90 Hz with a ramp of -12 dB/octave; zero phase rotation, 2) A low-resolution Butterworth wavelet with the amplitude spectrum having a low frequency of 8 Hz with a 12 dB/octave ramp and a high

frequency of 35 Hz with a -32 dB/octave ramp and no phase rotation, 3) An approximation of an extracted wavelet from the example seismic data that is a Ricker wavelet with a center frequency of 24 Hz and 120 degrees of phase-rotation. These wavelets and amplitude spectrums are shown in Figure 26.

LIMITATIONS OF SEISMIC MODELING

Typically, the synthetic seismogram is the tool used to relate reliable geologic information available in borehole logs to actual seismic data acquired very near the well. Many of the discrepancies that may exist between processed seismic data and well log data are fairly easily incorporated into the one-dimensional model. These include a band-limited and/or phase rotated seismic response, attenuation of the signal, and multiple reflections. However, there are numerous other facets of processed seismic data that cannot be accounted for in one-dimensional seismic models. Most problems arise from the fact that in seismic data, a subsurface reflection from a geologic boundary is developed over a large lateral area known as the Fresnel zone, while the synthetic model develops the reflection coefficient from a single point where the borehole intersects the geologic boundary. In

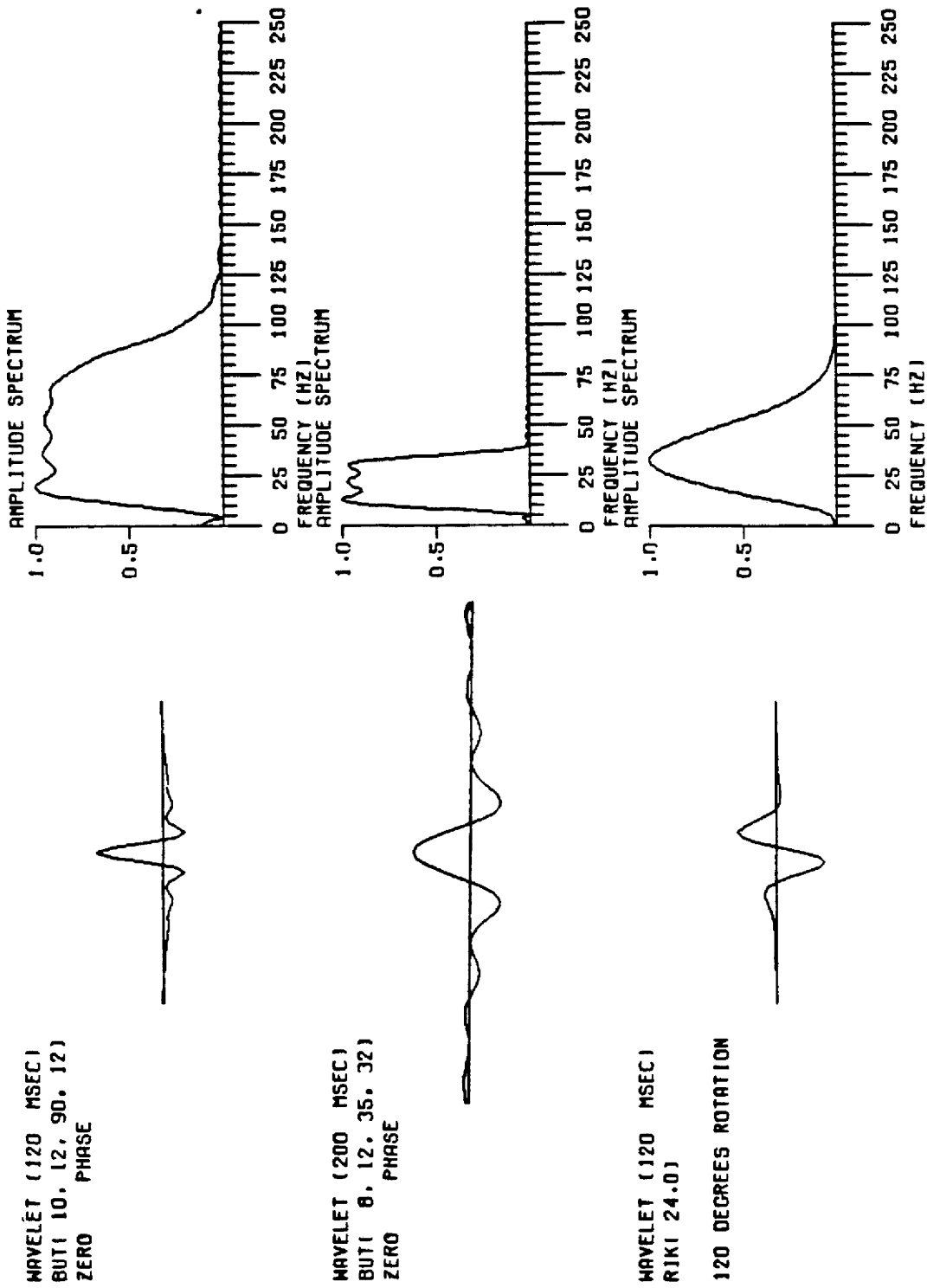


Figure 26. The three wavelets used in seismic modeling.

effect, this means that if the rock properties, i.e. geology, are not laterally homogeneous and flat over the area of the Fresnel zone, the acquired seismic data will lose some of its similarity to the normal-incidence model.

While the effect of the Fresnel zone is to decrease the lateral resolution with depth, the vertical resolution of actual seismic data also decreases with depth. Because the high frequencies of the downgoing energy are attenuated by the earth more than low frequencies, the realizable bandwidth of seismic data decreases with depth, consequently decreasing vertical resolution. In seismic modeling, usually a constant wavelet is convolved with the reflection coefficient series throughout the total depth section. Therefore, contrary to actual seismic data, frequency content and vertical resolution do not change with depth for the normal-incidence model. This discrepancy is important to this study because the seismic event of interest (Muddy) ranges between 700 ft to approximately 10,000 ft below surface in the study area. This problem could possibly be corrected for by using a time-variant frequency bandpass filter on the models to decrease the higher frequencies with depth. However, such a filter was not used in the study.

One-dimensional models made from borehole measure-

ments do not typically account for the effects of shear wave energy conversion within the earth. This may cause amplitude discrepancies between actual offset seismic data and the one-dimensional models.

One last but very important limitation of one-dimensional modeling results from the use of the common ray-tracing algorithms. In this approach, vertical changes in acoustic impedance must be approximated as a step function so that a corresponding reflection coefficient can be calculated. Therefore, a vertical gradational change in rock properties, as commonly found in sandstone/shale sequences, can only be approximated by a finite number of steps in the acoustic impedance curve.

RESULTS

The one-dimensional synthetic seismic models are present in the Appendix. On each model, the well operator, name, and location (section, township, range) appear at the top. The velocity data from the well, the reflection coefficients, and the synthetic traces are all aligned as a function of two-way travel time. Under the heading of velocity, the continuous curve denotes the interval velocities derived from the sonic log while the dotted line is the RMS velocity computed from the interval

velocities. While the reflection coefficients are self explanatory, wavelet 'A' is the high resolution zero phase Butterworth wavelet, 'B' is the low resolution zero phase Butterworth wavelet, and 'C' is the 120 degree phase-rotated Ricker approximation of the extracted wavelet shown in Figure 26. The thin horizontal lines that extend across each figure denote sandstone boundaries of the Muddy as defined from the gamma ray logs. While the top and the base of the Muddy interval are shown by the upper and lowermost lines, an intermediate solid line indicates the top of the basal sandstone and a dashed intermediate line denotes the base of the upper Muddy. Only one intermediate line is shown when there is five ft or less of shale between the two sandstones. The thick 100 ms time line is not to be confused with the lines denoting Muddy boundaries.

The primary objective of the seismic modeling was to determine how well each of the three wavelets could be used to detect variations in the Muddy interval. The simplest case will be discussed first, that of lateral variation in the single basal sandstone. The basal sandstone consists of both the valley-fill deposits and the regressive sandstones and is treated as a single unit in the modeling because there is no apparent acoustic impedance boundary

between the two sandstones.

The isopach of the basal sandstone (Fig. 17), shows that the thicknesses range from 15 ft to 103 ft. In order to more closely analyze how these various thicknesses affect the seismic amplitude of the one-dimensional models, simplified two-dimensional seismic models were constructed with a laterally thickening sandstone wedge encased between two lower velocity shales (Fig. 27). In the following analysis, the various seismic signatures of the simplified two-dimensional models are studied in detail. Forty one-dimensional models are also used in this study.

Figures 28, 29, and 30 show the vertical incidence time response for the high resolution Butterworth (A), low resolution Butterworth (B) and the extracted (C) wavelets. These are true relative amplitude seismic displays. The zero phase characteristics of the two Butterworth wavelets results in a positive peak occurring at a horizon boundary of increasing acoustic impedance. Consequently, the trough (negative amplitude) should correspond to a decrease in acoustic impedance. However, the extracted wavelet has a phase rotation of approximately 120 degrees. The asymmetry of this wavelet causes difficulty in locating the exact location in time of a change in

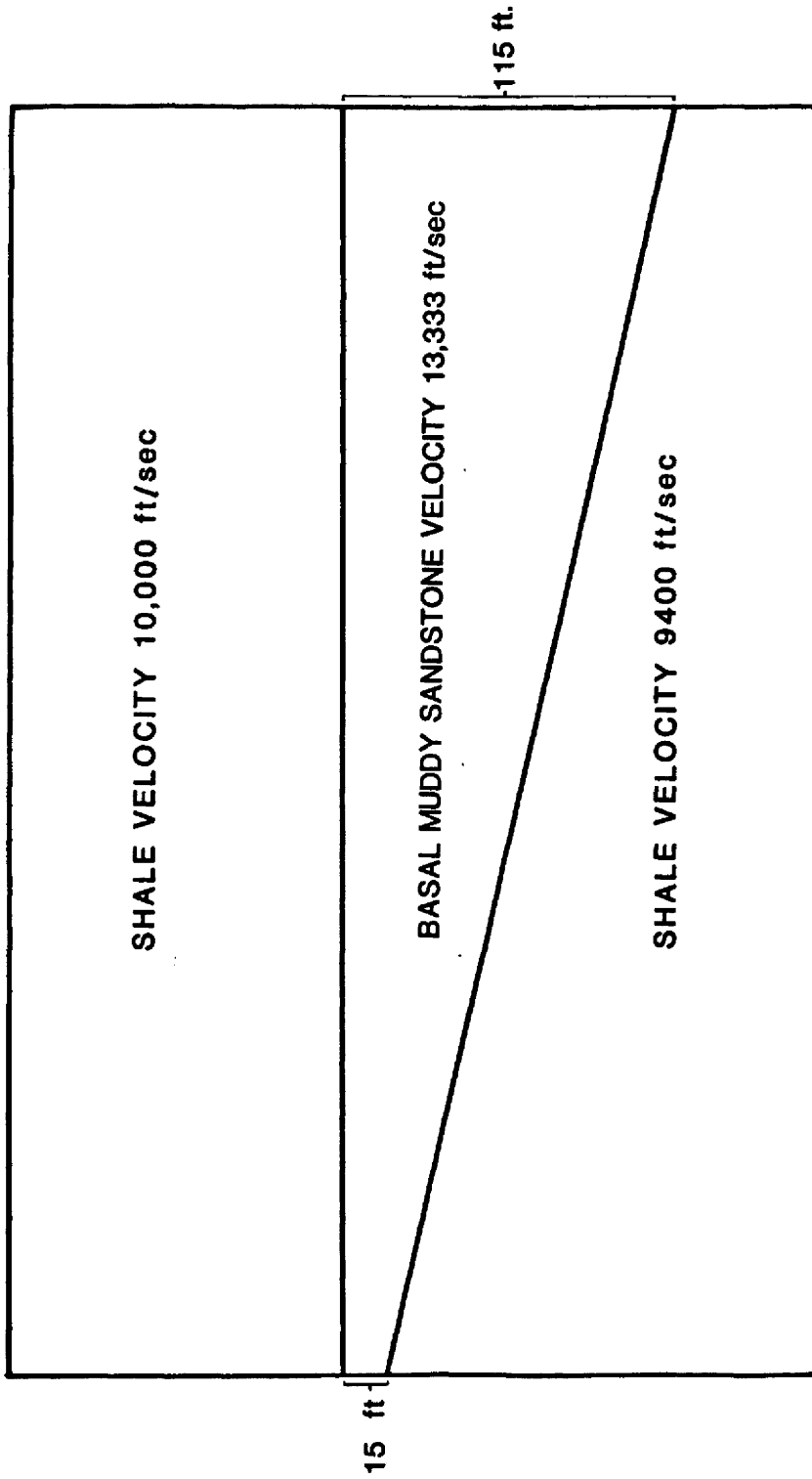


Figure 27. Laterally thickening two-dimensional single sandstone velocity model.

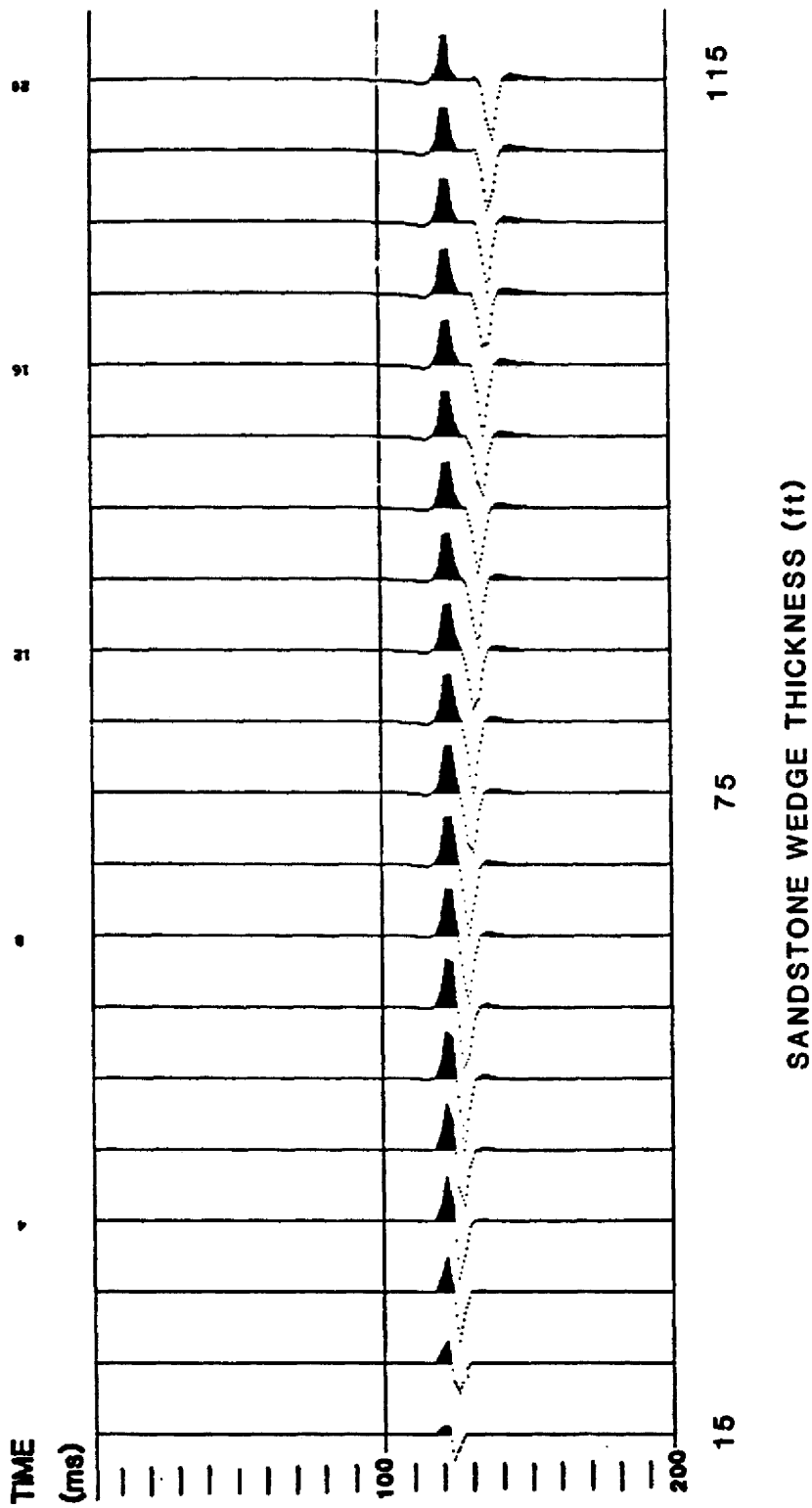


Figure 28. High resolution vertical incidence seismic response for the single sandstone model.

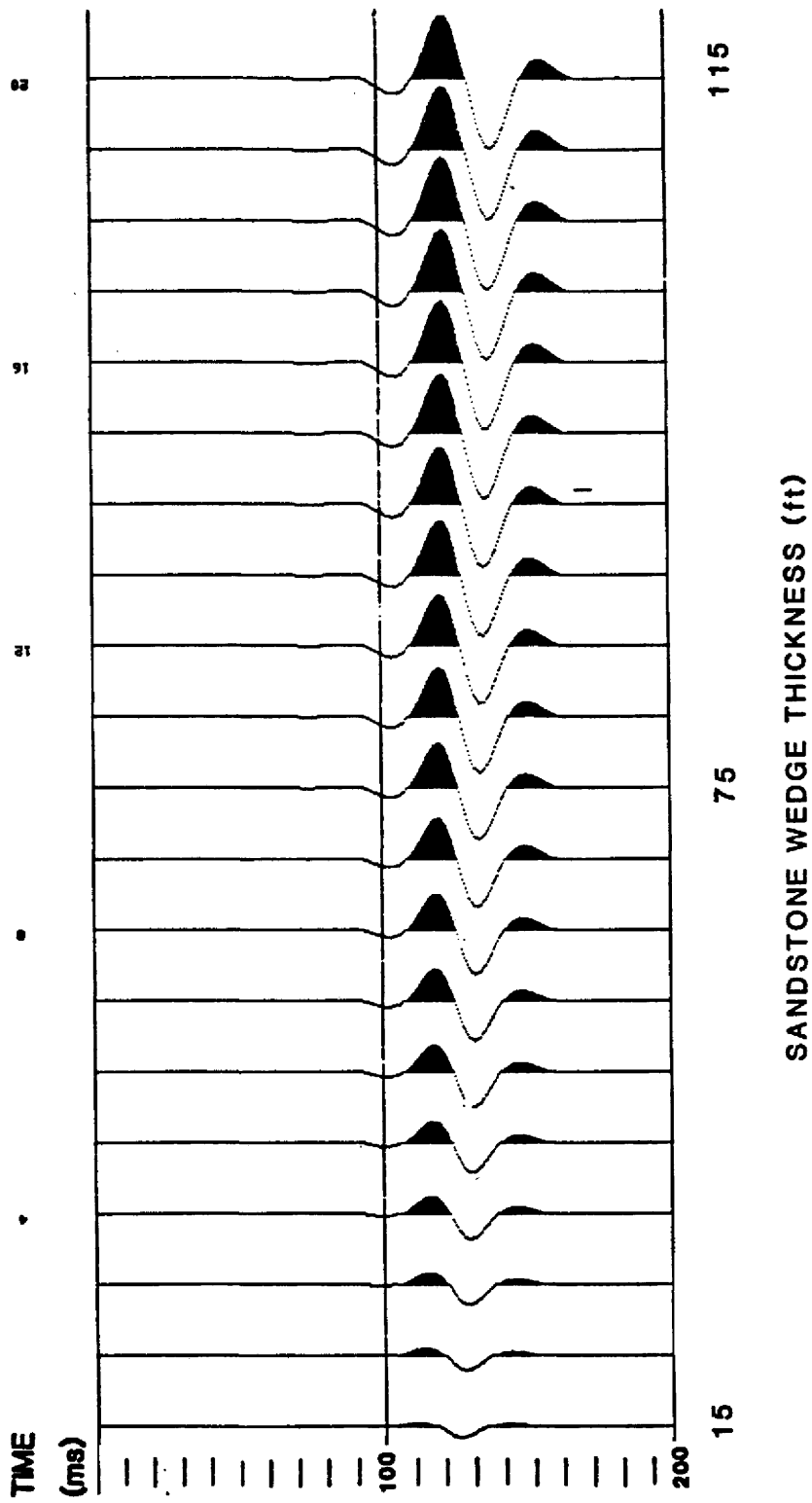


Figure 29. Low resolution vertical incidence seismic response for the single sandstone model.

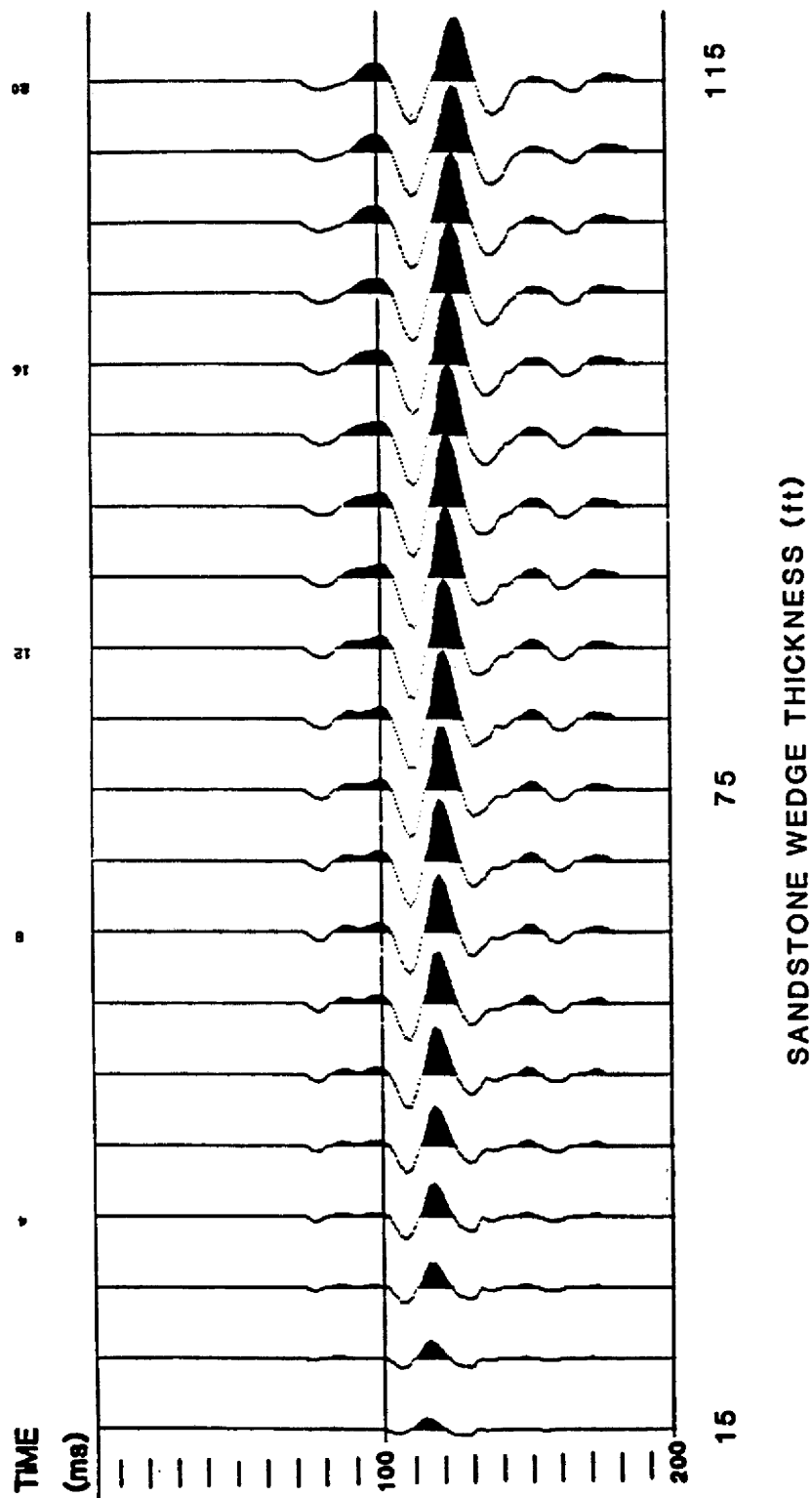


Figure 30. Vertical incidence seismic response for the single sandstone model utilizing the extracted wavelet.

acoustic impedance. The seismic resolution of a bed such as this sandstone wedge would occur if the response from the top and the base were vertically separated so that the two signals did not interfere with one another (Sheriff, 1980). In this strict sense of the word, not any of the three different wavelets can resolve the single sandstone, even up to the thickness of 115 ft

However, peak to trough measurements for the high resolution model can be translated to approximate sandstone thicknesses if the velocity is known. The high frequency content and extremely large bandwidth of this wavelet results in a very 'spikey' pulse with minimal side lobe effects. A consequence of the minimal side lobes is that interference between two wavelets is not appreciable unless the center peak and trough of the wavelets actually overlap. Although this type of signal interference occurs in the model for thicknesses below 45 ft (trace 7), peak-to-trough measurements in traces 1 through 6 will still provide thickness values with less than 20% error. Accuracy attained with the high-resolution wavelet is reasonable in most of the one-dimensional models that have a single sandstone in the Muddy. One exceptional case involves a very thick single sandstone with large velocity variations in it, as shown in the synthetic trace from

section 36, T43N, R91W (Appendix p. 140). The top of the sandstone is easy to locate with the large positive peak, but either of two troughs could represent the base.

The one- and two-dimensional models show that destructive interference occurring in sandstones of less than 45 ft results in lower amplitude responses for the high-resolution wavelet. No evidence of constructive interference (tuning) occurs for this wavelet due to lack of side lobe energy.

While the high resolution wavelet represents a very optimal seismic response that might only be possible with the very best in acquisition and processing parameters, the low resolution wavelet is the opposite. This low frequency wavelet has a very narrow frequency bandwidth, resulting in large side lobes. In Figure 29, vertical peak-to-trough measurements can provide approximate sandstone thickness values only for the sandstones over 100 ft thick. The large side lobes of this wavelet are responsible for destructive interference in this simple sandstone model. Abnormally large amplitude signal responses caused by constructive interference are often used to detect sandstone thickness when peak-to-trough measurements are known to be incorrect. Wavelets with unusually large side lobes work especially well in this type analy-

sis. However, the very low frequency content of this wavelet (B) results in a period of 40 ms, causing the tuning effect to occur at a sandstone thickness of 134 ft.

The most obvious feature of the low resolution two-dimensional model that changes with sandstone thickness is pulse amplitude. Amplitude for the primary peak and trough as well as the side lobes increase with sandstone thicknesses up to approximately 90 ft. All aspects of this seismic response are the same for sandstone thicknesses of 90 to 115 ft.

Bandwidth and dominant frequency of the extracted wavelet lies between the extremes exhibited by the two Butterworth wavelets. As seen in Figure 30, asymmetry of this wavelet leads to a more complex and significantly longer time response than that of the two other wavelets. Complexity of this wavelet tends to produce a large array of both constructive and destructive interference patterns that rapidly change with varying sandstone thickness in the wedge model of Figure 27. Exact location of the top and base of the sandstone in time cannot be correlated with a specific peak or trough, as is apparent in most of the one-dimensional models. A constant time shift can be applied so that the upper large amplitude trough corresponds to the top of the sandstone. However, vertical

time measurements between this trough and the large amplitude peak below show only a very crude relationship to the changing sandstone thicknesses. In the two-dimensional models, the most obvious feature that changes in response to sandstone thickness for this wavelet is the uppermost positive doublet that begins to occur at trace 3 (approximately 20 ft). In traces 3 through 14, amplitude of the basal portions of the doublet increases more than the top until the feature becomes a single peak in traces 15 through 20. A second feature that might be recognizable for determining sandstone thickness is amplitude of the central trough and peak. Both of these events gradually increase in amplitude from left to right, until a maximum occurs at trace 14 at approximately 80 ft of sandstone. A slight reduction in amplitude occurs as the sandstone continues to thicken. While the one-dimensional models clearly show a similar variation in peak and trough amplitude for the sandstone thickness, there is very little evidence of a small positive doublet above the major trough, as appeared in two-dimensional modeling. Instead there is only a small peak with a width and amplitude that varies independently of sandstone thickness.

In the next three models, a second sandstone of constant thickness was located 25 ft above the top of the

basal sandstone wedge as in Figure 31. This two-dimensional model presents a very simplified representation of the upper marine bar sandstone and the thicker valley-fill sandstone below. The same three wavelets were used in the two-sandstone model so that a comparison with the single-sandstone model would reveal if the upper sandstone is recognizable and the effect it may have on the seismic response of the lower sandstone.

High resolution Butterworth wavelet detects both sandstones separately and accurately (Fig. 32). While it would be difficult to accurately determine the exact thickness of the upper sandstone, one could easily recognize that the upper sandstone is thin in comparison to the average thickness of the valley-fill sandstone below. Presence of the upper sandstone causes an asymmetry in the large amplitude peak associated with the top of the basal sandstone. However, peak-to-trough measurements for the basal sandstone still give accurate values for the sandstone thickness. In the one-dimensional models, the marine bar sandstone can only be identified with the high resolution wavelet in a few cases. The model from the Tenneco well in section 24, T45N, R92W (Appendix, p. 149) clearly shows a peak that indicates the sandstone's presence; however, the center of the peak is a

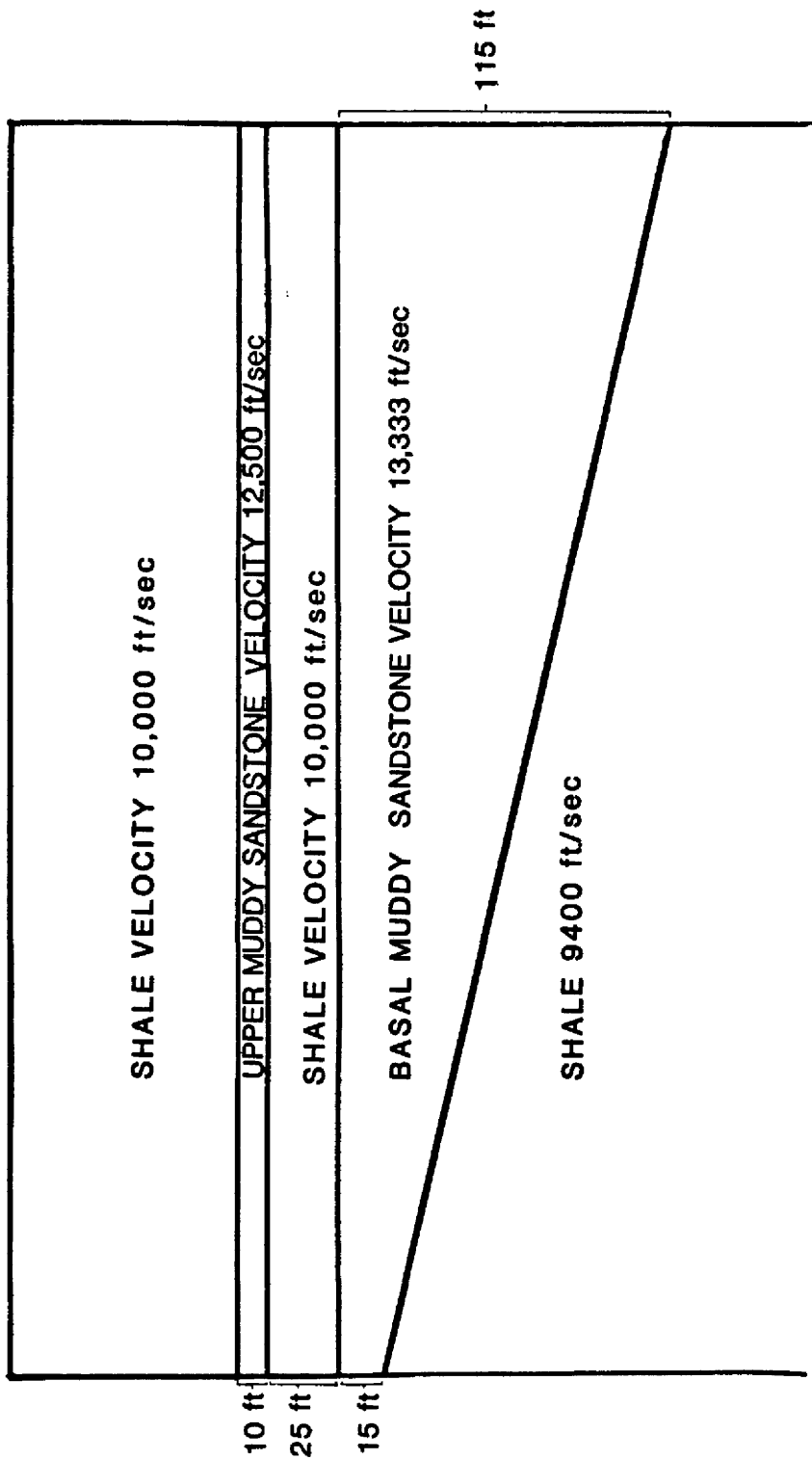


Figure 31. Two-dimensional velocity model consisting of a laterally thickening basal sandstone overlain by a thin upper sandstone.

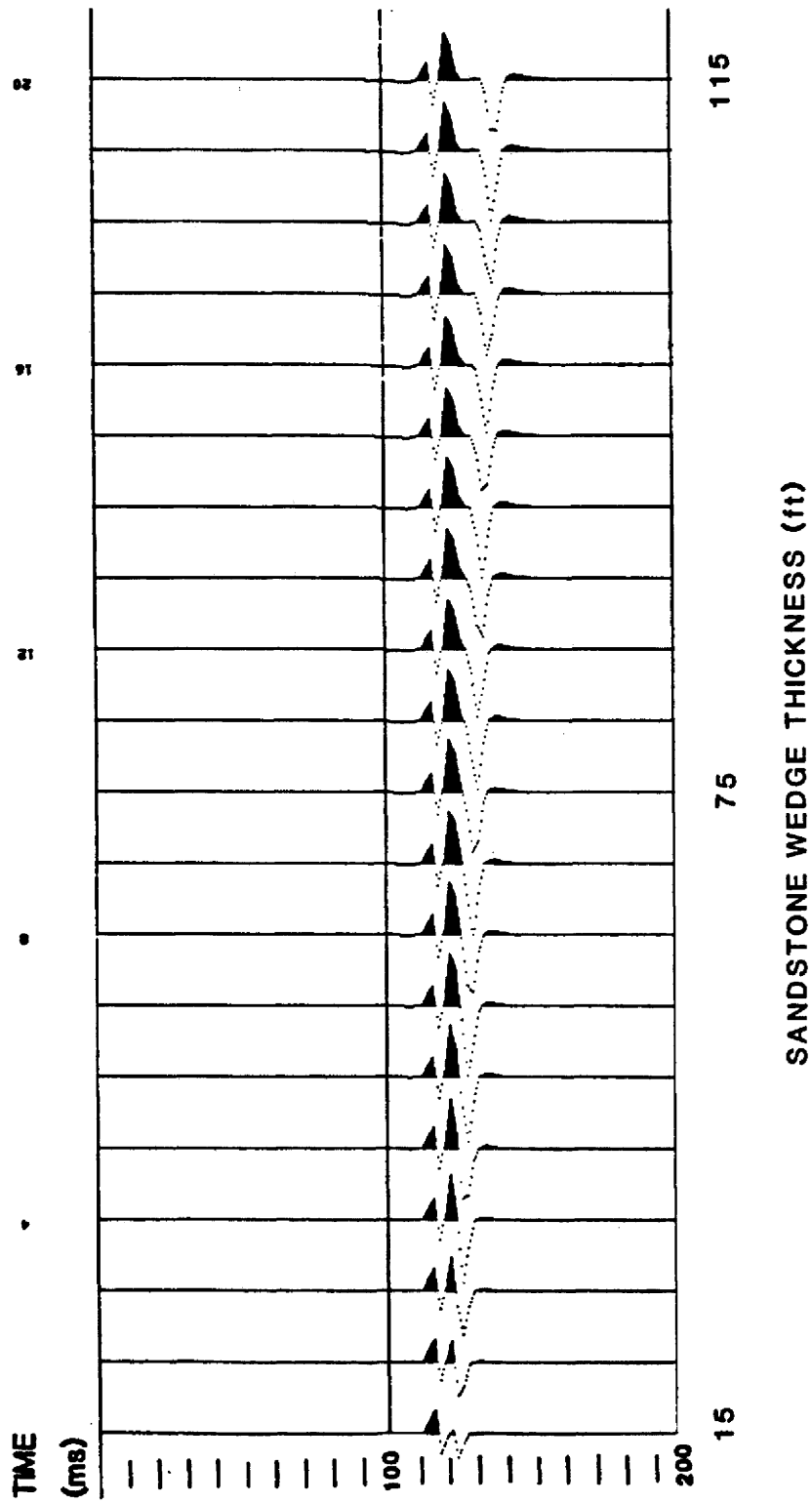


Figure 32. High resolution vertical incidence seismic response for the two sandstone model.

considerable distance above the top of the sandstone. While there are often one-dimensional models that have even thicker bar sandstones, they do not produce a recognizable seismic event for two apparent reasons. First, the upper sandstone is usually so close to the basal sandstone that both are displayed as a single event, and second, the upper sandstone usually has a very small velocity contrast with the surrounding shale.

The time response of the two sandstone wedge model appears almost identical with that of the single sandstone model when the low resolution Butterworth wavelet is used (Fig. 33). Presence of the bar sandstone may have no noticeable response in the one-dimensional models. However, it is apparent that when bar sandstone occurs over a substantial basal sandstone, this wavelet's peak is centered at the top of the upper sandstone instead of at the top of the basal sandstone.

Two-dimensional wedge models made using the extracted wavelet also show very little change with the addition of the bar sandstone (Fig. 34). The small peak above the major trough does become asymmetric toward the base, however this subtlety does not appear in the one-dimensional models. It is probable that lithologic variations in the Shell Creek shale affect this subtle

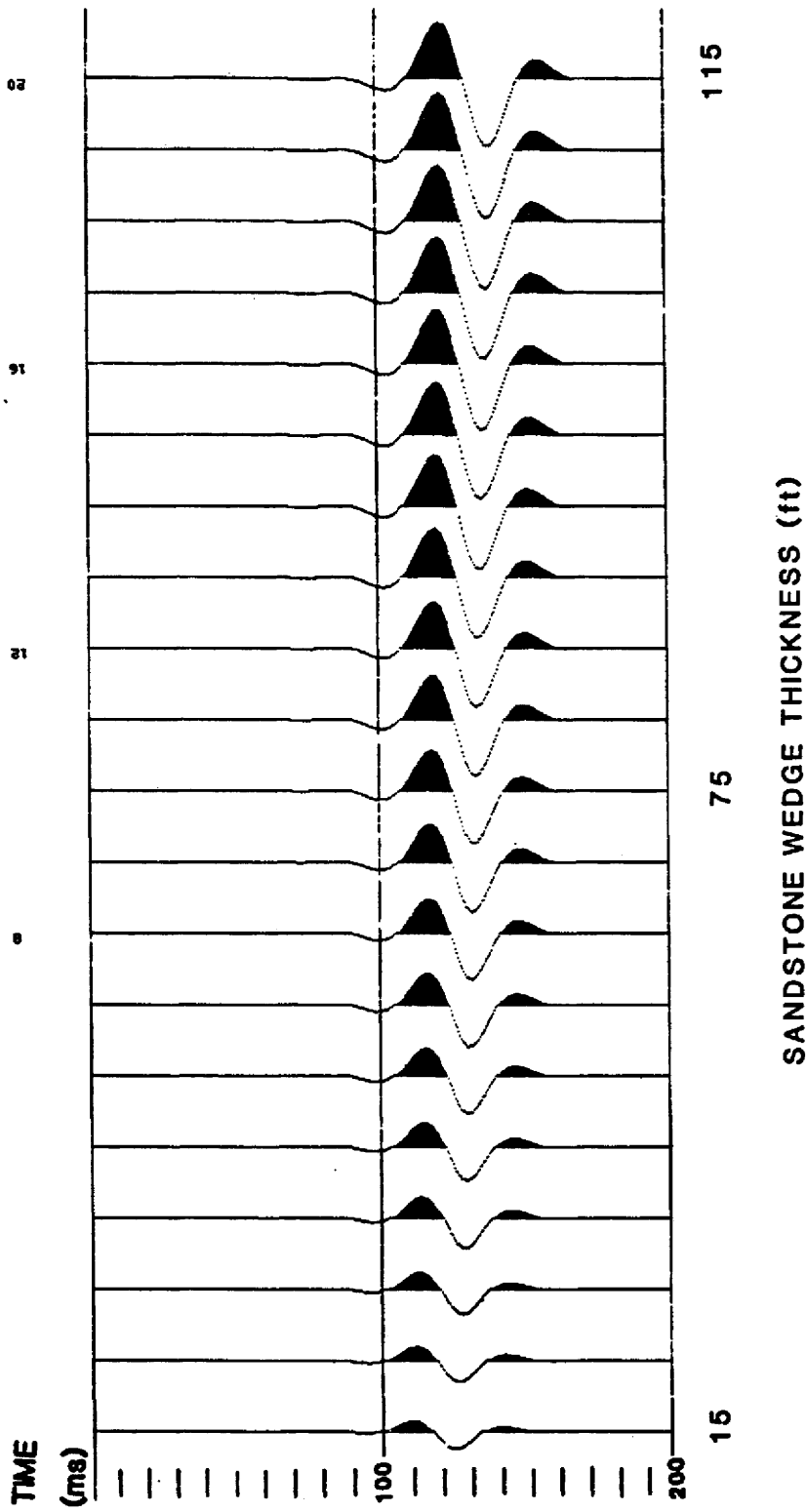


Figure 33. Low resolution vertical incidence seismic response for the two sandstone model.

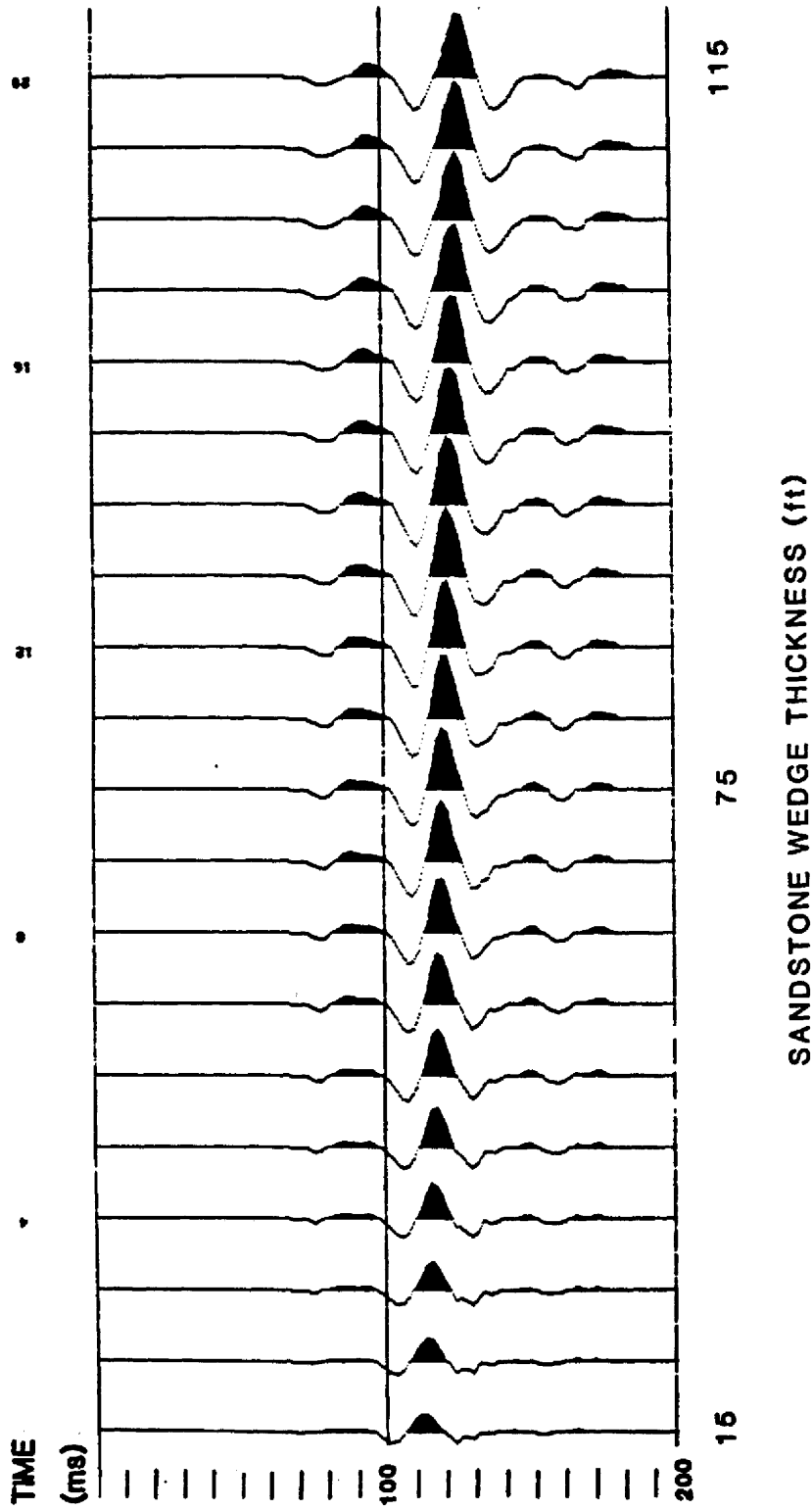


Figure 34. Vertical incidence seismic response for the two sandstone model utilizing the extracted wavelet.

response feature as much as, or maybe more than, Muddy thickness.

A more definitive indication of upper sandstone presence on this model is a lowering of the major trough amplitude. This amplitude decrease may be confused with a simple thinning of a single sandstone except that the amplitude of the major peak (below the trough) is not affected by the bar sandstone's presence as it would be by a thinning sandstone.

Plate II consists of a geologic cross-section through five wells in the study area that penetrated the Muddy. The three wells on the left have thin- to moderate-basal sandstones overlain by an upper bar sandstone. On the right side of this plate, the bar sandstone pinches out while basal sandstone thickness increases in the Pan American well. The Muddy interval cross-section is shown relative to one-dimensional seismic models derived from the five wells. This plate illustrates detection capabilities for the three wavelets used in this study.

In summary, the high resolution wavelet can be used to accurately determine the thickness of a basal sandstone 20 ft thick or more. A bar sandstone may be detected if it is greater than 15 ft thick and separated from the basal sandstone by at least 15 ft. The low resolution

wavelet can only be used to detect gross changes in total Muddy thickness. Sandstone thickness determination with the extracted wavelet is complicated by its phase-rotation. Thicker basal sandstones increase the amplitude of both the major peak and trough of this wavelet's seismic response. Thick upper bar sandstones are occasionally detectable by recognizing amplitude variations in the major trough of the seismic response produced using this wavelet.

FACTORS AFFECTING MODELING RESULTS

General relationships established apply to most of the one-dimensional models; many exceptions are found in the models and certainly must exist in real seismic data. Various unpredictable geologic factors such as thin spurious silts or minor compositional changes within the Muddy undoubtedly affect the seismic response of this unit. While there is no practical way of accounting for these types of geologic influences, there are other less specific factors affecting the seismic response that can be considered in this study.

Gradational Boundaries

Gradational geologic boundaries between sandstone

and shale were only briefly mentioned earlier under the heading of 'Limitations of Seismic Modeling'. A transitional geologic boundary usually is expressed in terms of acoustic impedance as a ramp. One-dimensional synthetic models use a large number of closely spaced thin layers to approximate a transitional zone. However, in the simplistic two-dimensional models, no attempt was made to synthesize a gradational boundary. In general, the overall effect of convolving a wavelet with the acoustic impedance ramp is to generate a low frequency reflection. A short length transition zone, less than the pulse period, results in a stretched response in time with a lower than normal amplitude. If the transition zone is over a long vertical distance, then a zero phase wavelet will result in a very lengthy, low-amplitude doublet response (Anstey, 1980).

Velocity and reflection coefficient information included with each of the one-dimensional models indicates that gradational boundaries between the Muddy and the surrounding shale occur with equal frequency for the top and bottom contacts. Many researchers in the field of seismic stratigraphy believe that such transitional boundaries vastly deteriorate the reliability of the synthetic seismogram (Neidell and Poggialiomi, 1977).

However, detail of actual sonic and gamma ray logs from wells used in the models reveal that many of the supposedly gradational basal contacts are actually very sharp boundaries. The few wells with gradational basal Muddy contacts were interpreted as locations where the unconformity, that typically separated the valley-fill sandstone from the Thermopolis shale, ramps up to separate a remnant of regressive sandstone from the valley-fill sandstone above it. Therefore, in the case of an occasional true basal transition zone where the unconformity separates two sandstones, the simplistic four-layer model recognized no gradational boundary at all, the synthetic seismogram portrays a transition zone along with many surrounding fabricated transitional boundaries, while the real seismic data may result in an isolated low frequency trough associated with the contact.

Porosity

Variations of sandstone porosity are also likely to alter the seismic response for the Muddy. Porosity is usually directly proportional to interval transit time as measured by a sonic tool in a borehole. Figure 35 is a map of the average interval transit time for the basal Muddy in the study area. As expected, the map

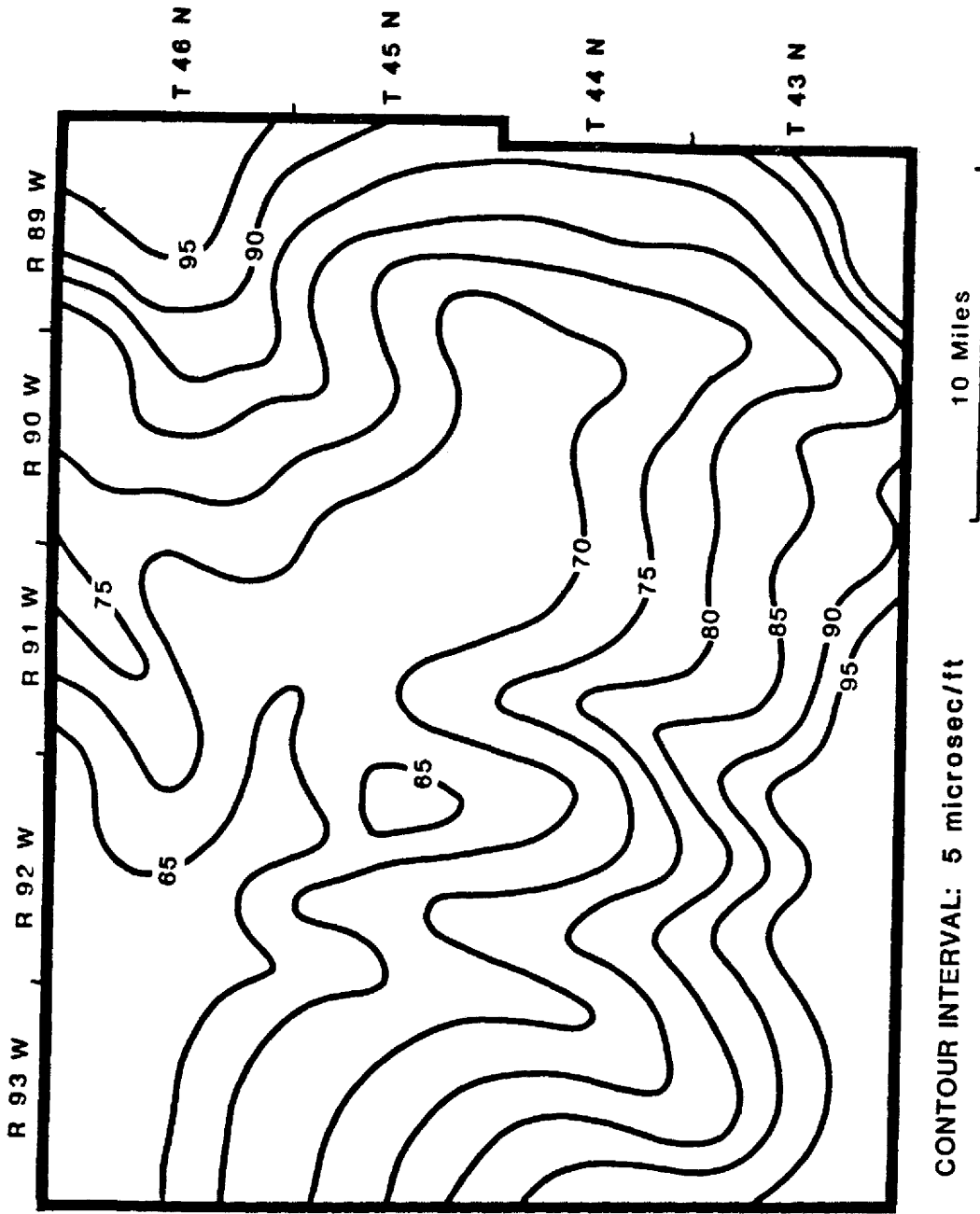


Figure 35. Contour values of interval transit time taken from the basal Muddy sandstone sonic log response.

of relative porosity generally correlates well with the map showing Muddy depth of burial (Fig. 12). This is probably related to the effects of compaction and is discussed in more detail later in this thesis. By calculating the interval velocity of the Muddy from the interval transit time in Figure 35, it becomes apparent that the velocities vary by more than 50% across the study area. Therefore, even if the sandstone is resolved accurately so that the peak-to-trough time of the seismic response corresponds exactly to the bed boundary, drastic errors in bed thickness may be calculated by using a velocity from a well up or down dip from the area.

While the interval transit time values for Figure 35 are for the valley-fill sandstone of the Muddy, sonic logs and the velocity curves for each of the models show that the marine bar sandstones has higher interval transit time values than do the basal sandstones. Because many of these bar sandstones have very low gamma ray counts, thus excluding shale as a possibility, high interval transit time values may indicate that upper bar sandstones have better overall porosity than that of the valley-fill sandstones. This stands to reason since the marine sandstones were probably reworked more than valley-fill sediments, hence they have better porosity due to better sorting. If

the slower velocity of the upper sandstone is indicative of porosity, then higher porosity would result in lowering the acoustic impedance contrast between this sandstone and the surrounding shale. This, in turn, would result in a lower amplitude seismic response, which may be interpreted as the response to a thinning of the sandstone.

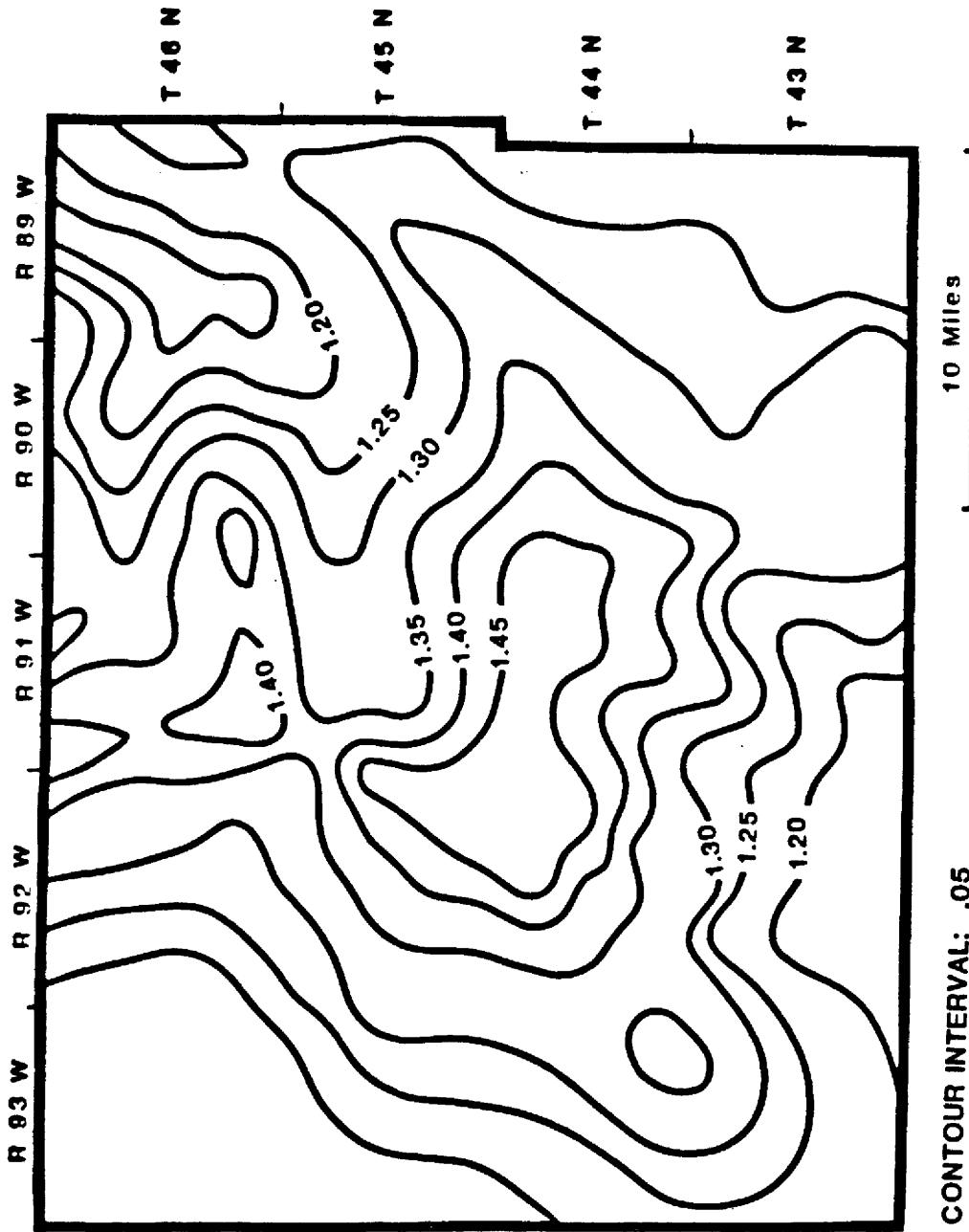
While porosity is a sought after property of a sandstone in oil and gas exporation, the presence of porosity in the Muddy marine bar sandstones may only duplicate the response of a thinner sandstone.

Depth of Burial

The changes in seismic data that occur in vertical and lateral resolution with depth were discussed under the section titled 'Limitations of Seismic Modeling'. This is a limitation because it is very difficult to correct vertical ray-trace models for this effect found in real data. Therefore, the response signatures that were found for the Muddy using one- and two-dimensional models may only be valid for certain depths. The high resolution wavelet may be correct for very shallow depths of, for example, less than 3000 ft, while the low resolution wavelet may be correct for very deep reflections. It is not likely that both the high and low resolution wavelets used in this

study would exist in the same seismic section. However, the two wavelets do illustrate how frequency bandwidth affects vertical resolution.

As shown earlier, velocity of the Muddy changes drastically with depth. If velocities of the surrounding shale change with depth at a rate similar to that of the Muddy, acoustic impedance changes between the Muddy and the shale would not change with depth. Figures 36 and 37 show contoured values calculated from the ratio of Muddy velocity to the Shell Creek shale and Thermopolis shale velocity. Both maps indicate that velocity of the Muddy increases much more with depth than does surrounding shale velocity. It is also interesting to note that velocity contrast between Muddy and Thermopolis shale varies substantially more than that between the Muddy and the Shell Creek shale. The large degree of variation in these Muddy contacts most likely affects the amplitude of seismic reflections associated with the top and base of the Muddy. Results of one-dimensional modeling show that reflection amplitude is the primary seismic signature associated with sandstone thickness for the lower resolution wavelets. Presumably, there would be no possible way for one to distinguish between reflection amplitude changes caused



CONTOUR INTERVAL: .05

SCALE 10 Miles

Figure 36. Contour map of variation in the ratio of Muddy sandstone velocity to shell Creek Shale velocity.

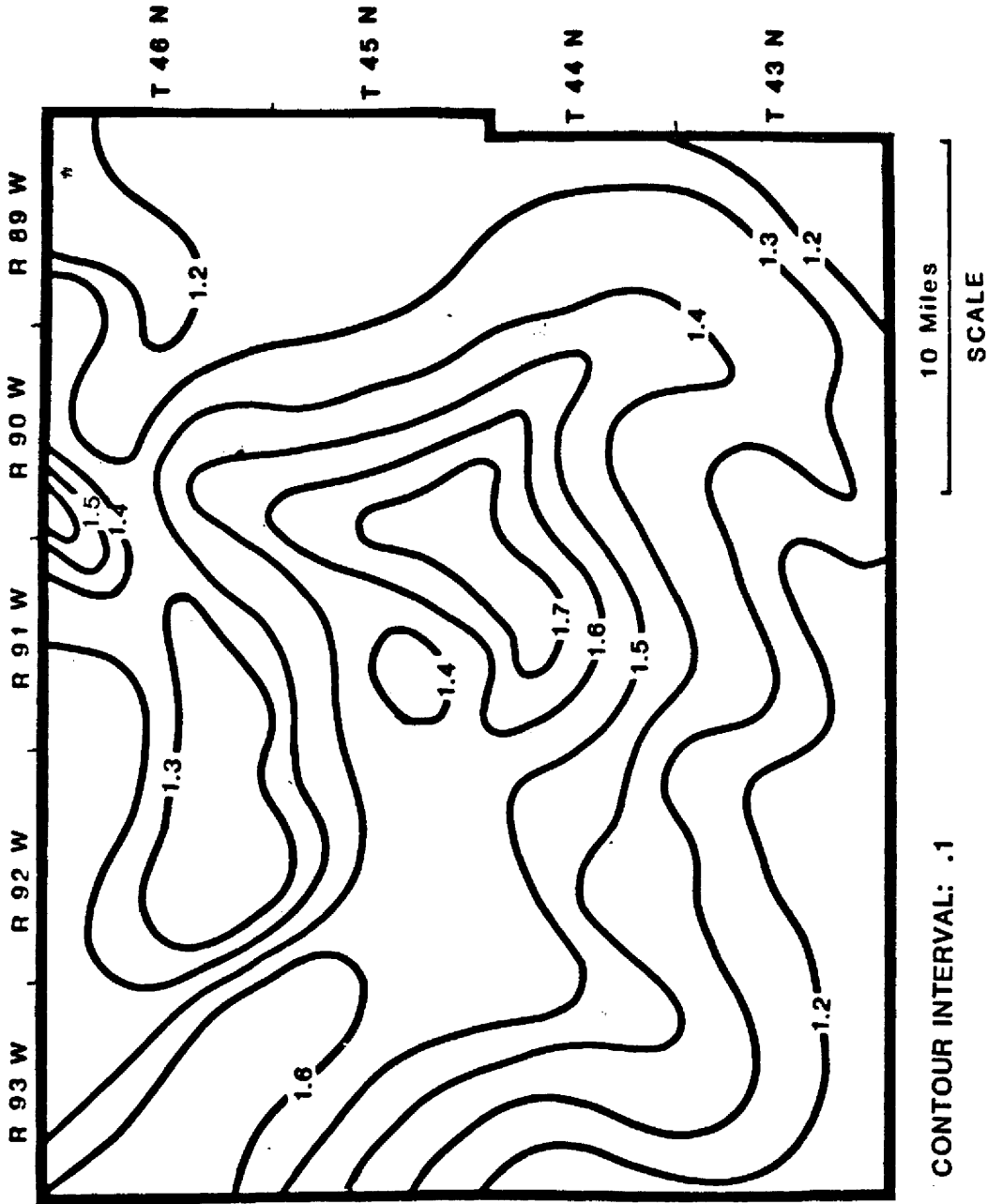


Figure 37. Contour map of variation in the ratio of Muddy sandstone velocity to Thermopolis shale velocity.

by variations in velocity contrast from changes in sandstone thickness. However, if major velocity trends and anomalies in Figures 36 and 37 are taken into account when looking at amplitude anomalies, there is less chance of confusing effects of velocity anomalies with those of changes in Muddy thickness.

Gas Effects

If one is trying to use a seismic signature to define sandstone thickness for purposes of hydrocarbon exploration, then it is very important to realize the effect that partial gas saturation will have on the signature. The Texaco #37 Unit located in section 31, T43N, R90W (Appendix, p. 126), is the only well in the study area that has a recognizable gas effect in the Muddy. While the gamma ray log indicates that the basal Muddy in this well is 103 ft thick, the sonic log shows sandstone-like velocities only for the upper 10 to 20 ft of this basal unit. The extremely low velocity of the gas filled portion of this sandstone leads to a large negative reflection coefficient at the base. The one-dimensional model from this well shows that there are no distinctive seismic signatures associated with this gas effect. In fact, the presence of gas in

this 100 ft sandstone gives a seismic response indicating a sandstone of only 20 to 30 ft thick. However, if one has enough well control and is familiar with the geology of the area, then one may realize that it is unlikely for the sandstone to be so thin at this location, thereby recognizing the possibility of a thicker gas saturated sandstone.

Rock Fractures

Rock fractures commonly occur in competent sandstone units in response to regional structural deformation. Such fractures possibly exist in the Muddy as a result of Laramide deformation in late Cretaceous time. Velocity measurements of fractured Muddy derived from a borehole sonic tool may not accurately portray the velocity of a seismic pulse propagating through the same fractured unit. Therefore, seismic model responses based on sonic log data may differ from the actual seismic response as a result of rock fractures.

SEISMIC DATA ANALYSIS AND INTERPRETATION

ACQUISITION AND PROCESSING PARAMETERS

The seismic response of the Muddy was also examined on three regional seismic lines that lie in the study area (Fig. 38). These data were shot and processed by Grant Geophysical using standard commercial acquisition and processing parameters. The 28 Hz geophones were positioned in-line at a group interval of 110 ft. The energy source consisted of 10-pound charges of dynamite buried 80 ft below ground surface. Shots were spaced at 220-ft intervals. A 48-trace recorder was used to attain the twelve-fold CDP coverage. The data was processed at a 2 ms sample interval. Processing sequence is shown in Figure 39.

WAVELET EXTRACTION

In order to display the Muddy seismic response over approximately 100 miles of data, the time interval of interest was windowed and displayed for every one-hundredth trace. In Figure 40 (also Plate III), the Muddy interval seismic response is shown. As stated earlier, one of the wavelets used in the one- and two-dimensional modeling was extracted from the seismic data. The wavelet extraction was performed using the C.G.G. modeling soft-

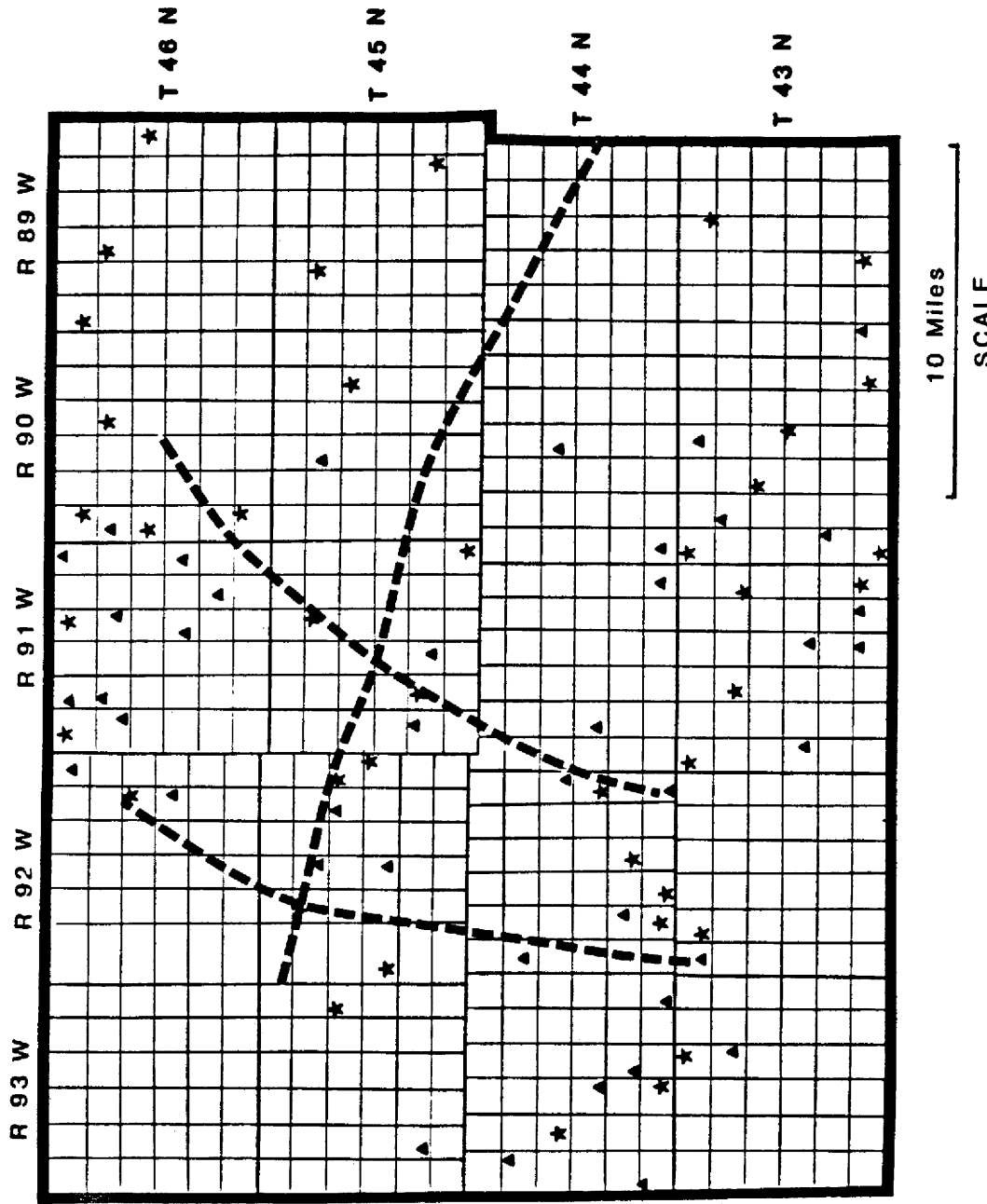


Figure 38. Location of the three Grant Geophysical seismic lines.

1. DEMULTIPLEX AND GAIN RECOVERY
2. INSTRUMENT PHASE COMPENSATION
3. SPIKING DECONVOLUTION
 - 100 ms OPERATOR
 - 5 PERCENT PREWHITENING
 - DESIGN WINDOW: 400-2500 ms
 - 900-2500 ms
4. BANDPASS FILTER
 - 9/12-80/90 Hz
5. SINGLE WINDOW SCALING
 - WINDOW: 800-2500 ms
6. TRACE EDIT
7. VELOCITY ANALYSIS/P.M.S.
8. STRUCTURE STATICS
9. NMO APPLICATION
10. FIRST-BREAK MUTE
11. SURFACE CONSISTENT RESIDUAL STATICS
12. CDP TRIM STATICS
13. CDP STACK
14. BANDPASS FILTER
 - 15/20-60/75 Hz
15. SINGLE WINDOW SCALE: 400-2300 ms
16. FILM DISPLAY: 7.5 in/sec 12 traces/in

Figure 39. Processing sequence used for the three seismic lines.

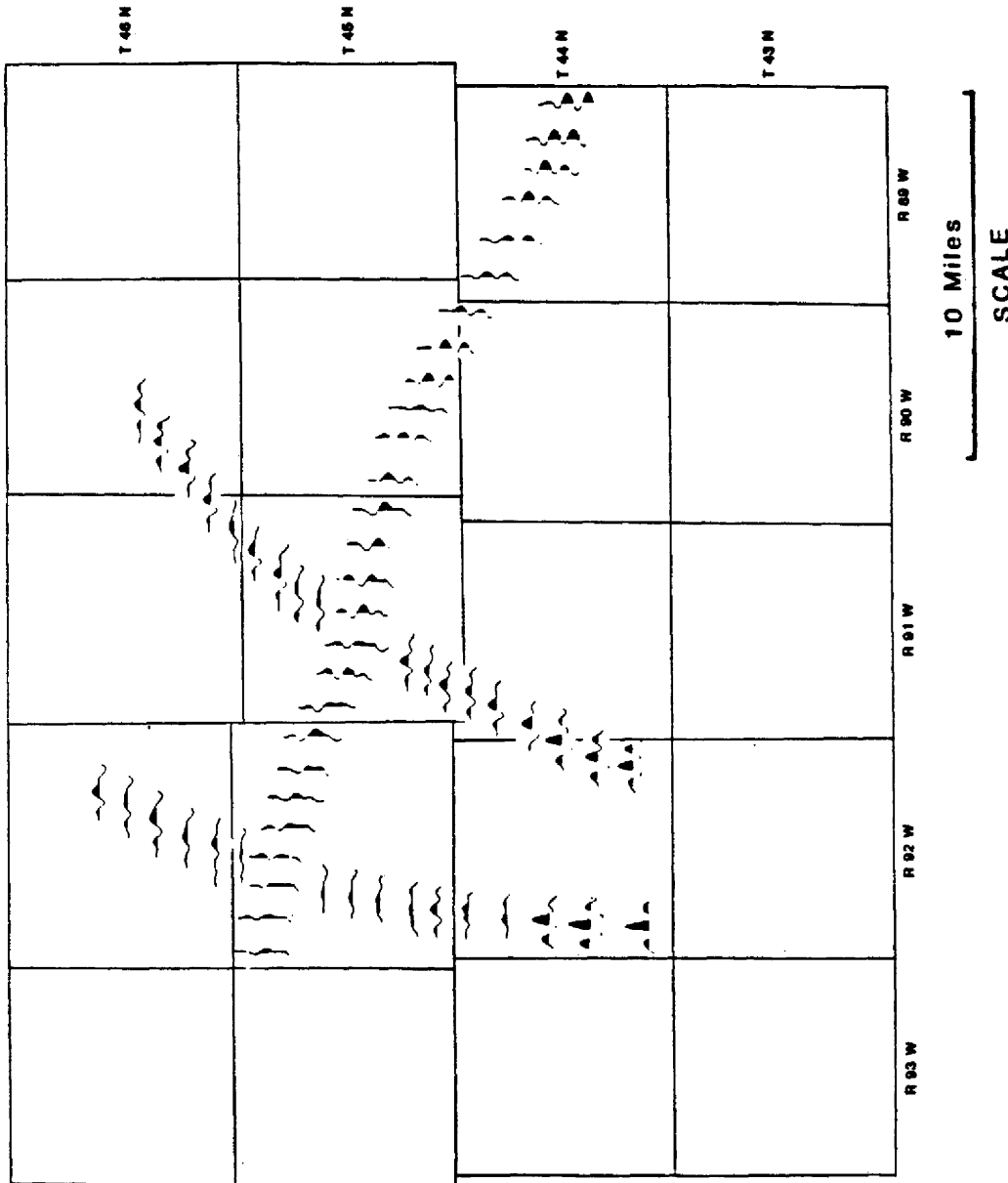


Figure 40. Grant Geophysical seismic data over the Muddy interval. Every one hundredth trace was plotted.

ware. This routine does an autocorrelative wavelet extraction by comparing multiple seismic traces with the reflection coefficients series derived from a sonic log of a nearby well. The Continental well, located in section 24, T44N, R92W (Appendix, p. 134), was used for the extraction on this data. The wavelet extraction process requires that sonic log information be supplemented by a check shot survey. The Continental well was used because it was the only one near a seismic line with an available check shot survey. The extracted wavelet was approximated by a rotated Ricker wavelet, primarily based on waveform and amplitude spectrum. Figure 41 shows the correlation between the actual seismic trace, a synthetic made with the extracted wavelet, and a synthetic made with the phase-rotated Ricker. Although the purpose of the modeling was to re-create the seismic response of wavelet processed data, the rotated Ricker wavelet was used in the one- and two-dimensional models as a representative of the conventionally processed data from the area.

MUDDY SEISMIC SIGNATURE RECOGNITION AND INTERPRETATION

While the conventional processing produces good quality data with high frequency content in the area, wavelet processing assures a consistent zero phase wavelet in the

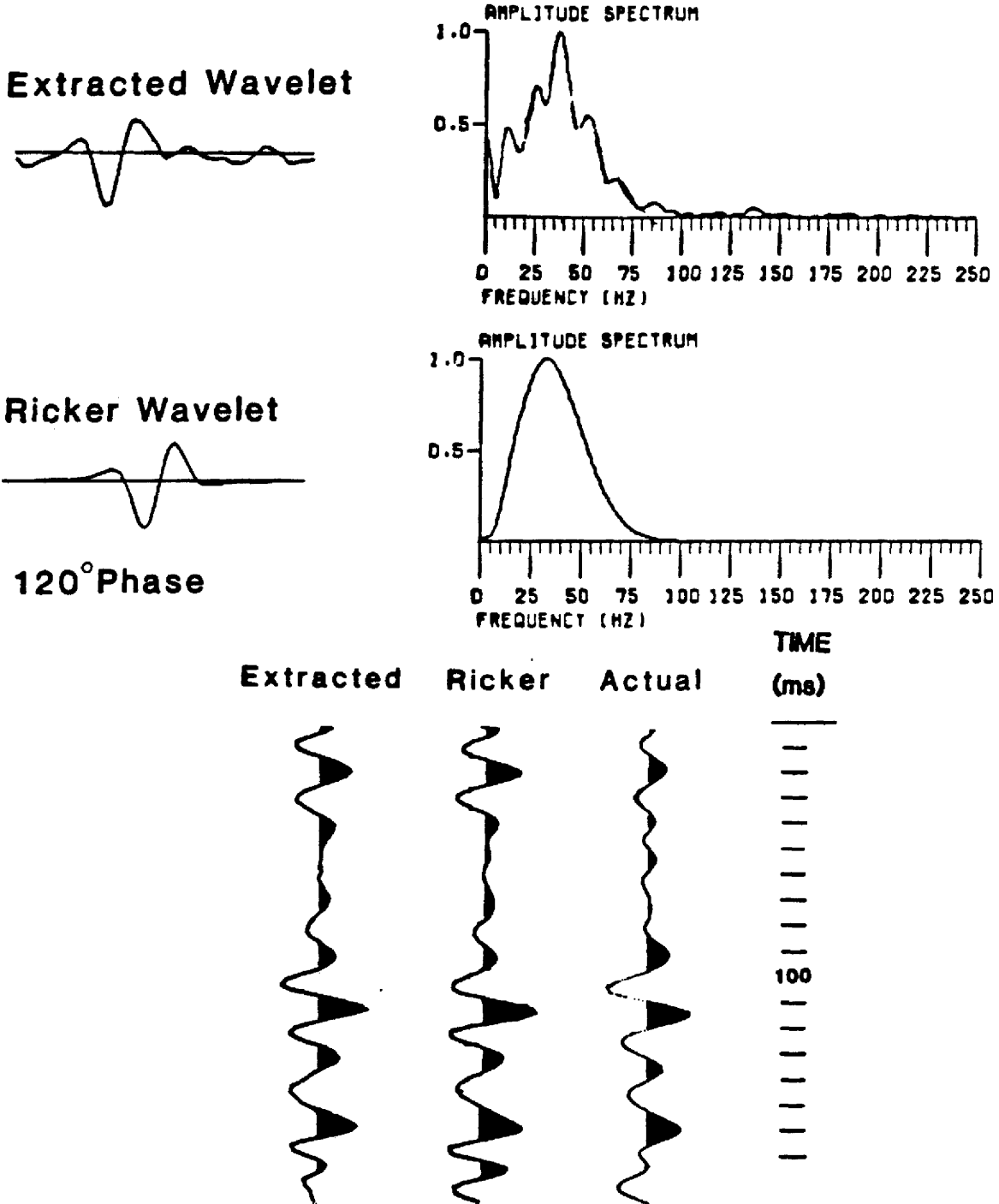


Figure 41. Comparison of models utilizing the extracted wavelet and a phase-rotated Ricker wavelet with actual seismic data trace.

data. Although wavelet processing is a difficult and costly process, stratigraphic interpretation of the resulting section is much more valid and accurate than for data with conventional deconvolution.

A comparison of the actual data with selected one-dimensional models is shown in Figures 42, 43 and 44. Each of these models is no more than 1.5 miles from the seismic data that are used for the comparison. There is a reasonably good correlation between the models and the actual data, especially for the Muddy interval, located about the midpoint of each trace. Seismic data near the six models that contain only a basal Muddy (Figures 42 and 43) exhibit good similarity in Muddy response amplitude and waveform. The 120 degree phase rotation associated with the extracted wavelet is roughly consistent throughout the data. However, there are moderate differences in frequency content between the models and data that appear to be due to depth of burial. One- and two-dimensional models using the extracted wavelet indicate that in the case of a single basal Muddy increasing thicknesses resulted in increasing seismic peak and trough amplitude. Due to the similarity between the models and actual data in Figures 42 and 43, a similar relationship between amplitude and basal sandstone thick-

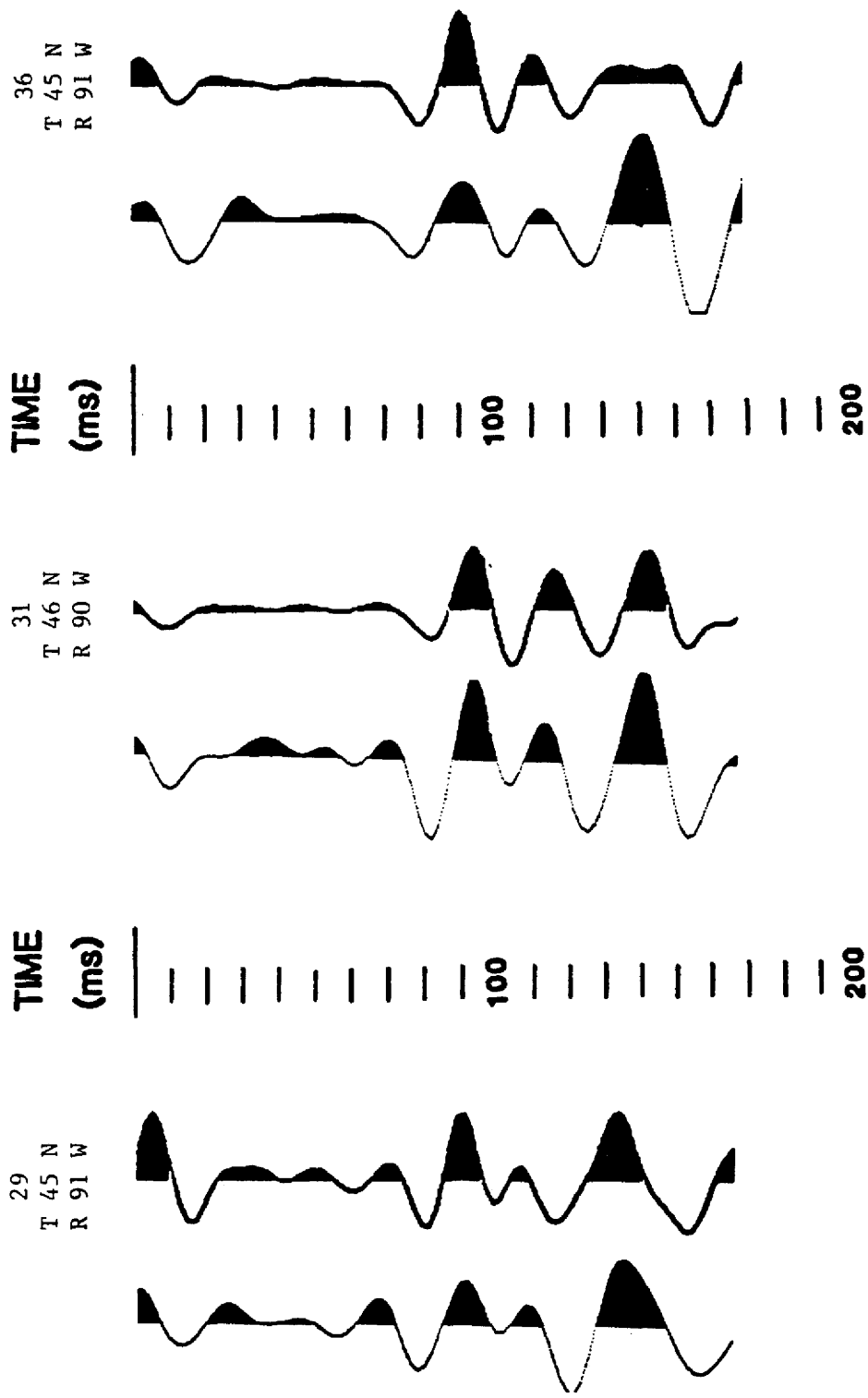


Figure 42. Comparison between actual data and three seismic models that each contain the basal Muddy sandstone, but not the upper sandstone. Location is listed over the model trace.

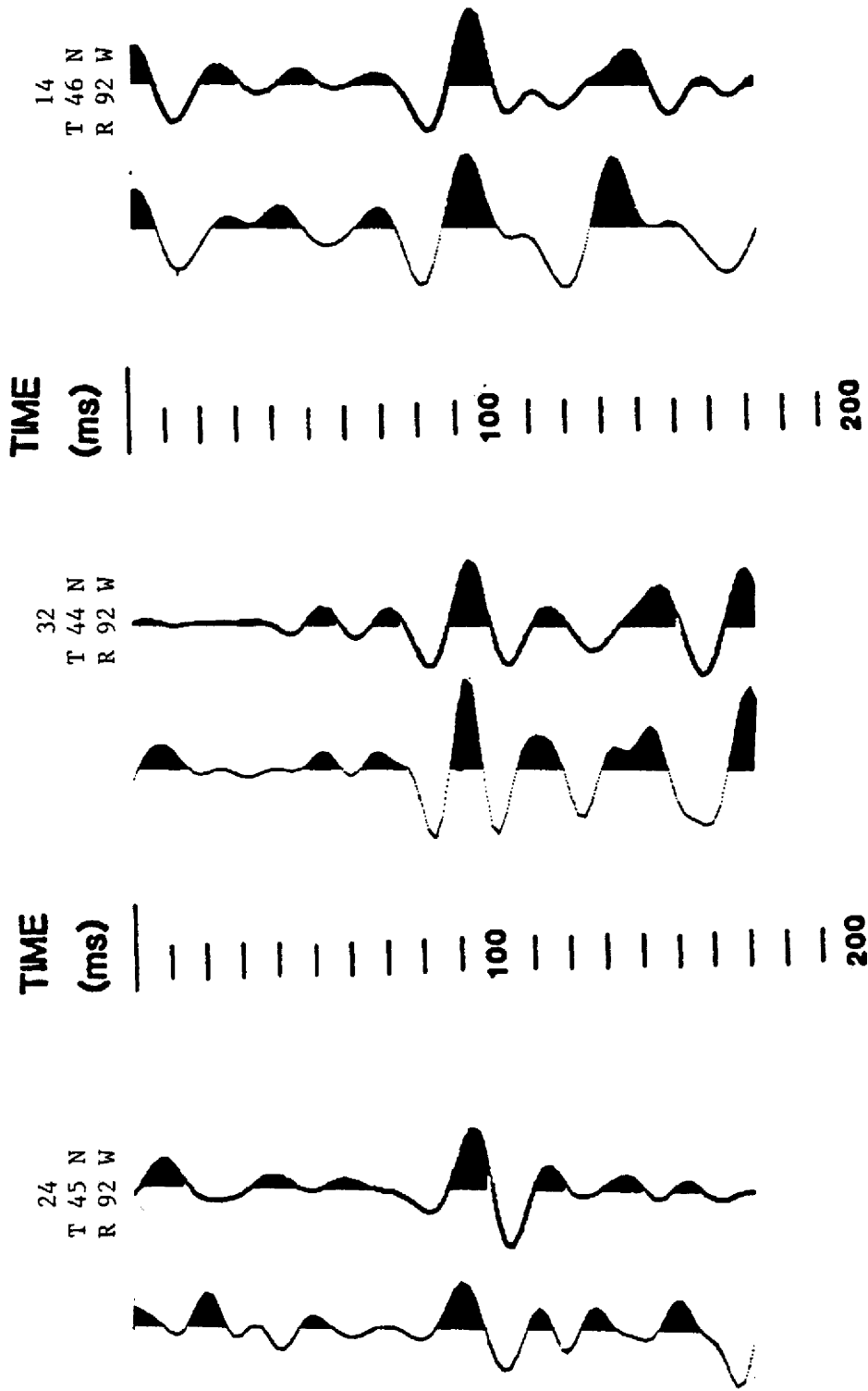


Figure 43. Comparison between actual data and three seismic models that each contain basal Muddy sandstone, but not the upper sandstone. Location is listed over the model trace.

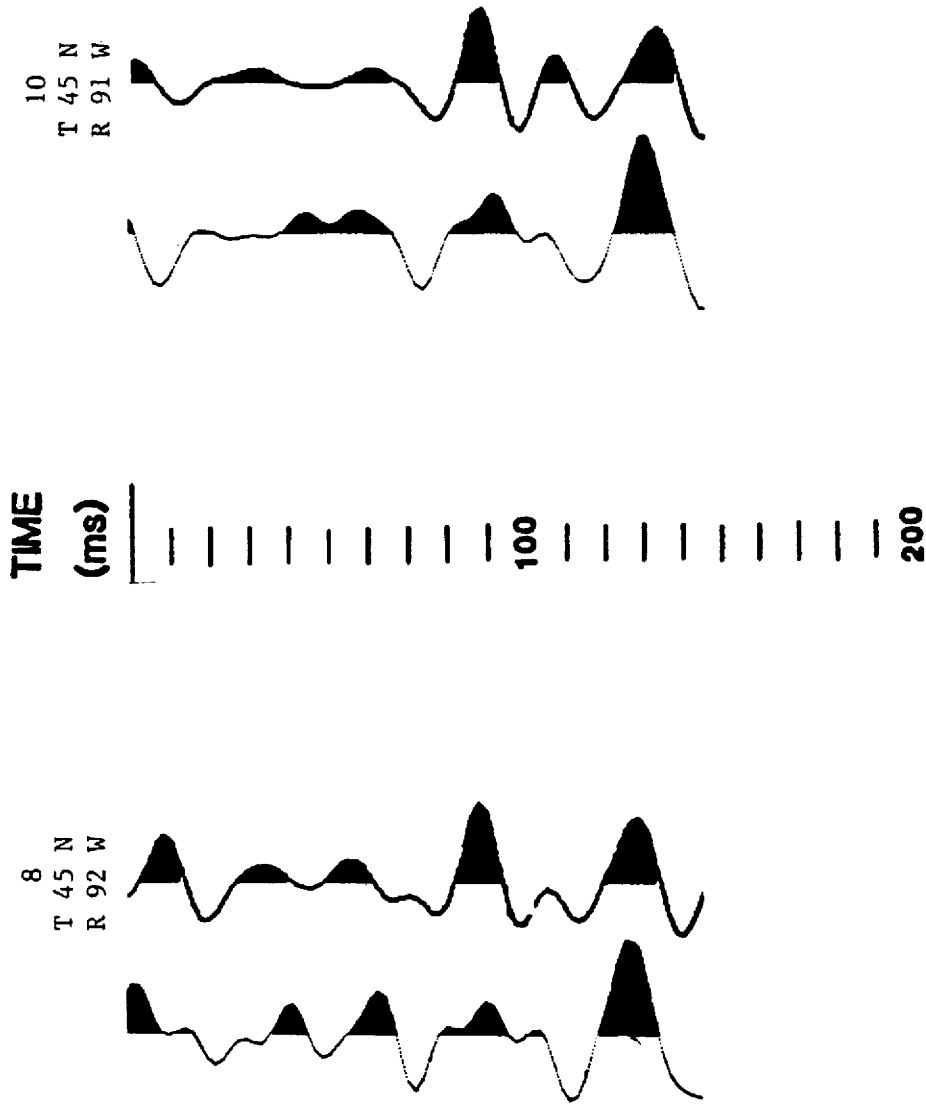


Figure 44. Comparison between actual data and two seismic models that each contain the basal and upper Muddy sandstones. Location is listed over the model trace.

ness is likely to exist for the actual data. This amplitude relationship is confirmed when the seismic data of Figure 40 (also in Plate III) is examined with respect to the basal sandstone isopach of Figure 17. By honoring both well data and seismic amplitude information, the basal sandstone isopach map of Figure 17 can be enhanced, revealing more stratigraphic detail (Figure 45).

Only two (of the eight) models in the study area that are located close to the actual data contain both basal and upper Muddy sandstones. Marine bar sandstones in two wells are recognizable by gamma ray responses in Plate I. These two models (Fig. 44) show very little evidence of the marine bar presence. However, actual seismic data near each of these models exhibits a distinctive seismic signature in the Muddy response apparently associated with the presence of upper Muddy sandstone. This seismic signature can best be described as an asymmetric low-amplitude, low-frequency peak. In Figure 40, this signature is present at several locations in the western portion of the study area. However, central and southern portions of T45N, R92W exhibit the most consistent and developed display of this low-amplitude signature. The upper sandstone isopach (Fig. 18) verifies that the thickest bar sandstones occur in the central and southwest portion of

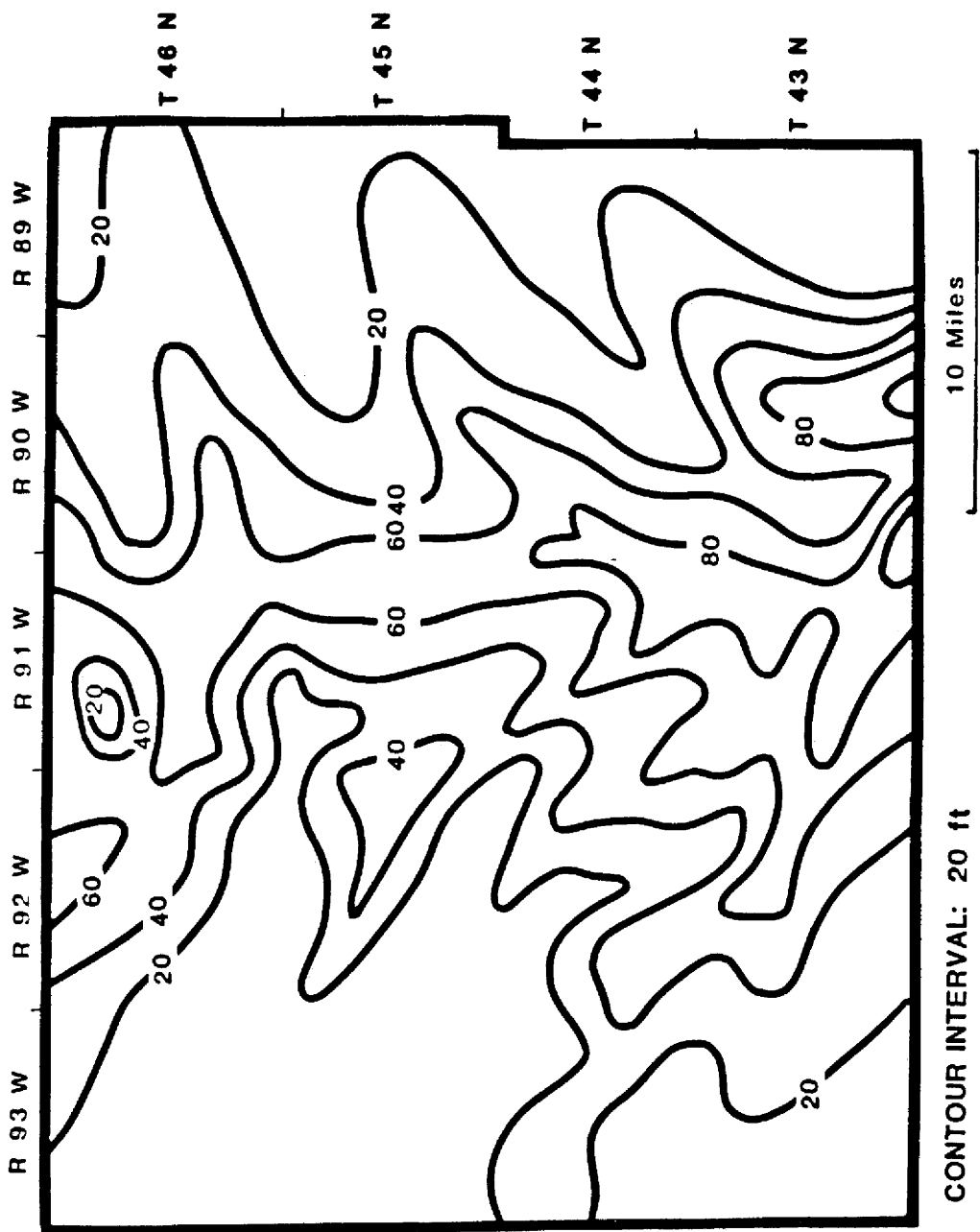


Figure 45. Isopach of basal muddy sandstone utilizing well control and seismic data.

T45N, R92W.

Close examination of the seismic data with respect to both basal and upper Muddy isopach maps reveals how the basal sandstone affects the low-amplitude bar signature. A thin basal sandstone overlain by a bar sandstone results in an extremely low-amplitude, low-frequency, positive response, as exhibited by the third trace from the west on the east-west line of Figure 40 (Plate III). A thicker basal sandstone overlain by the bar sandstone tends to slightly increase the amplitude of the Muddy response and gives way to a positive doublet as shown in traces 7 and 9 on the same line in the eastern portion of T45N, R92W and western portion of T45N, R91W. If the low-amplitude signature in the seismic data is used to locate Muddy bar sandstones, the upper sandstone isopach of Figure 18 can be modified to include more detail about the extent of these offshore bars (Fig. 46). The updated isopach shows that the large single linear body of upper Muddy sandstone on the west side of the study area in Figure 46 is actually several smaller linear sandstone bodies. Each of these sandstone trends may be composed of several smaller overlapping bars. Presence of the upper sandstone seismic signature in the actual data is difficult to speculate about because this signature is not

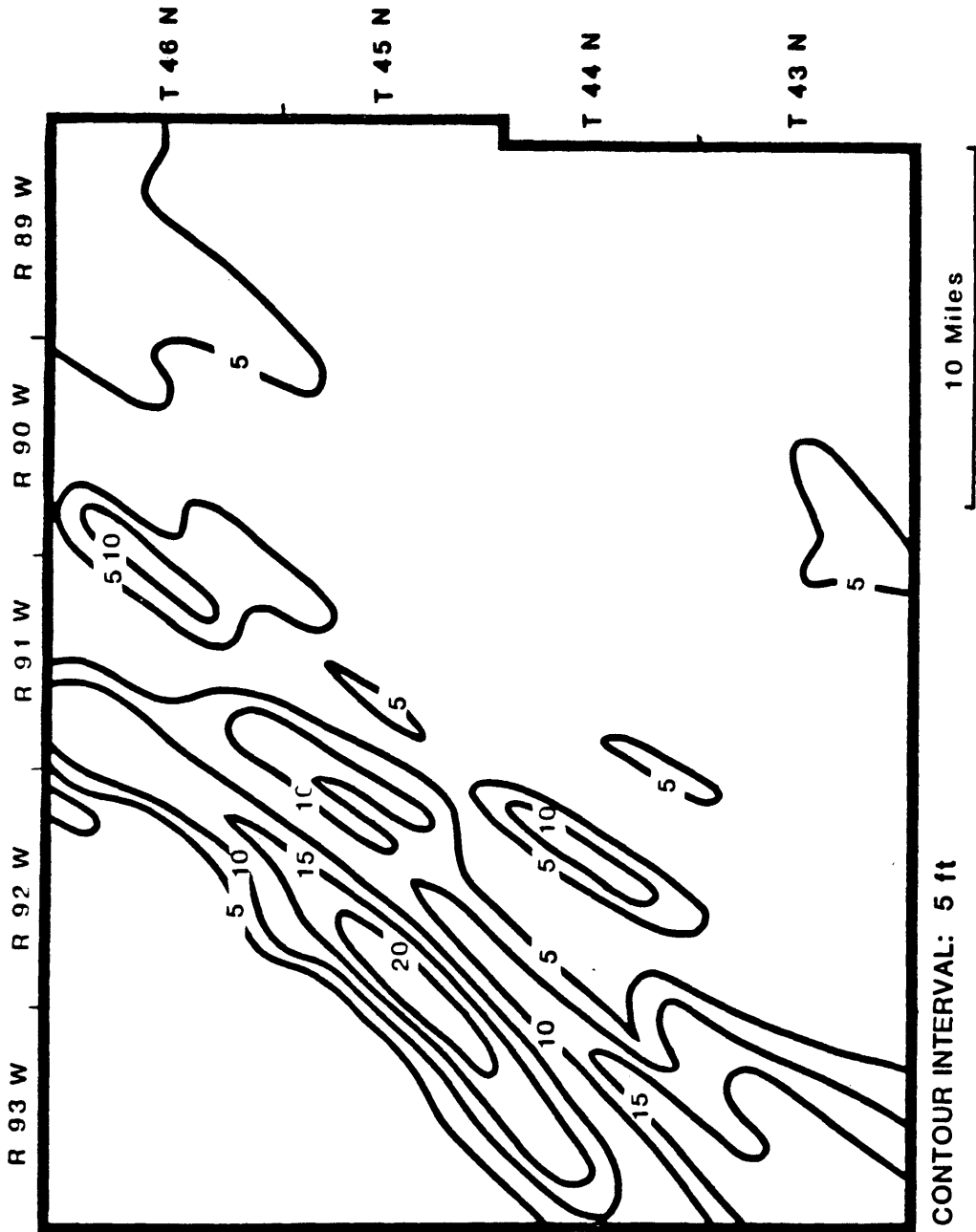


Figure 46. Isopach of upper Muddy sandstone utilizing well control and seismic data.

apparent in the models. However, as previously shown, a gradational boundary can produce a low-frequency, low-amplitude response. Three factors in the Muddy interval may result in a gradational boundary. First, the gamma ray response in Plate I shows that the upper sandstone usually has gradational upper and lower boundaries with the surrounding shale. Second, the upper sandstone is usually much thinner and lower in velocity than the basal sandstone. This may result in an 'impedance ramp' between the Shell Creek shale and the basal sandstone. Third, the presence of a regressive sandstone between the valley-fill sandstone the Thermopolis shale will cause a gradational base to the basal sandstone. While the third factor should only influence the seismic response of a regressive sandstone, the geologic model predicts that both regressive and marine bar sandstones are likely to occur together on Muddy paleotopographic highs.

Examples of the Muddy interval seismic response from actual data are shown in Figures 47, 48, and 49. These examples illustrate changes in seismic signature associated with presence of the offshore bar sandstone. Figure 50 shows the general location of each real data example. A schematic diagram of the three sandstones as interpreted from the well logs and seismic data is shown in

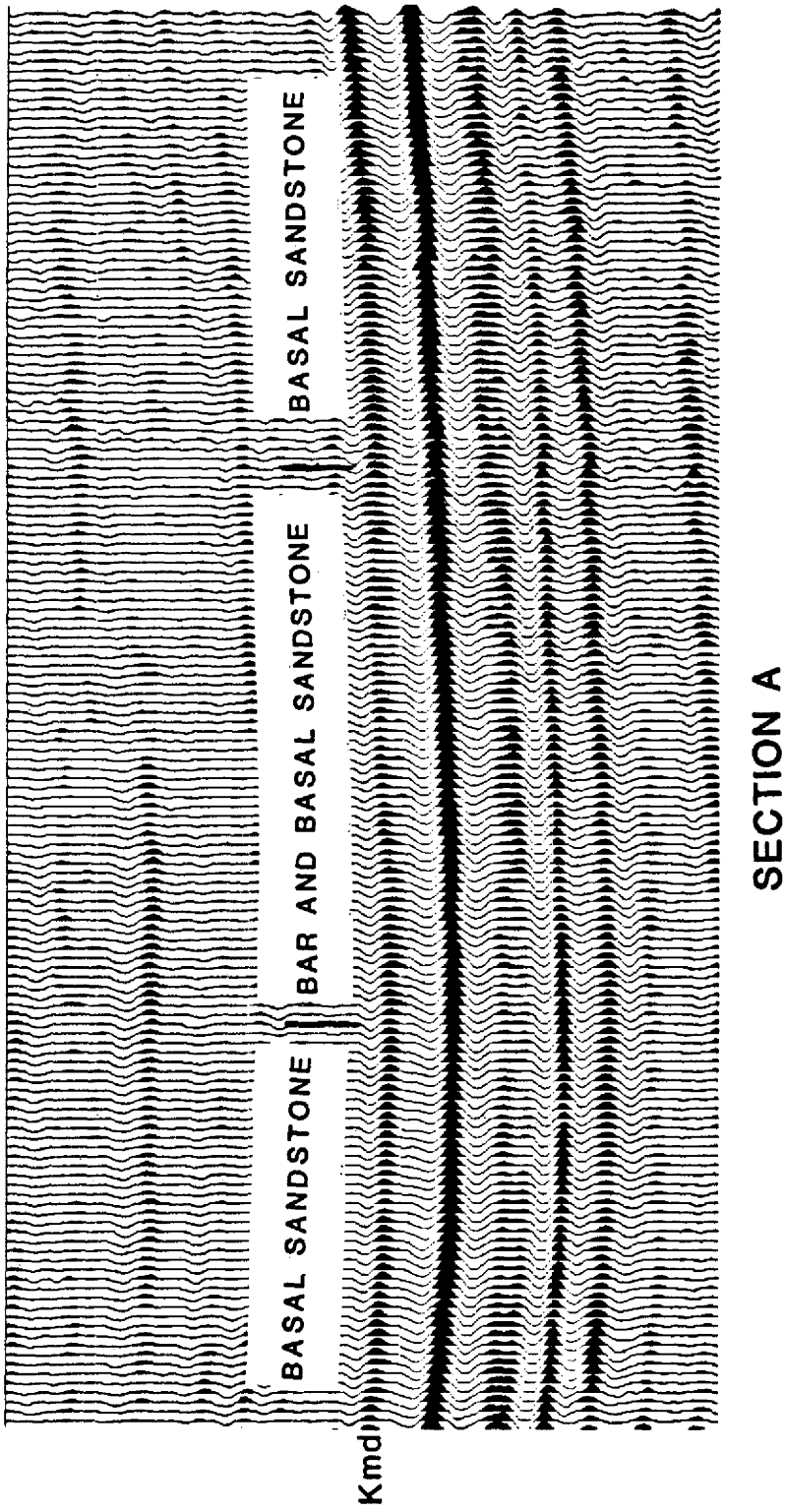


Figure 47. Change in Muddy seismic response due to presence of upper bar sandstone.

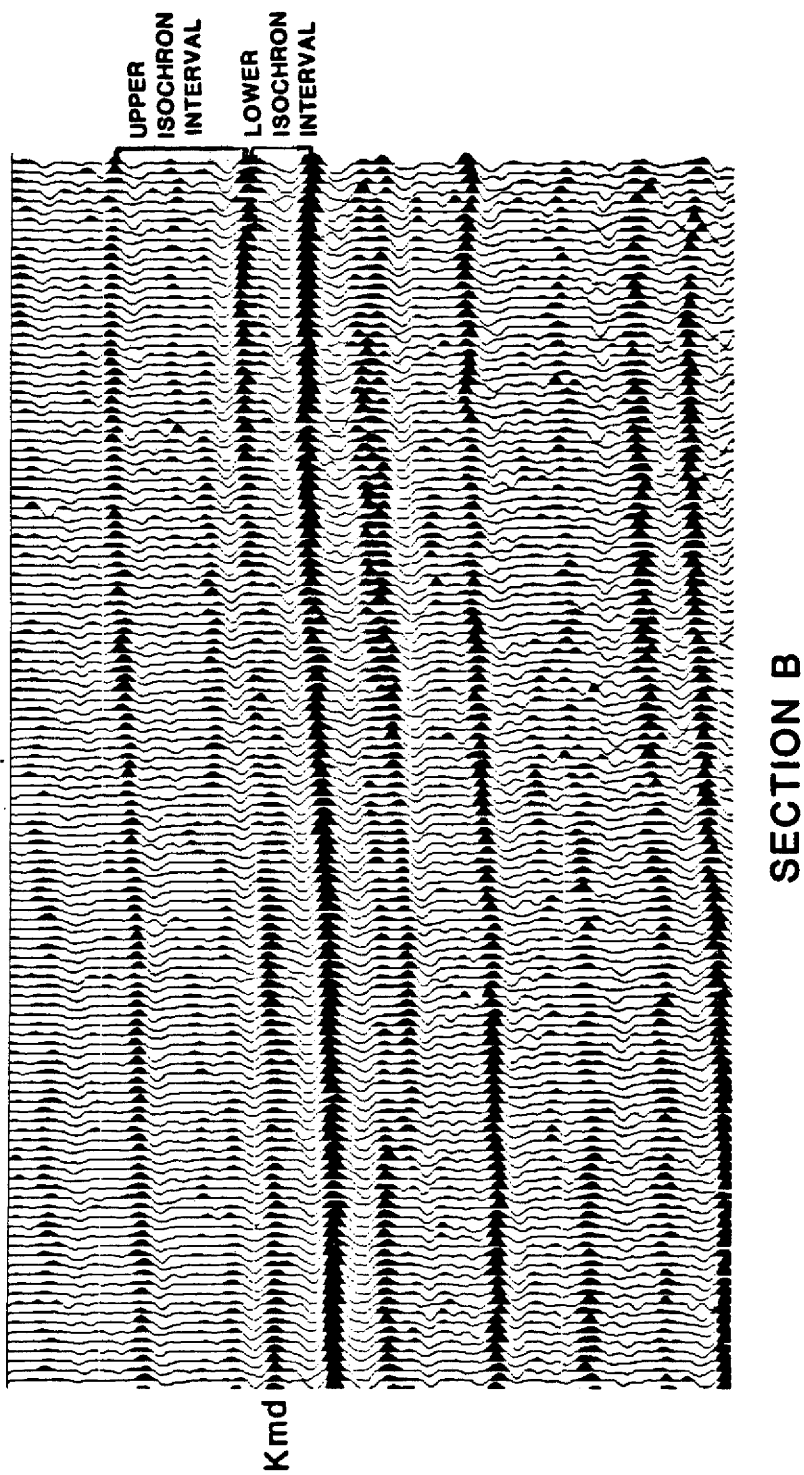


Figure 48. Seismic response due to alternating facies in the Muddy.

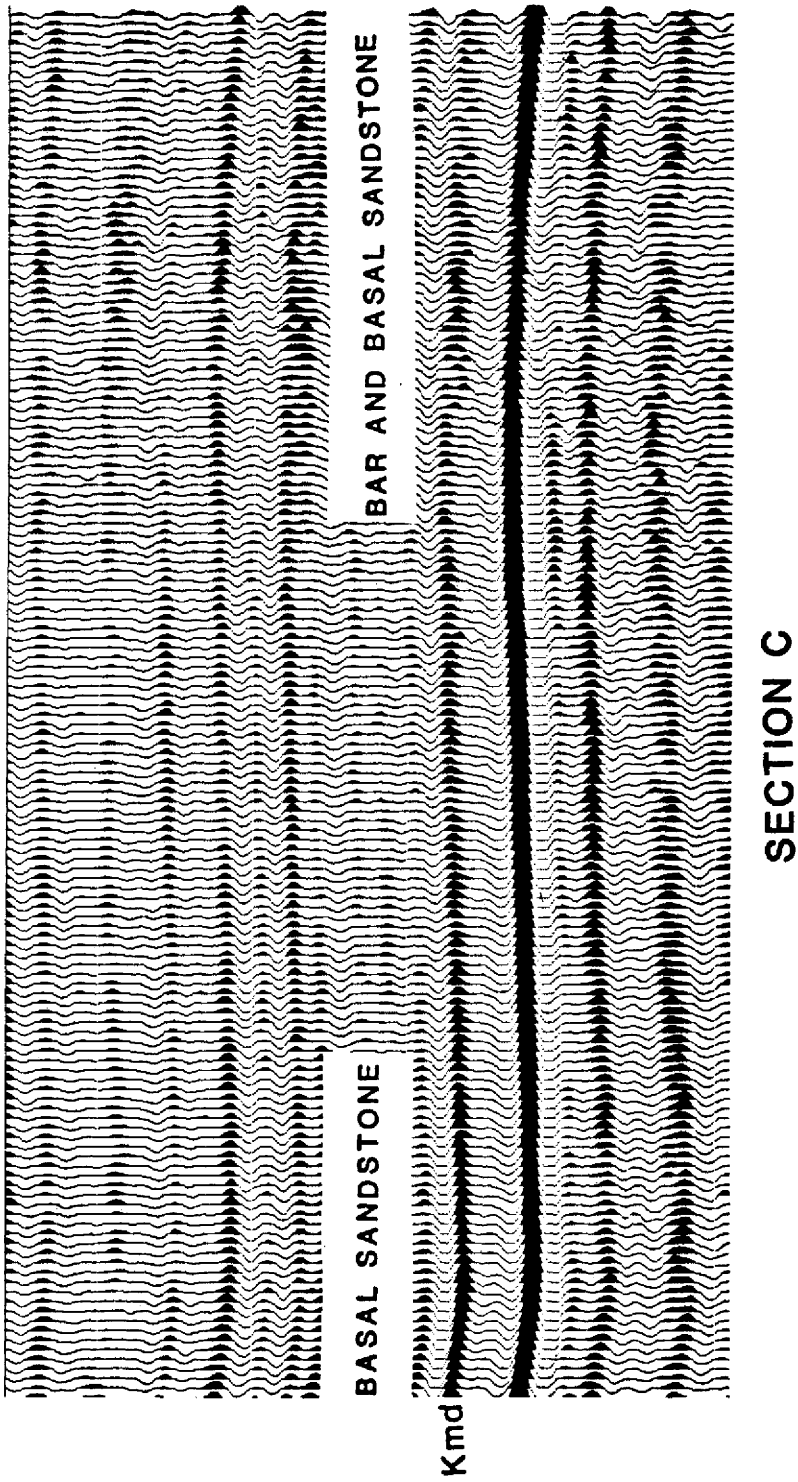


Figure 49. Change in Muddy seismic response due to a gradual change from basal sandstone only to a basal and upper bar sandstone.

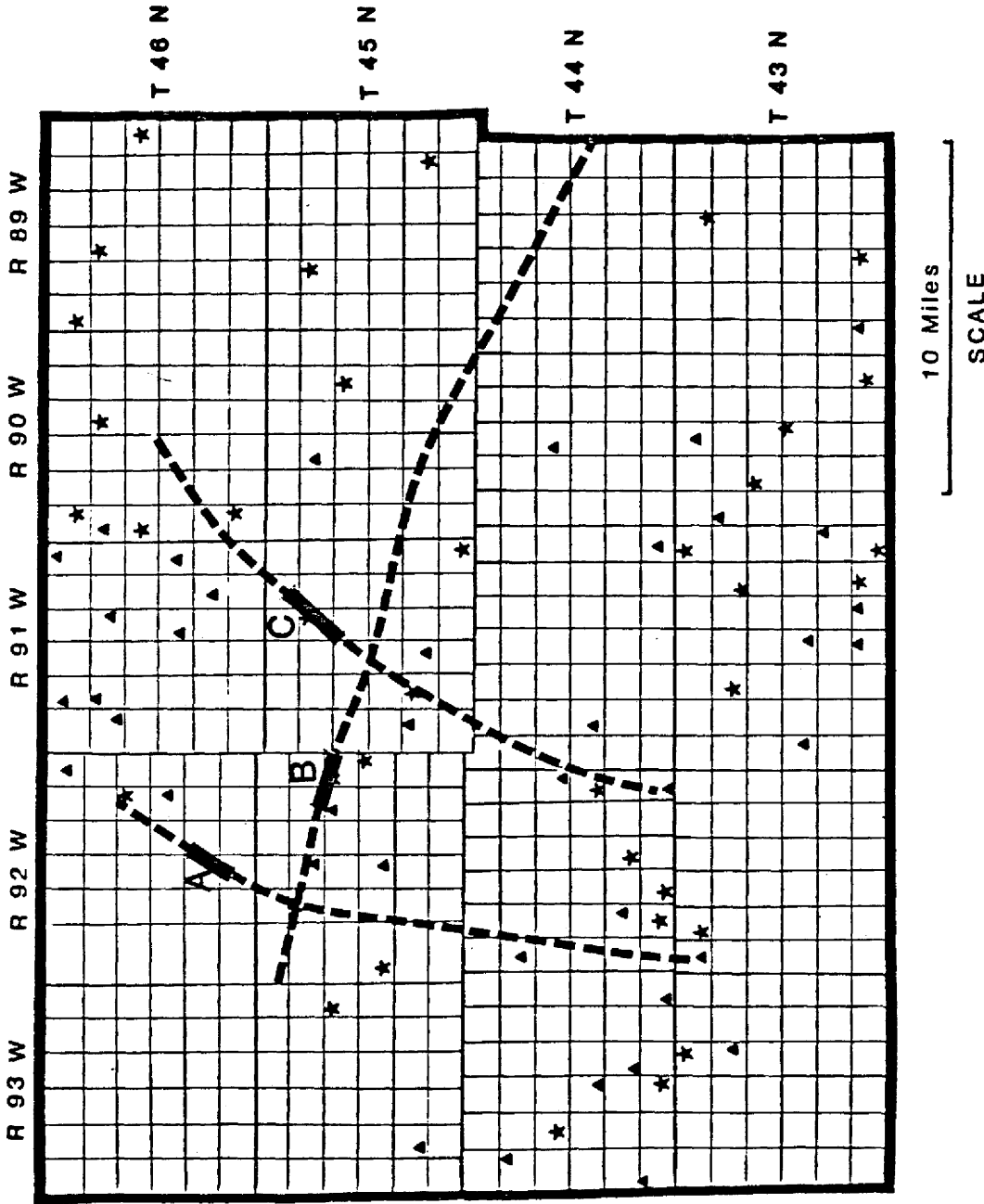


Figure 50. Map of study area showing general locations of the three example seismic sections from Grant Geophysical seismic data.

Figure 51. The seismic data is included in this diagram to show its relationship to the various sandstones. The basal sandstone occurs throughout the study area, therefore only trends of thick basal sandstone deposits are denoted by dashed lines. Thicker basal sandstone deposits result in an obvious increase of seismic amplitude for all but the northwest portion of the study area. In the northwest area, presence of upper bar sandstone changes the basal sandstone amplitude signature. Positions of the upper Muddy deposits are shown by the fine sandstone pattern in Figure 51. As noted previously, the low-amplitude, low-frequency seismic signature of the upper sandstone varies as a function of basal unit thickness. However, the upper sandstone signature is usually recognizable. Figure 51 also shows how ancient marine bars of the Muddy tend to be located between basal sandstone thicks, in areas that were topographically high during Muddy time.

The regressive deposits, denoted by the coarse sand pattern, were mapped using only gamma ray logs. These sandstones are also positioned at paleotopographic highs, between large incised valleys that were filled by valley-fill sediments.

The similarity of trends found in the Muddy Paleo-

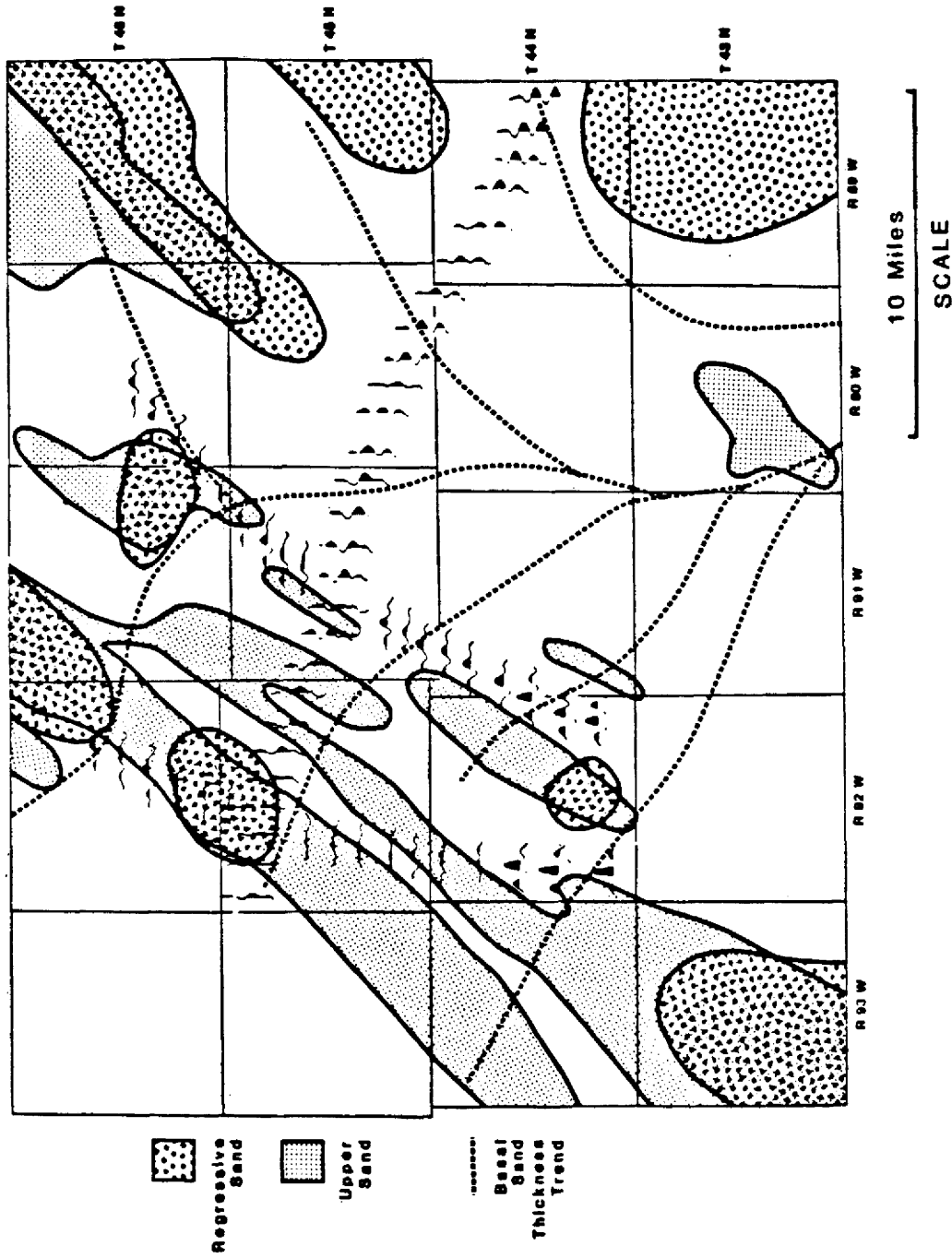
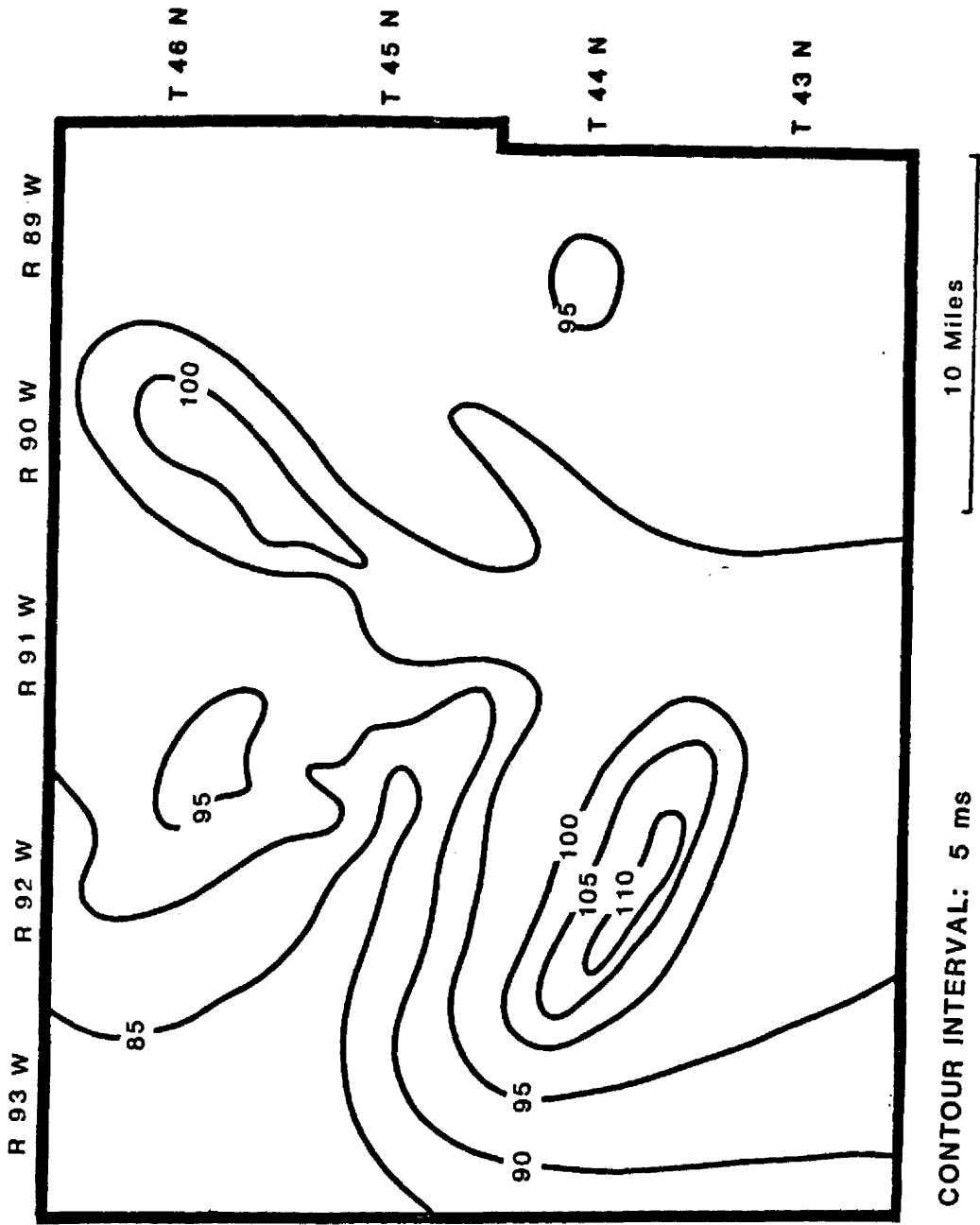


Figure 51. The extent of the three Muddy sandstone units interpreted from the seismic and well data.

topograph (Figs. 13 and 14), lower Cretaceous shale isopachs (Figs. 19 and 20), and basal Muddy sandstone isopach (Fig. 17) provides significant evidence of regional structural control over lower Cretaceous depositional patterns. Isochron maps of intervals above and below the Muddy were constructed from the three seismic lines of Figure 38. The time interval used for these maps is shown on Figure 48. The predominant northwest and northeast trends in the isochron maps (Figs. 52 and 53) give further evidence of a relationship between lower Cretaceous deposition and regional geologic structure.

Isochron data used in conjunction with various Muddy facies seismic signatures are important ingredients of an exploration model in southeast Big Horn basin. This model predicts that Muddy regressive deposits and off-shore bars tend to occur on paleostructural highs (isochron thins), while valley-fill deposits should thicken in paleostructural lows (isochron thicks). The small Muddy bar development in T43N, R90W (Fig. 51) serves as an example of how this exploration model can be applied. This small bar may continue in a northeast direction along the expected depositional trend, however, the feature cannot be mapped to the northeast due to lack of well and seismic control. Isochron maps (Figs. 52 and 53) indicate a Muddy



CONTOUR INTERVAL: 5 ms

10 Miles

SCALE

Figure 52. Isochron map of an interval above the Muddy. Map produced from Grant Geophysical seismic data.

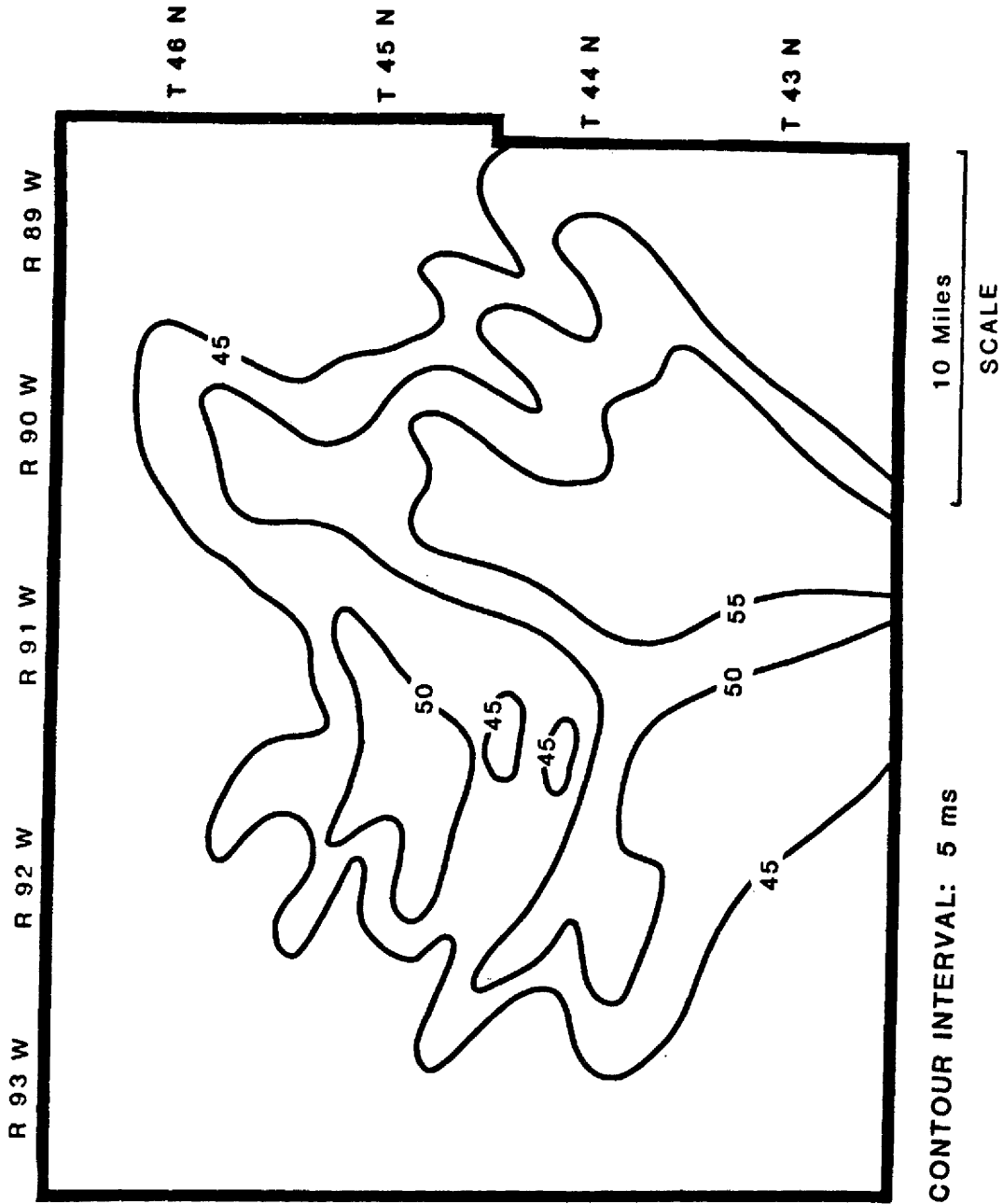


Figure 53. Isochron map of an interval below the Muddy. Map produced from Grant Geophysical seismic data.

paleostructural low situated northeast of the small bar deposit. Additional seismic data near the bar could provide the explorationist with isochron and Muddy seismic response information necessary for properly mapping the Muddy bar extent.

FUTURE WORK

Seismic models made with the extracted wavelet revealed a distinctive amplitude signature associated with basal sandstone thickness. This signature was later verified in the geologic model. On the other hand, the low-amplitude, low-frequency response associated with the marine bars was detected only when actual data was compared with the geologic model. Seismic models did not reveal this anomalous response. The gradational boundary associated with offshore bar deposits is believed to be responsible for the low-amplitude, low-frequency seismic response. Gradational boundaries are not accurately portrayed by most simple normal-incidence modeling methods. This may explain why the seismic models do not detect the marine bar sandstones. However, there are numerous other properties associated with marine bars or the valley-fill deposits that may have caused the characteristic seismic signature found in the conventionally processed data. Laramide strain features such as fractured sandstone units within the Muddy may be responsible for the anomalous seismic signature.

Future work on this topic might include using a more sophisticated modeling approach to analyze the marine bar seismic response. If other modeling techniques do not re-

veal the bar sandstone signature, then wavelet processing of the actual data may be considered. The wavelet-processed data should contain a more simple and consistent wavelet. This approach enables one to more accurately model the seismic data by using forward and inverse modeling techniques. The non-confidential data used in this study are kept on file at the Geophysics department of the Colorado School of Mines, Golden, Colorado.

SUMMARY AND CONCLUSIONS

Analysis of eighty wells in the study area reveals that the Muddy interval is comprised of three genetic sandstone facies; a regressive sandstone deposit, valley-fill deposits, and offshore bar sandstones. Valley-fill deposits are present over a large portion of the study area, however, they thicken in areas where depositional topography was low. Regressive deposits and offshore bar sandstones occur only in specific areas that tended to be topographically high during Muddy deposition. Where present, the regressive sandstone and the offshore bar sandstones usually result in a gradational base and top on the Muddy interval. Northwest and northeast lower Cretaceous depositional trends in the study area are possibly the result of regional structural control.

One- and two-dimensional ray-trace modeling of the Muddy interval indicates that actual basal sandstone thickness can be determined from vertical peak-to-trough measurements on the seismic response using a zero phase 10- to 90-Hz Butterworth wavelet. This wavelet can detect the presence of the upper bar sandstone, however, absolute thickness of the upper sandstone can not be determined.

In the models made using the zero phase 8 to 35 Hz

Butterworth wavelet, only crude relative approximations of the total Muddy interval thickness can be made. These thickness approximations are based primarily on relative amplitude of the seismic response, because vertical peak-to-trough measurements for this wavelet show little if any relationship to interval thickness.

Major increases in basal sandstone thickness tend to increase the amplitude of the Muddy response in conventionally processed data. Occurrence of bar sandstones in this data are denoted by a recognizable seismic signature which consists of a low-amplitude, low-frequency positive doublet. Gradational sandstone/shale boundaries associated with marine bars are the most likely cause of this anomalous response.

While the upper bar sandstone tends to have a higher porosity than the basal sandstone, both sandstones lose porosity with depth, presumably due to compaction. The only way to account for possible amplitude anomalies resulting from changes in porosity and other compaction features is to locate and map regional trends of the Muddy velocity field. While this method may work for large regional anomalies, local variations of sandstone porosity will not likely be accounted for and may be mistaken for changes in sandstone thickness.

Gas saturated sandstones within the Muddy interval have a seismic response equivalent to a shale. Recognition of a Muddy gas sandstone would only be possible in areas of extremely dense well control. Otherwise, the gas-saturated sandstone would be interpreted as a very thin sandstone.

An exploration model for southeast Big Horn basin is based on a relationship between regional structure and Muddy depositional facies. Isochron and isopach variations can be used to define Muddy paleostructural features. Oil and gas explorationists should expect a porous upper Muddy bar sandstone to be located over paleostructural highs and trending in a northeast direction. The thicker valley-fill deposits should occur over paleostructural lows and trend northwest and northeast.

REFERENCES CITED

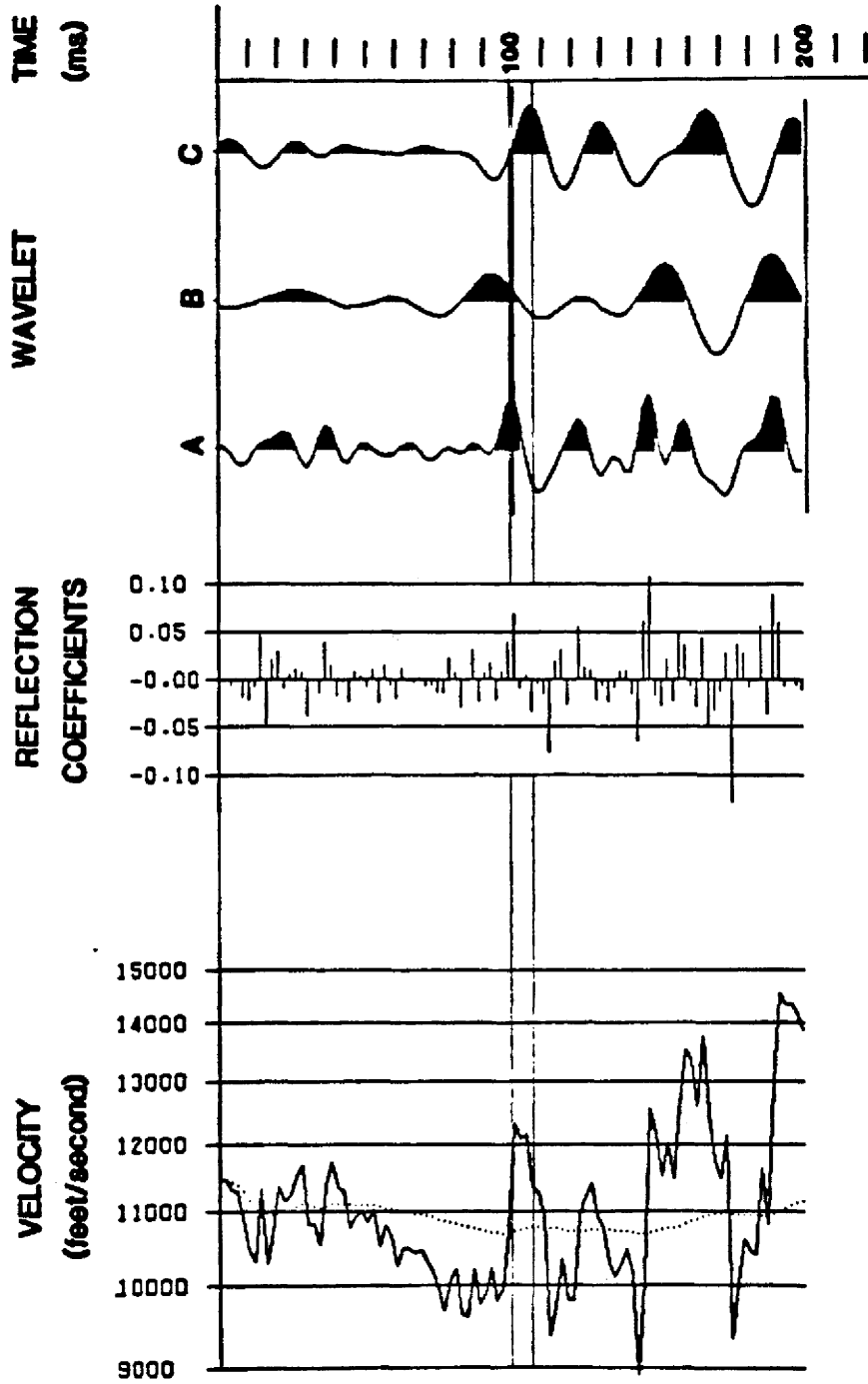
- Anstey, Nigel A., 1980, Seismic Exploration for Sandstone Reservoirs: Boston, International Human Resources Development Corporation, p. 26.
- Baker, D.R., 1962, The Newcastle Formation, Weston County, Wyoming: a Non-Marine (Alluvial Plain) Complex: WGA Guidebook, Seventeenth Annual Field Conference, pp. 148-162.
- Collier, A.J., 1922, The Osage Oil Field, Weston County, Wyoming: U.S. Geological Survey Bulletin 736-D.
- Curry, W.H. III, 1962, Depositional Environments in Central Wyoming during the Early Cretaceous: WGA Guidebook, Seventeenth Annual Field Conference, pp. 113-117.
- Dresser, Hugh W., 1974. Muddy Sandstone - Wind River Basin: WGA Earth Science Bulletin, March 1974, pp. 5-13.
- Eicher, Don L., 1962, Biostratigraphy of the Thermopolis, Muddy, and Shell Creek Formations: WGA Guidebook, Seventeenth Annual Field Conference, pp. 72-93.
- Gopinath, Tumkur R., 1977, Depositional environments of the Muddy Sandstone (lower Cretaceous), Wind River Basin, Wyoming: The Mountain Geologist, vol. 15, no. 1, (January 1978), pp. 27-47.
- Haun, John D. and Barlow, James A. Jr., 1962, Lower Cretaceous Stratigraphy of Wyoming: WGA Guidebook, Seventeenth Annual Field Conference, pp. 15-22.
- Hintze, F.F. Jr., 1915, The Basin and Greybull Oil and Gas Fields: Wyoming Geological Office, Bulletin 10.
- Larberg, G.M. Byrd, 1981, Depositional Environments and Sand Body Morphologies of the Muddy Sandstones at Kitty Field, Powder River Basin, Wyoming: WGA Guidebook No. 31, pp. 117-135.
- Moberly, Ralph Jr., 1962, Lower Cretaceous History of the Big Horn Basin, Wyoming: WGA Guidebook, Seventeenth Annual Field Conference, 1962, pp. 94-101.

- Neidell, Norman S. and Poggiagliolmi, Elio, 1977, Stratigraphic Modeling and Interpretation - Geophysical Principles and Techniques: AAPG Memoir, No. 26, p. 390.
- Paul, R.A., 1957, Depositional History of the Muddy Sandstone, Big Horn Basin, Wyoming (Doctor of Philosophy thesis): University of Wisconsin, 261 pages.
- Sheriff, Robert E., (1980), Seismic Stratigraphy: Boston, International Human Resources Development Corporation, p. 127.
- Vail, P.R., Mitchum, R.M., and Thompson, S. III, 1977, Global Cycles of Relative Changes of Sea Level: Payton, C.E. ed., Seismic Stratigraphy - Applications to Hydrocarbon Exploration: AAPG Memoir 26, pp. 83-98.
- Weimer, R.J. and Sonnenberg, S.A., 1982, Wattenberg Field, Paleostucture - Stratigraphic Trap, Denver Basin, Colorado: Oil and Gas Journal, pp.204-210.
- Weimer, R.J., Emme, J.J., Farmer, C.L., Anna, L.O., Davis, T.L., and Kidney, R.L., 1982, Tectonic Influences on Sedimentation, Early Cretaceous, East Flank Powder River Basin, Wyoming and South Dakota: Colorado School of Mines Quarterly, V. 77, No. 4, 61 pages.
- Whitford, S.D., 1959, A Regional Study of the (Upper Cretaceous) Muddy Sandstone in Wind River Basin, Wyoming: Unpublished M.S. Thesis, Northwestern University, Evanston, Illinois, 70 pages.
- Wilson, Charles W. Jr., 1936, Geology of Nye-Bowler Lineament, Stillwater and Carbon Counties, Montana: AAPG Bulletin, Vol. 20, No. 9, pp. 1161-1188.
- Wulf, George R., 1962, Lower Cretaceous Albian Rocks in Northern Great Plains: AAPG Bulletin, Vol. 46, No. 8, p.1412.

APPENDIX OF
ONE-DIMENSIONAL SEISMIC MODELS

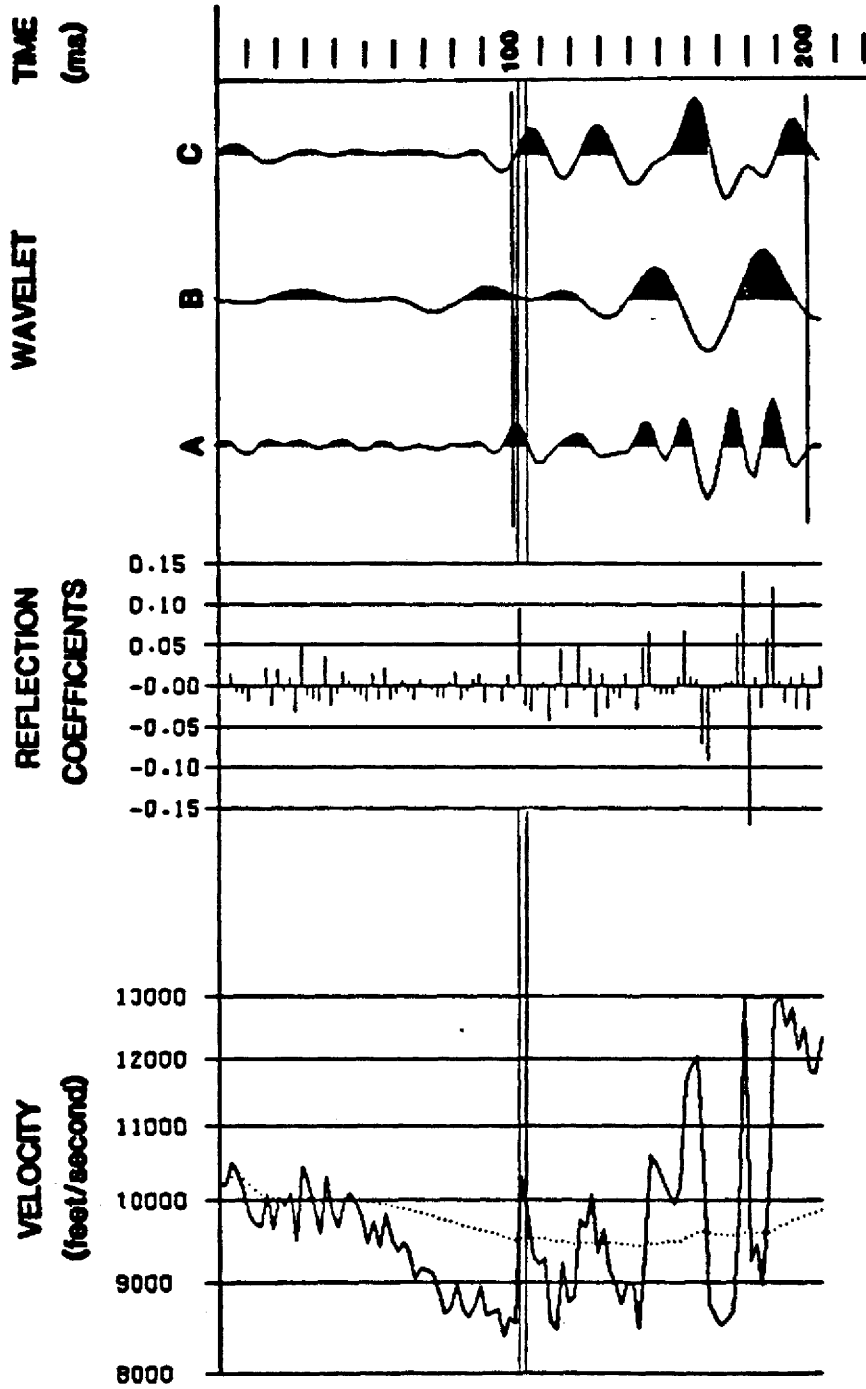
3 T43N R89W

BENEDUM #1 GOVT.



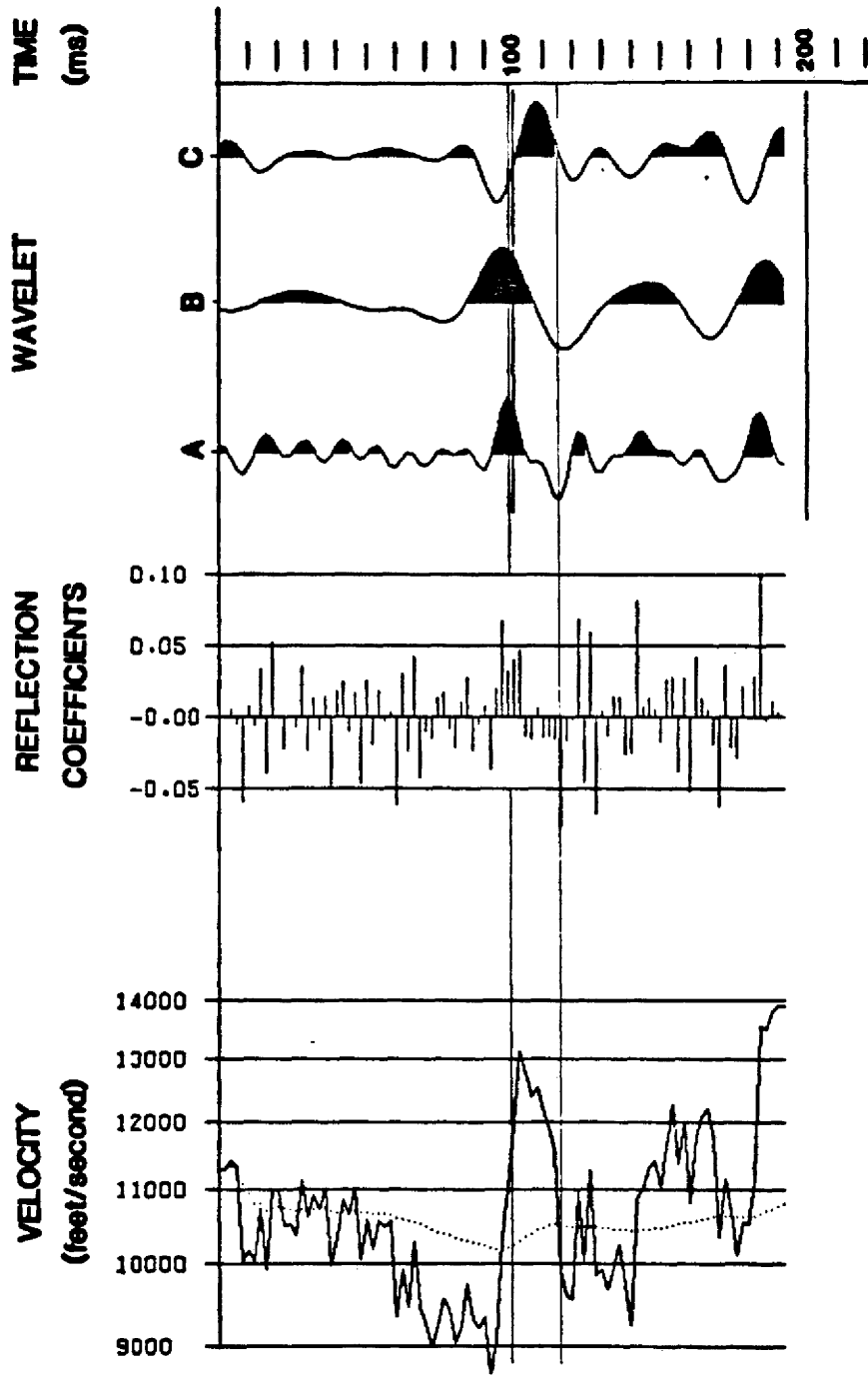
33 T43N R89W

DELTA D-1 FEDERAL



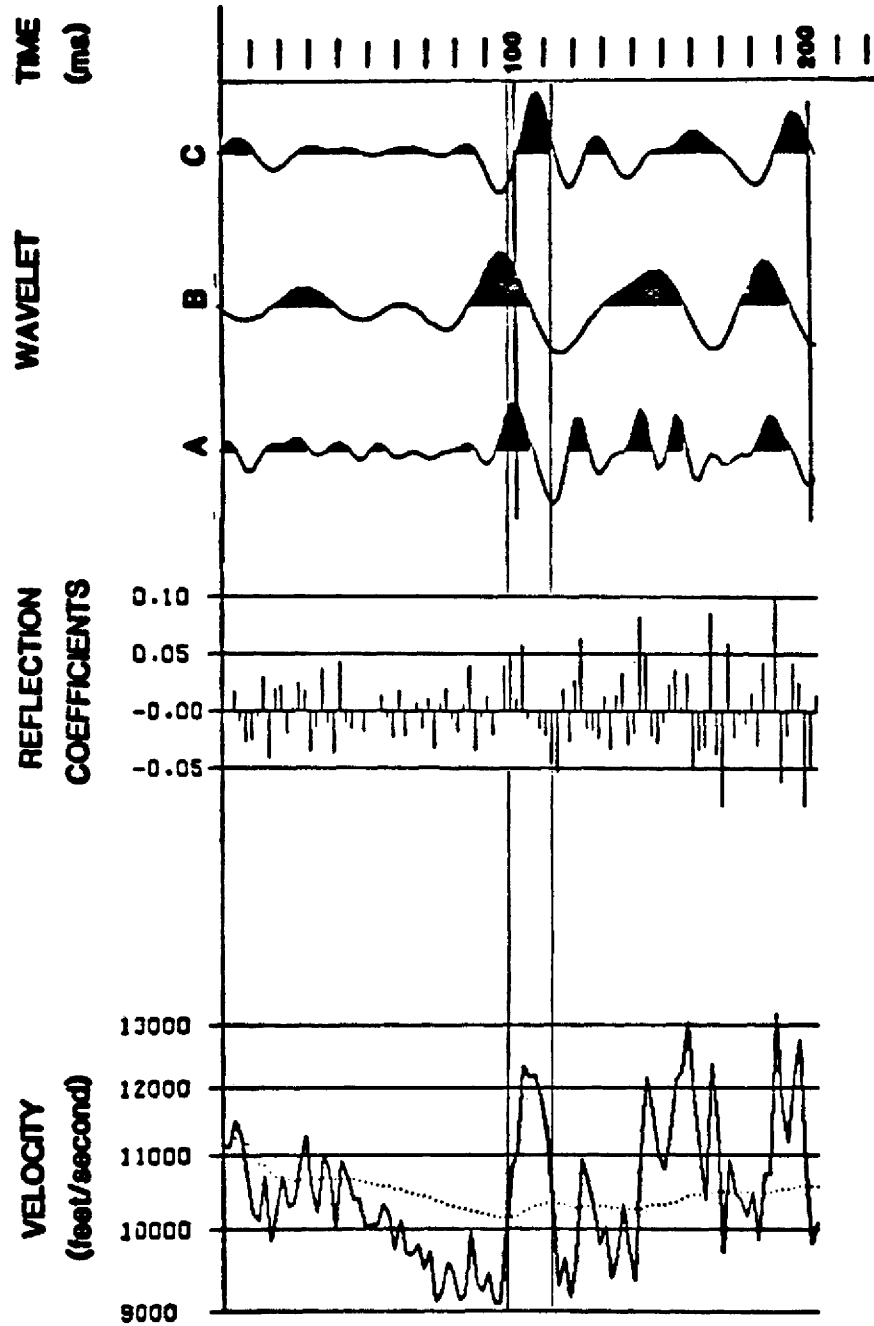
6 T43N R90W

PROFESSIONAL PETROL. #1 GOVT.



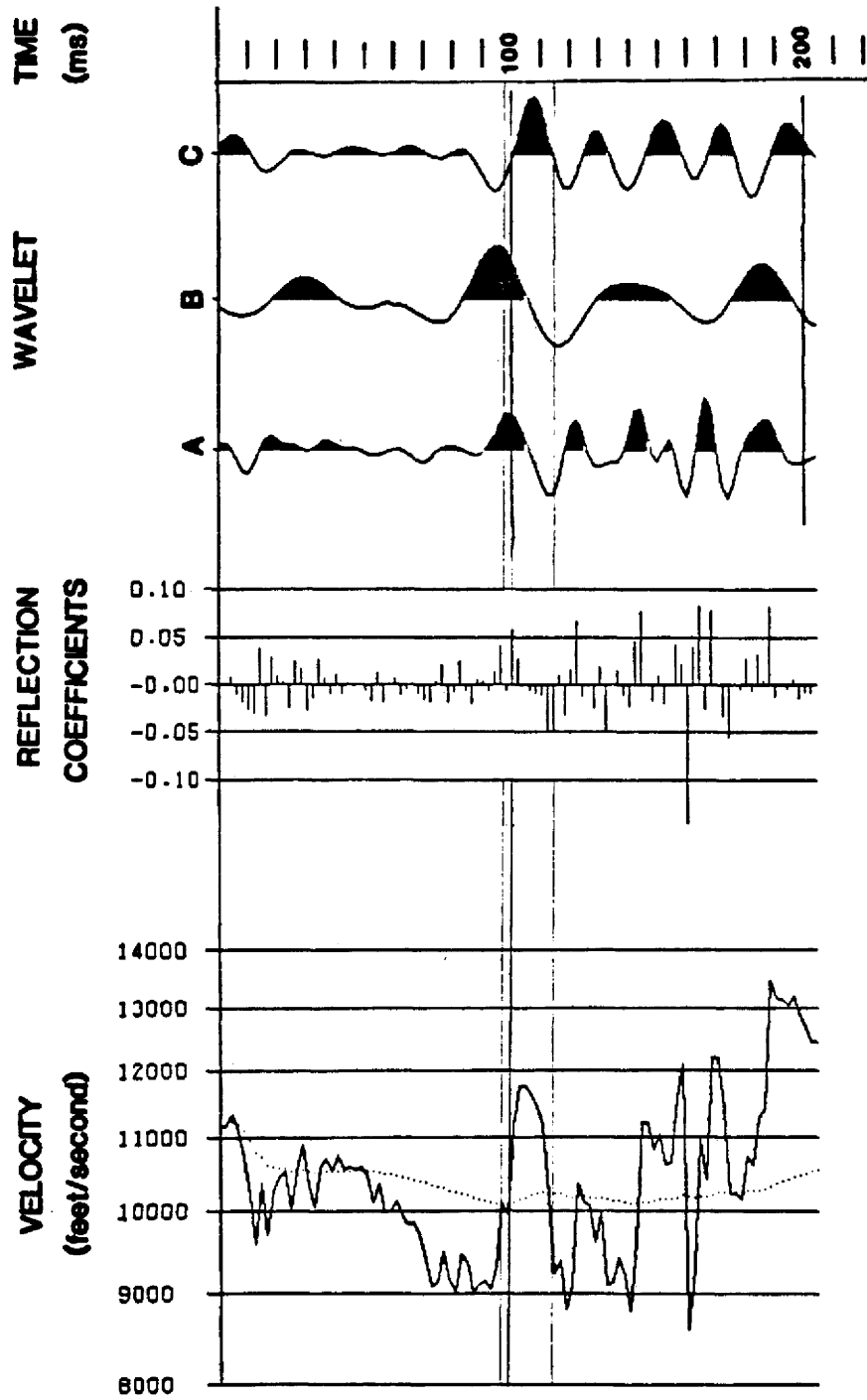
16 T43N R90W

ARROWHEAD #11-16 STATE



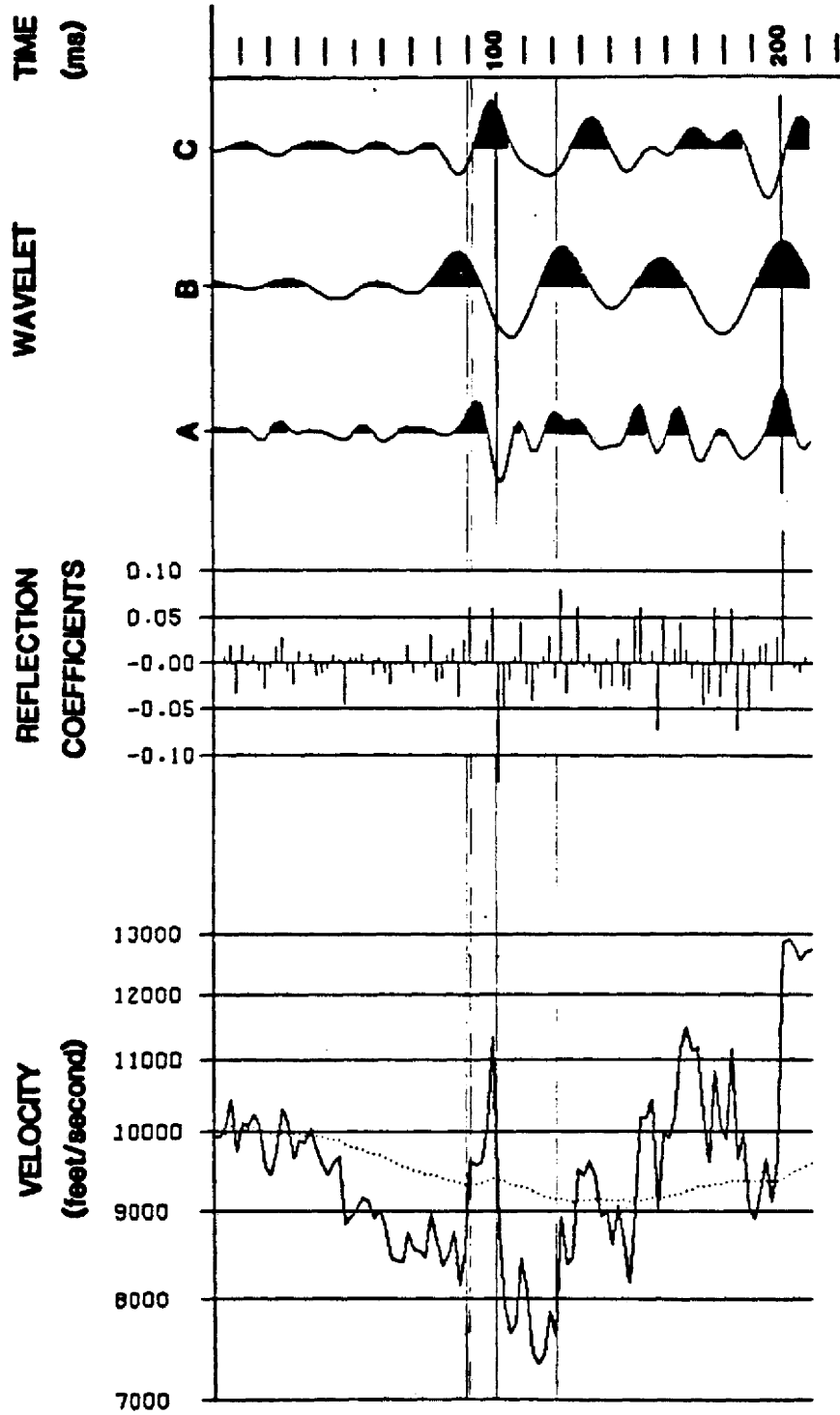
22 T43N R90W

AMERADA PET. #1 USA-HALES



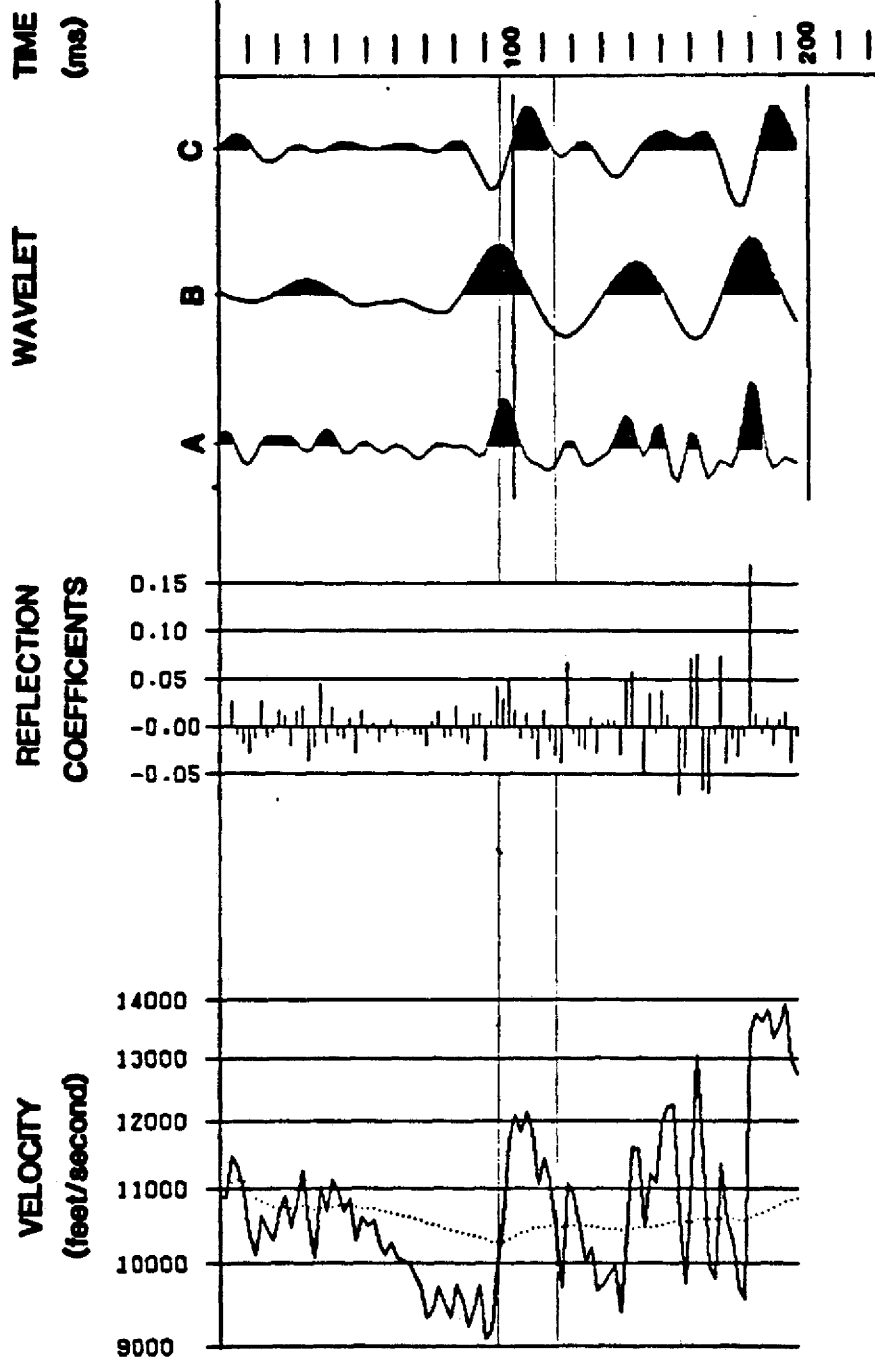
31 T43N R90W

TEXACO #37 UNIT



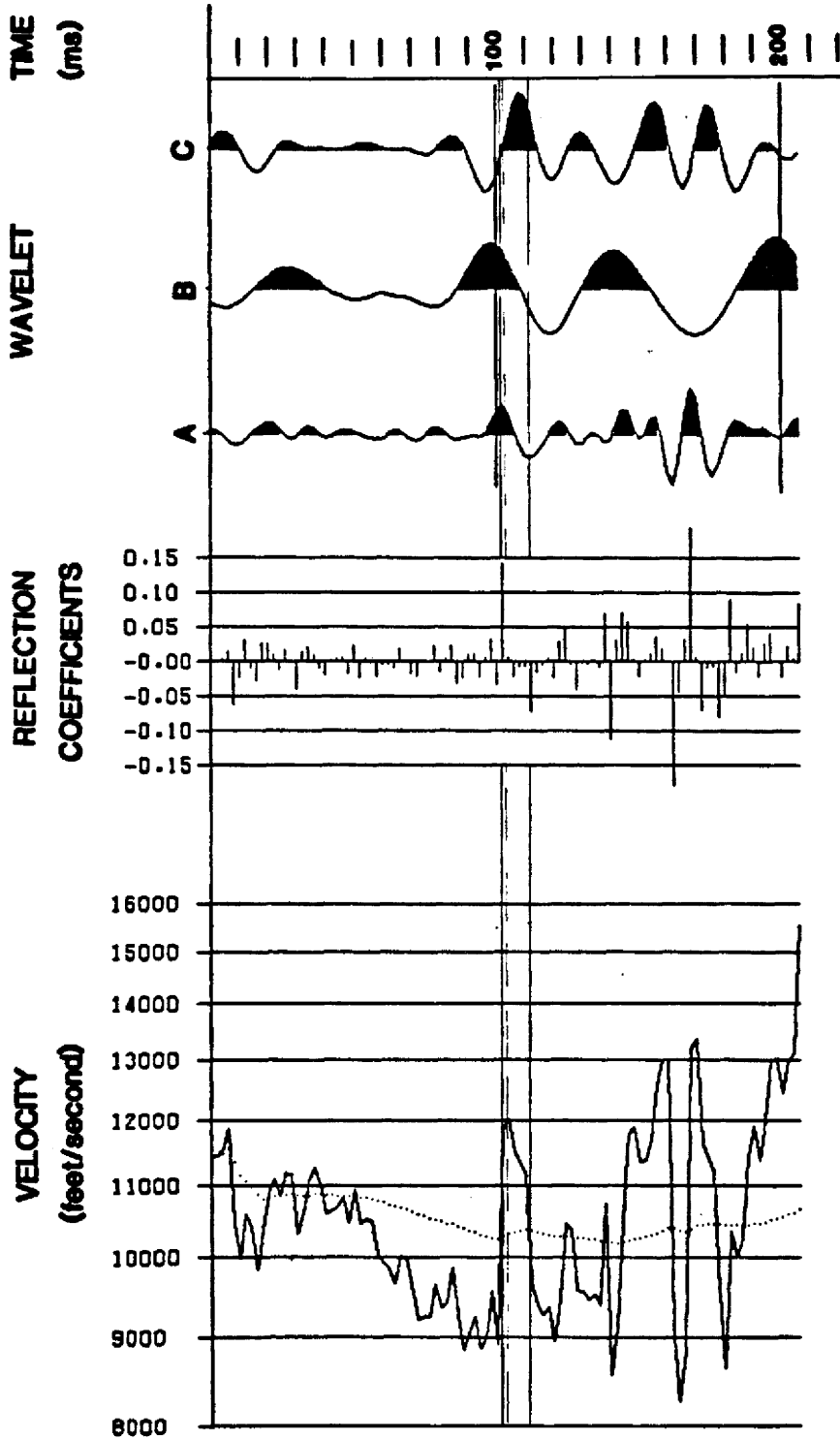
36 T43N R90W

MURPHY OIL #1 STATE SCHOOL



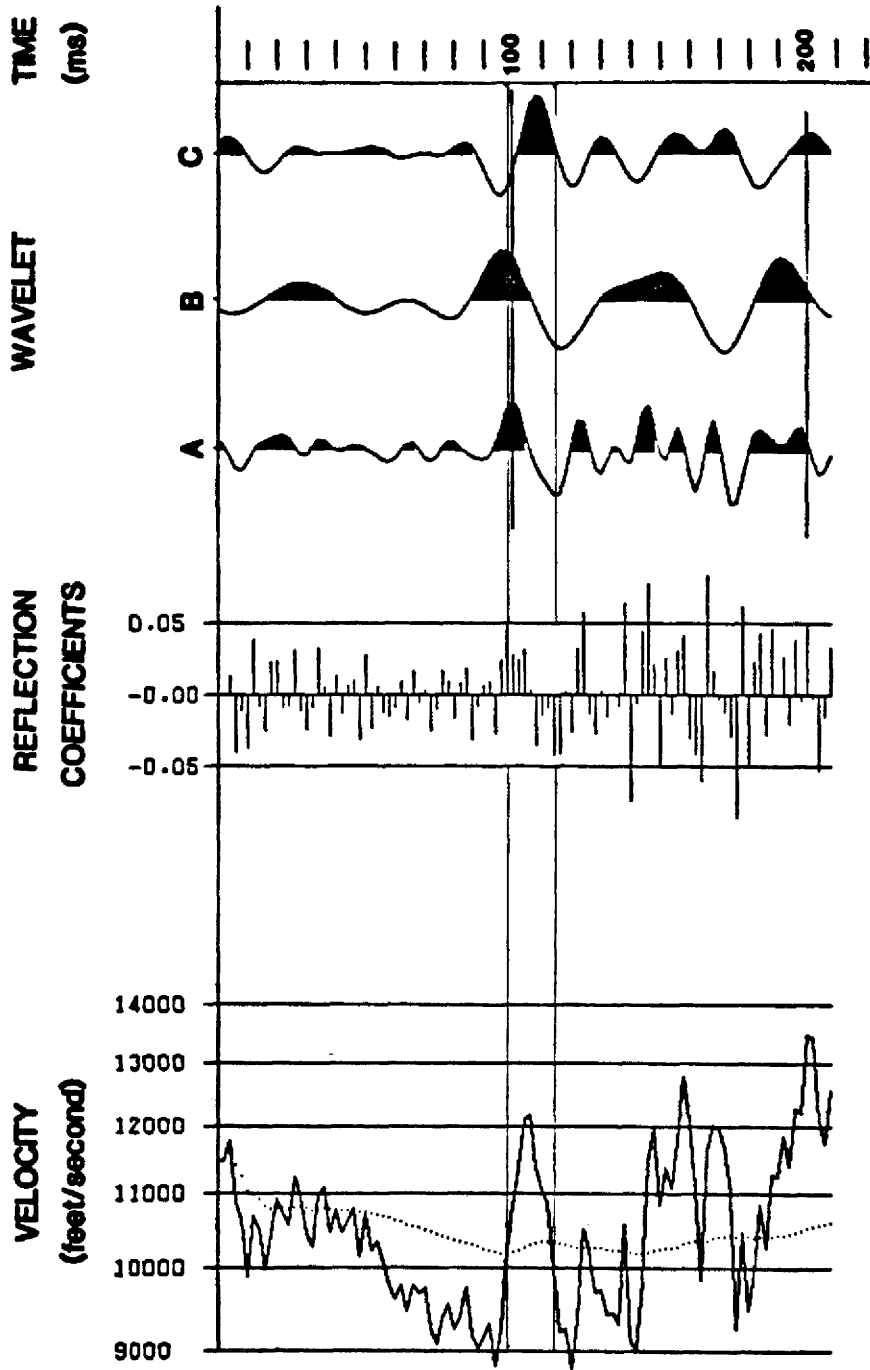
6 T43N R91W

FARMERS UNION EXCHANGE #22 SHAD



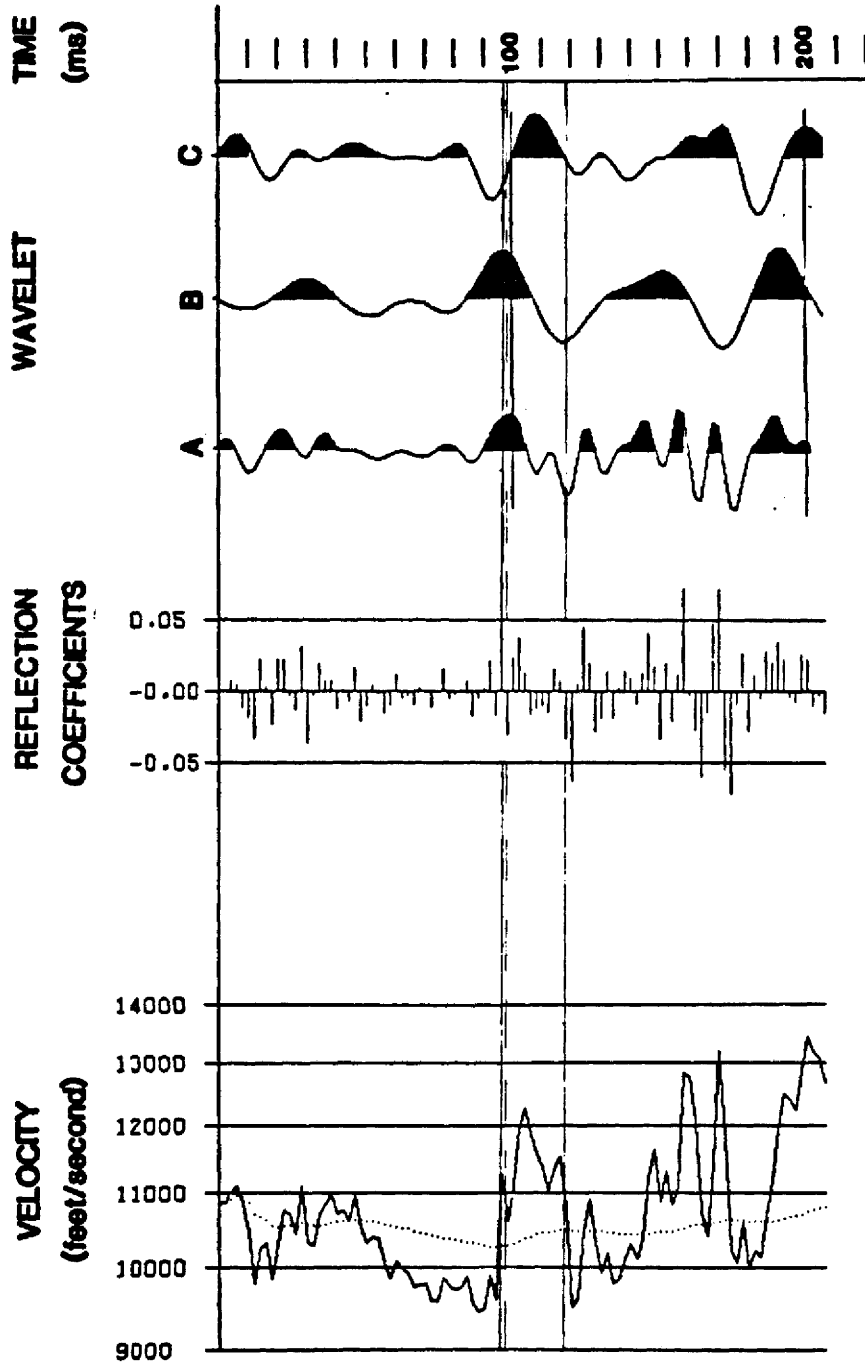
9 T43N R91W

FARMERS UNION EXCHANGE #23 SHAD



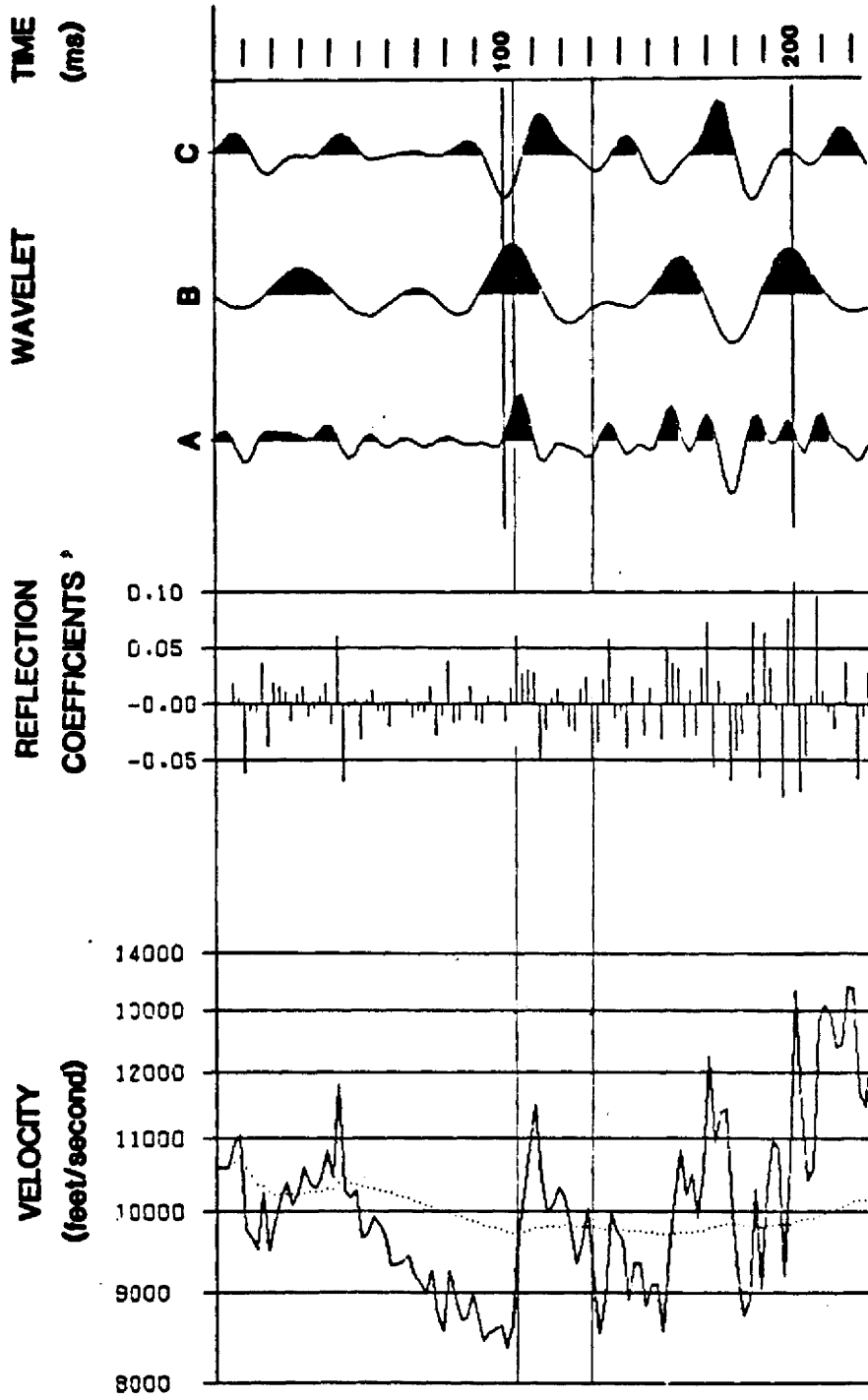
12 T43N R91W

DELTA #1 BIRDWELL-TENSLEEP



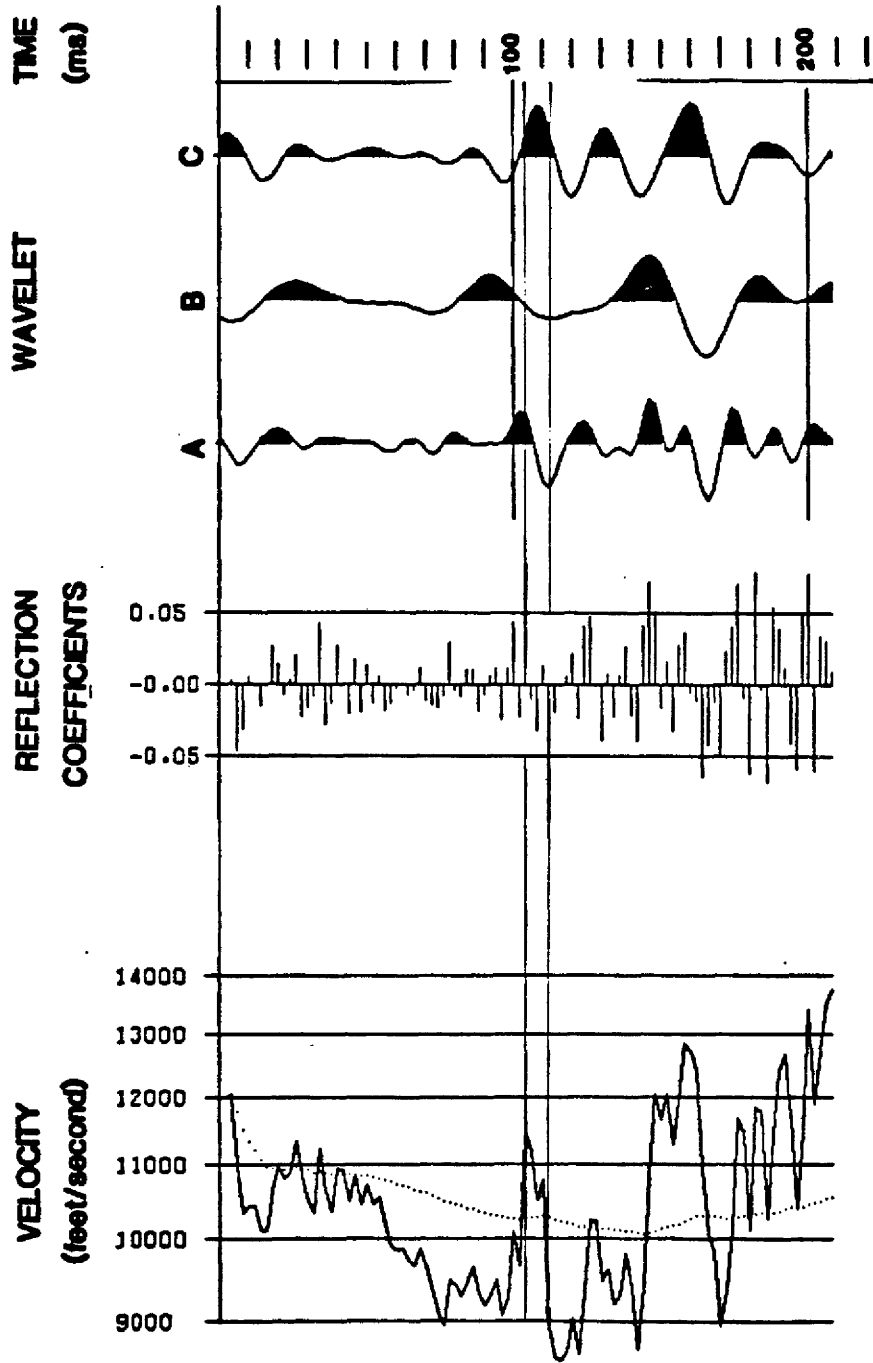
36 T43N R91W

TEXACO #38 BLACK MOUNTAIN UNIT



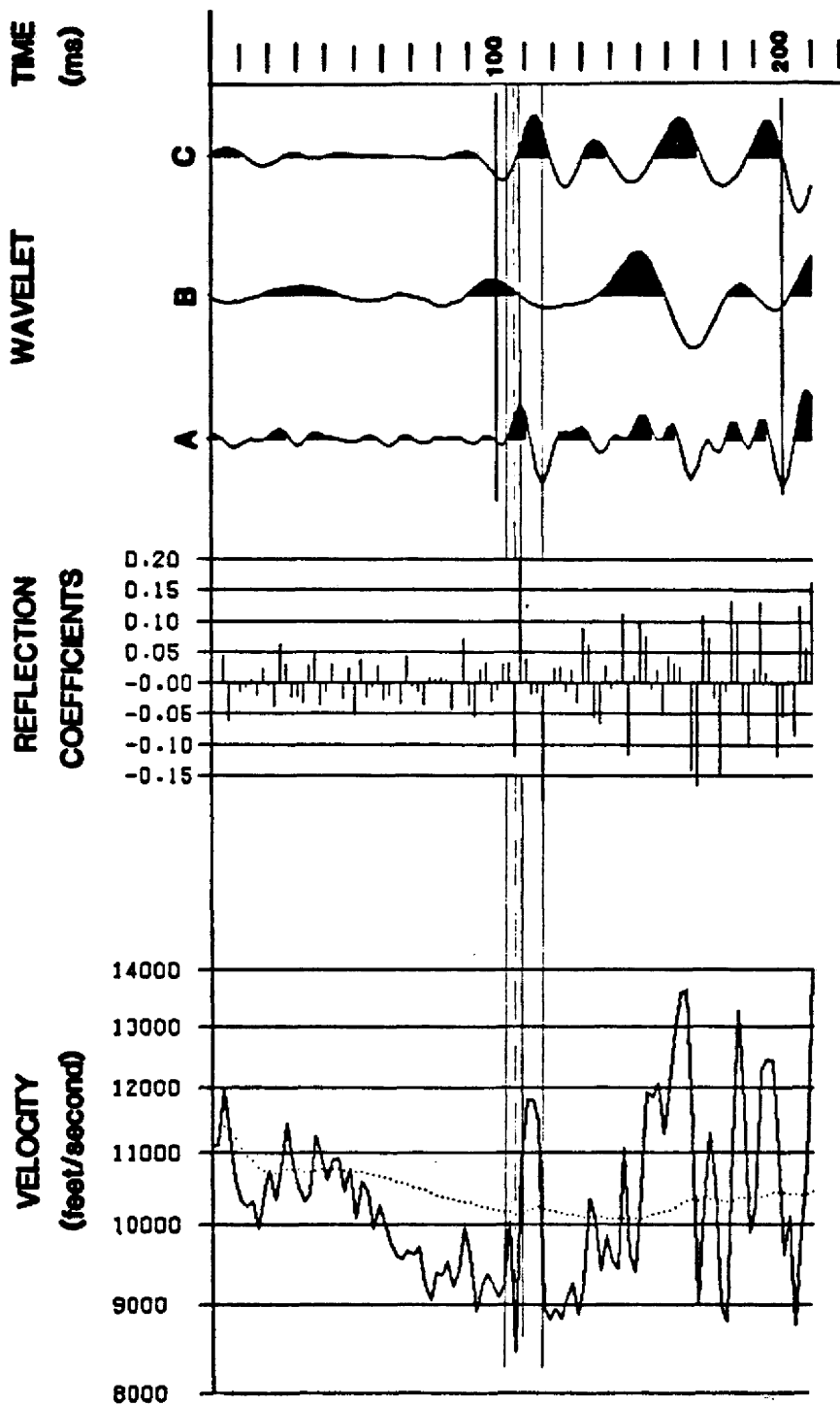
6 T43N R92W

CORONADO #1 OZMAN GOVT.



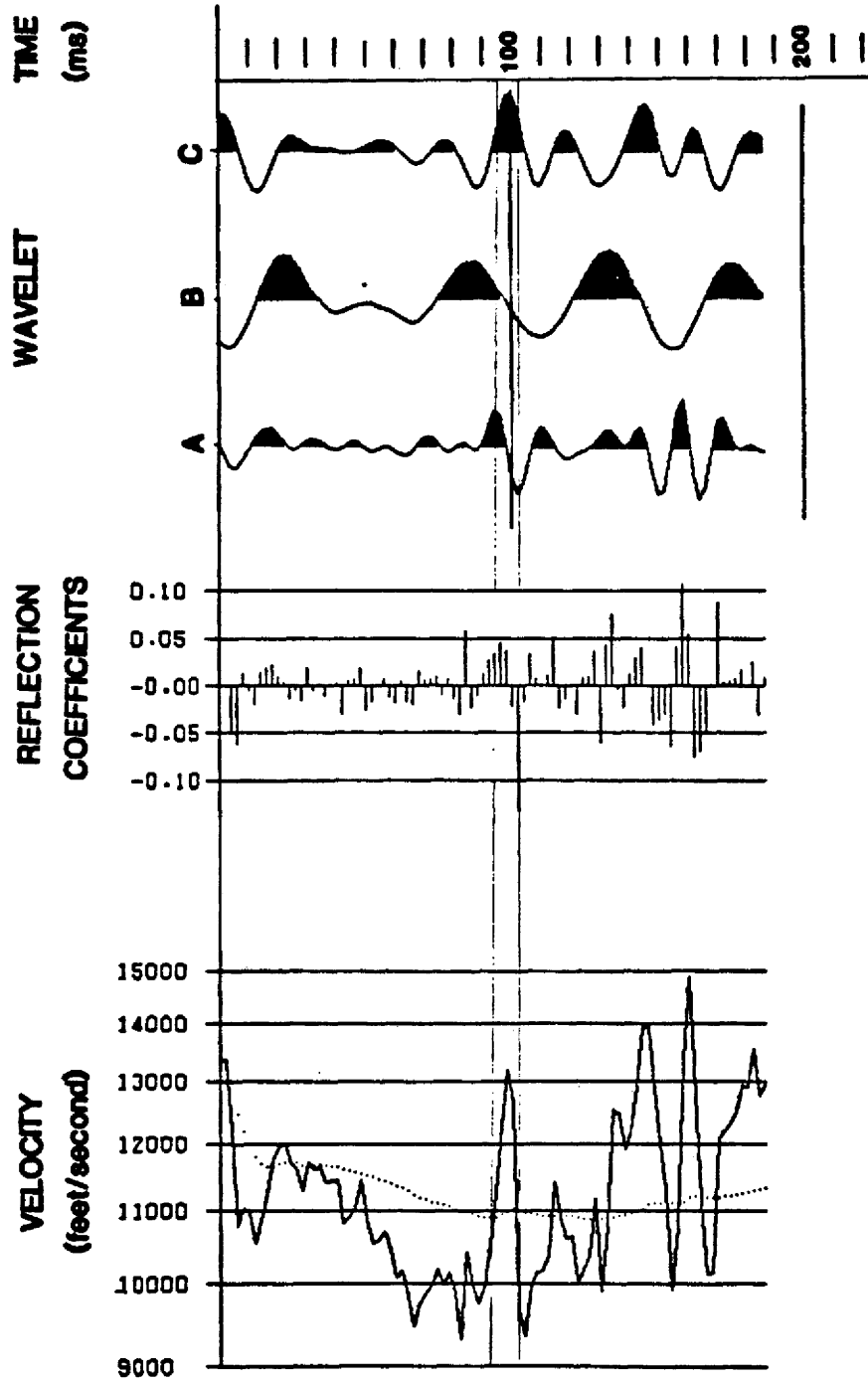
3 T43N R93W

CORONADO OIL #1 NELSON-GOVT.



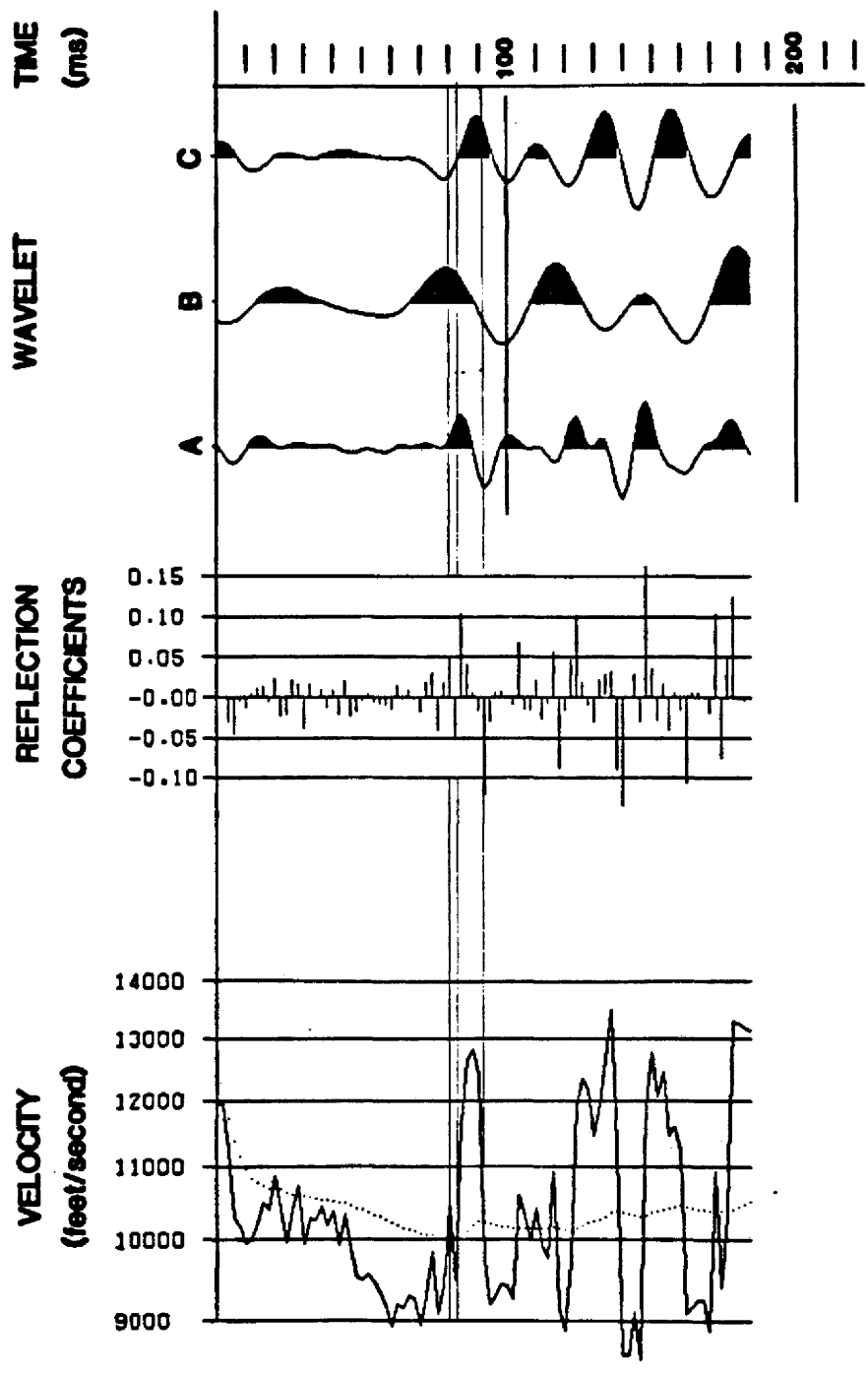
24 T44N R92W

CONTINENTAL #1 -24 MUD CREEK



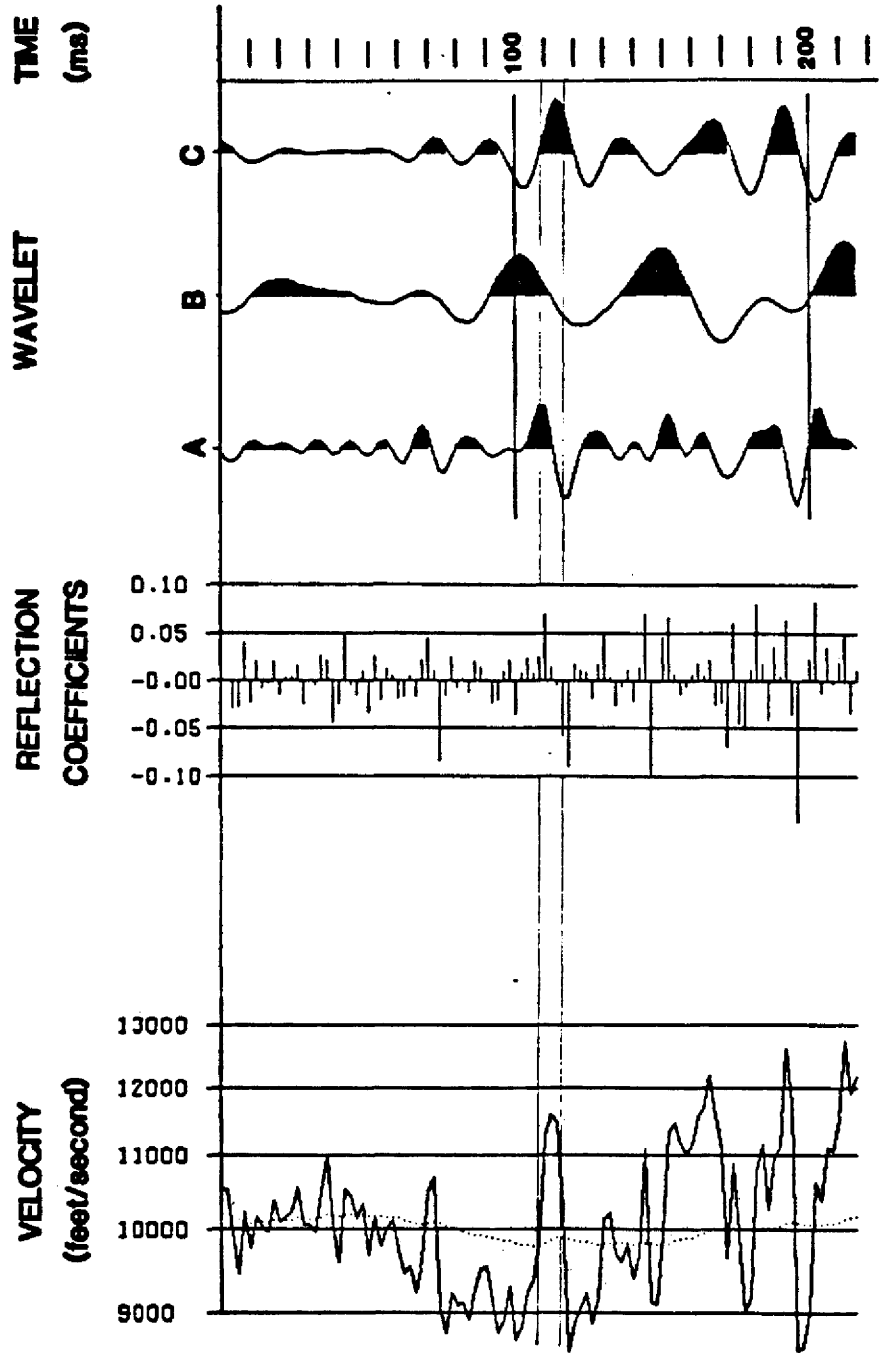
27 T44N R92W

HELIS #27-1 NW MURPHY DOME



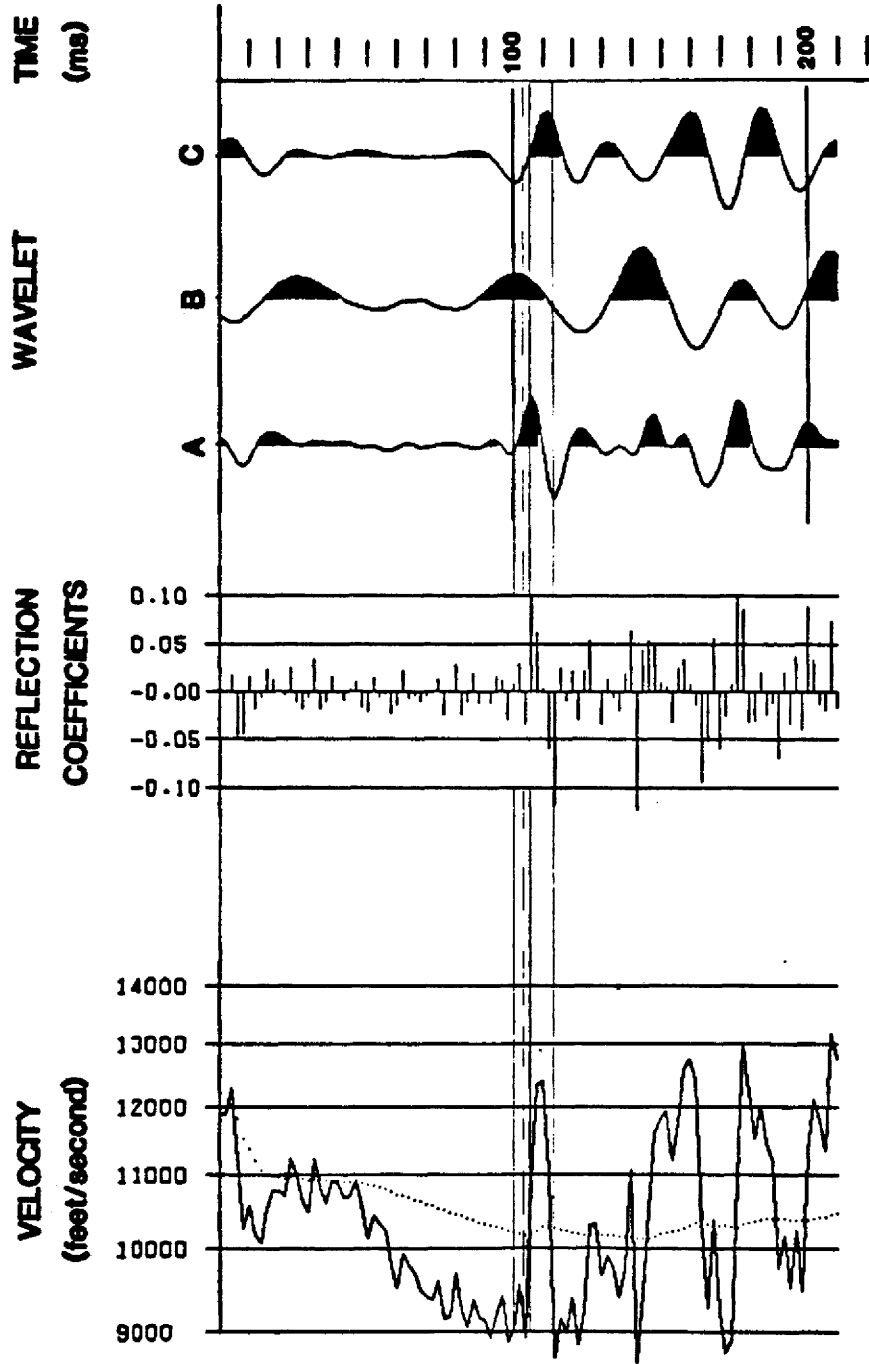
32 T44N R92W

CONTINENTAL OIL #1 GOVT.-MANN



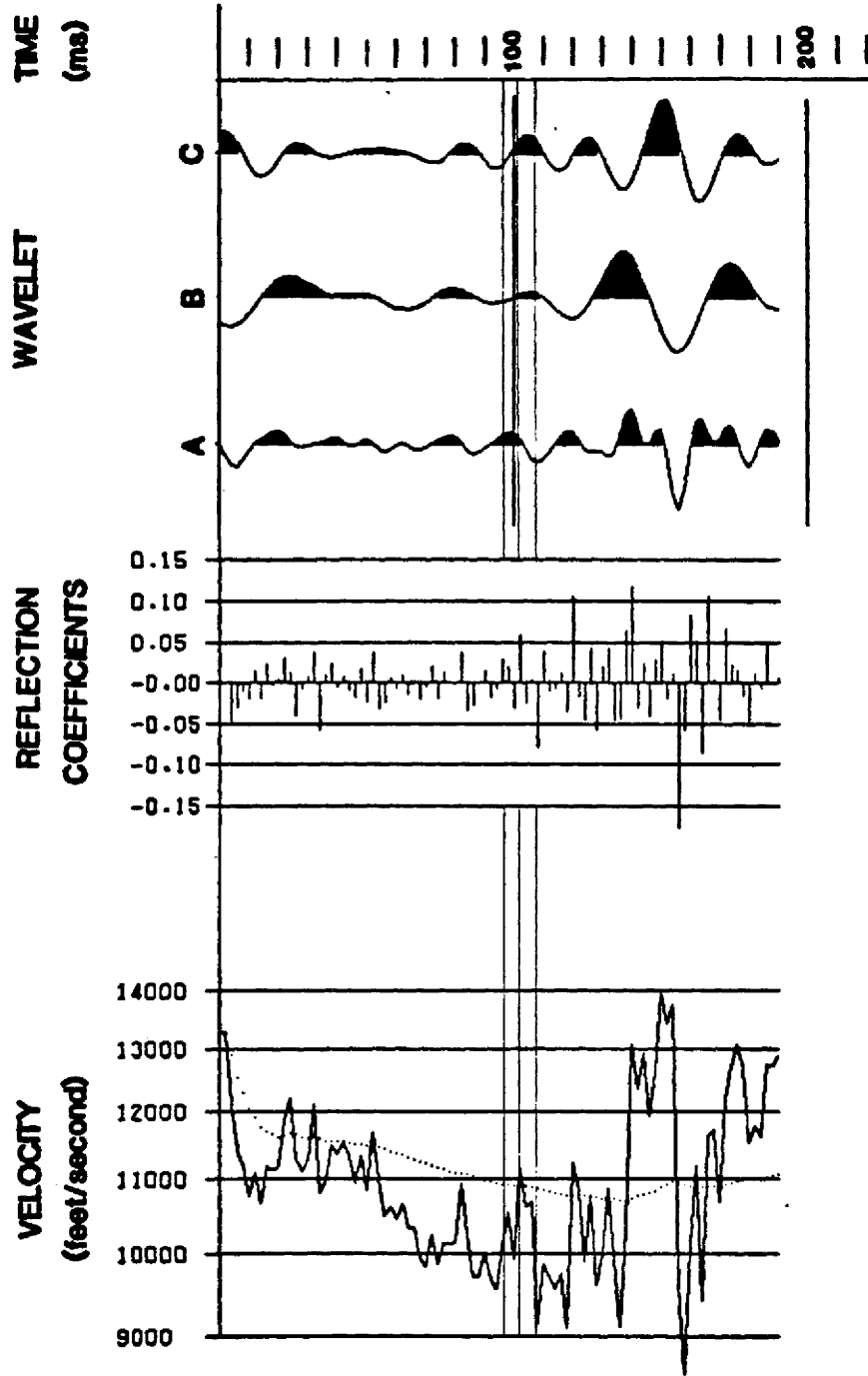
33 T44N R92W

MANNING #1 GOVT.-CONOCO



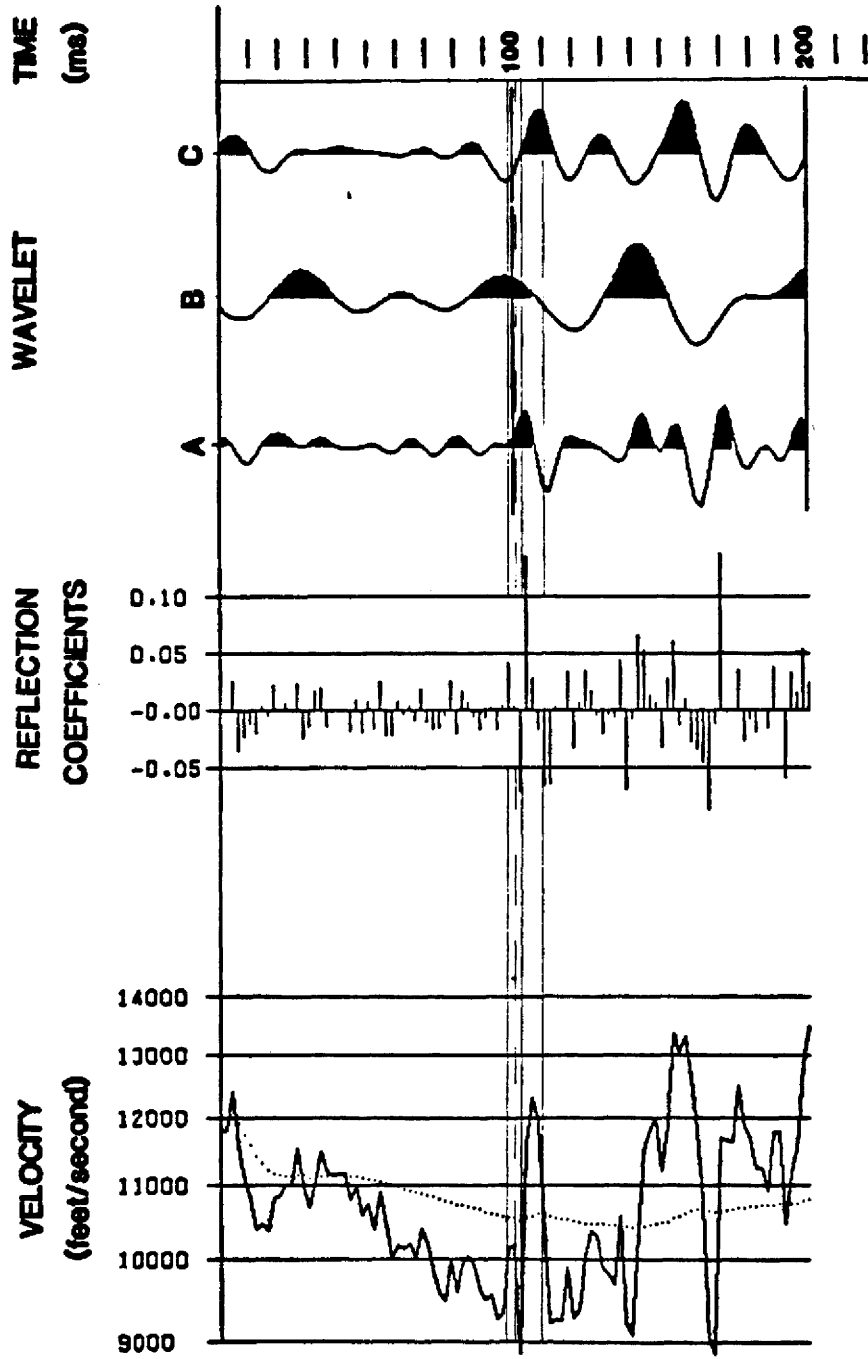
17 T44N R93W

GREAT WESTERN DRILLING #1 FED.-MELTON



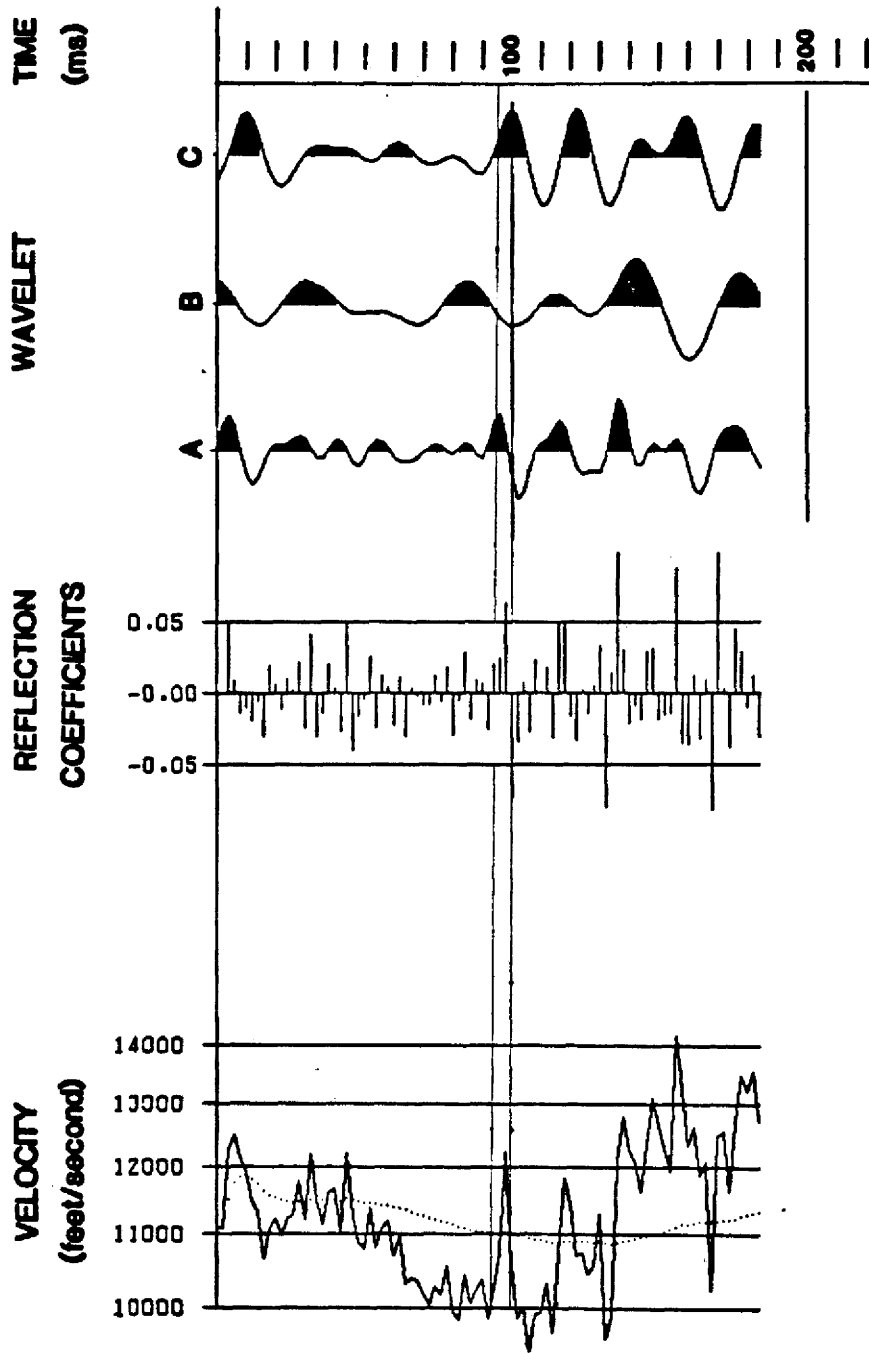
33 T44N R93W

SPELMA PRENTICE #1 VANNAY



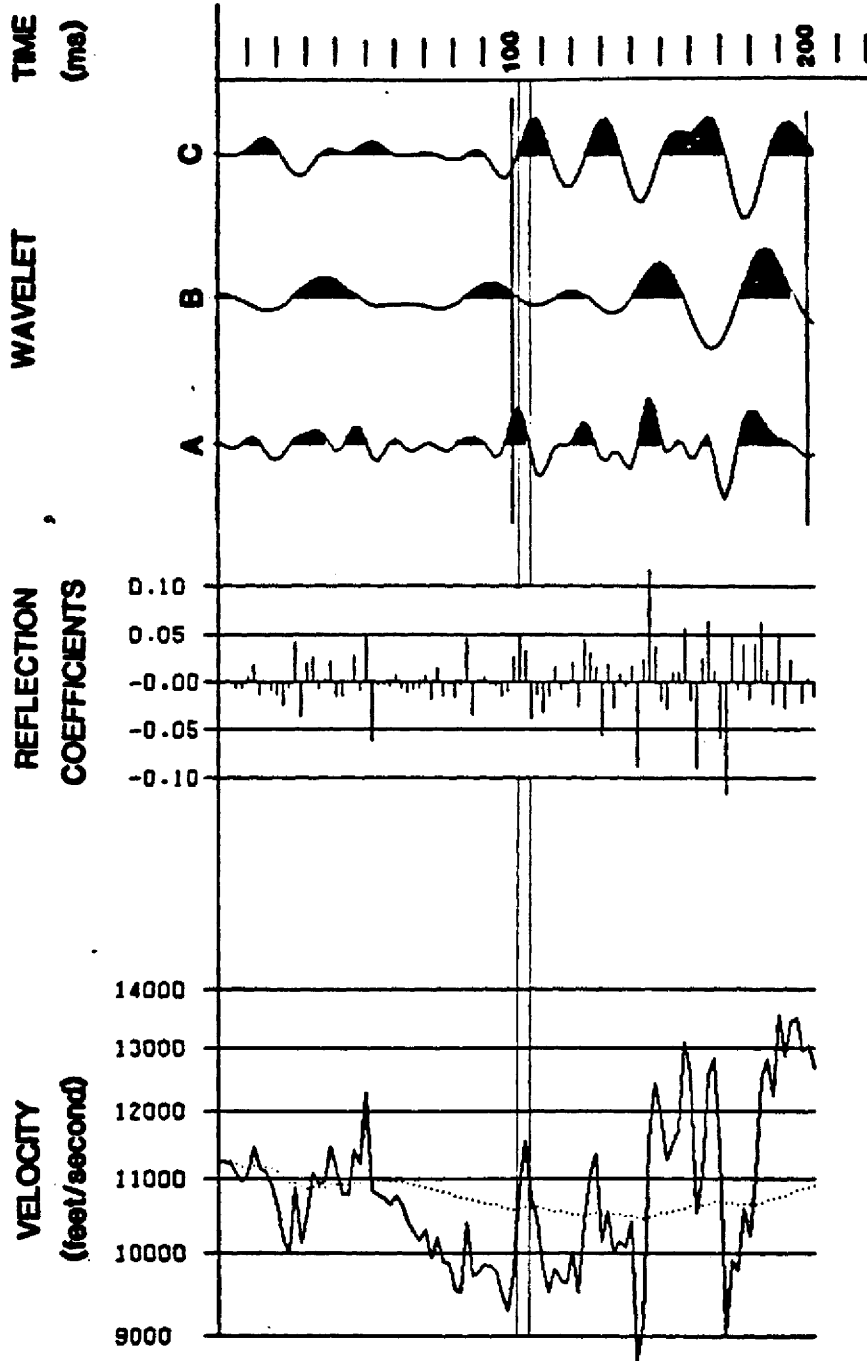
8 T45N R89W

ASHLAND OIL #1-8 GOVT.



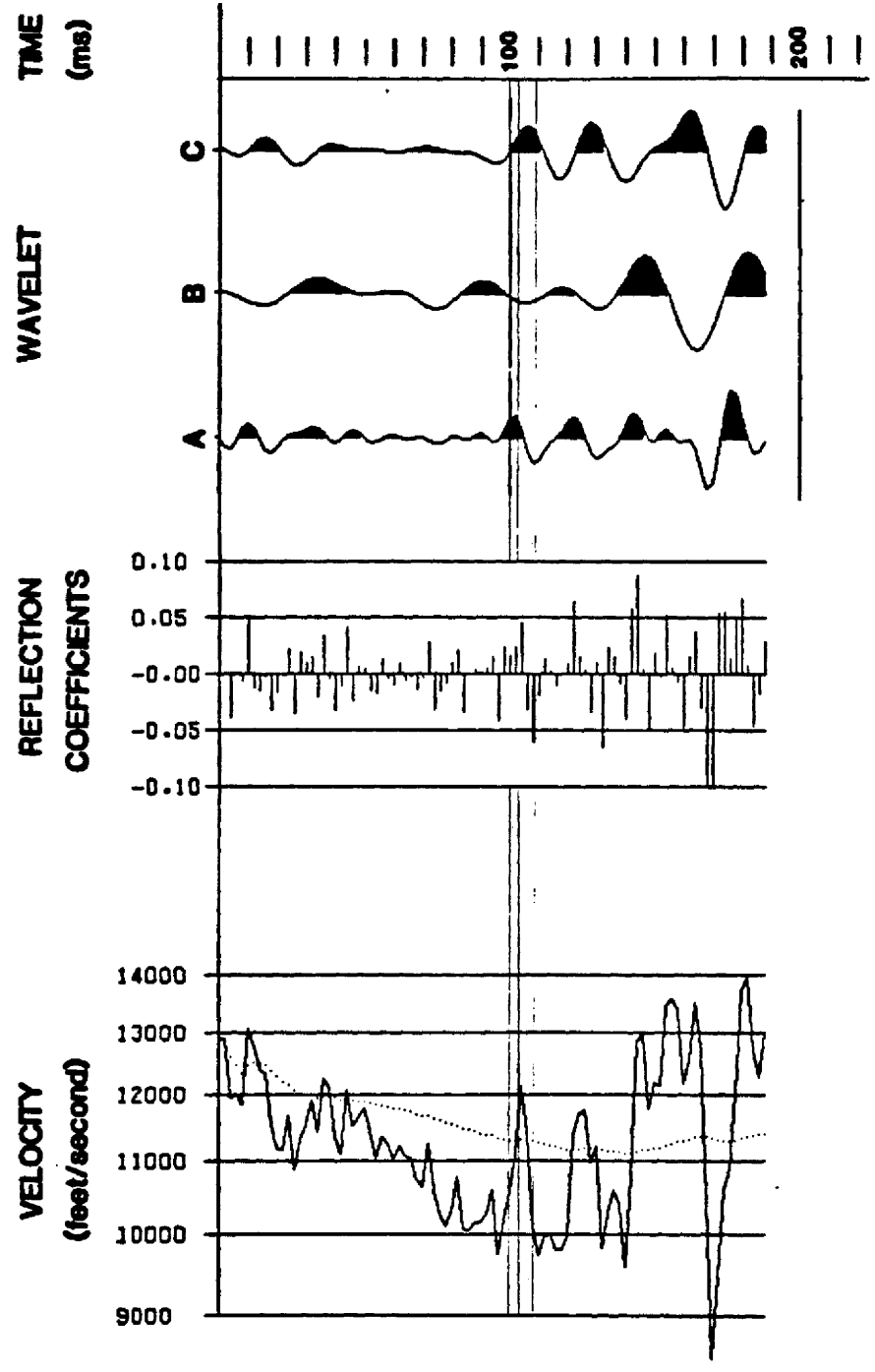
26 T45N R89W

MARATHON OIL #1 GOVT.-NERO



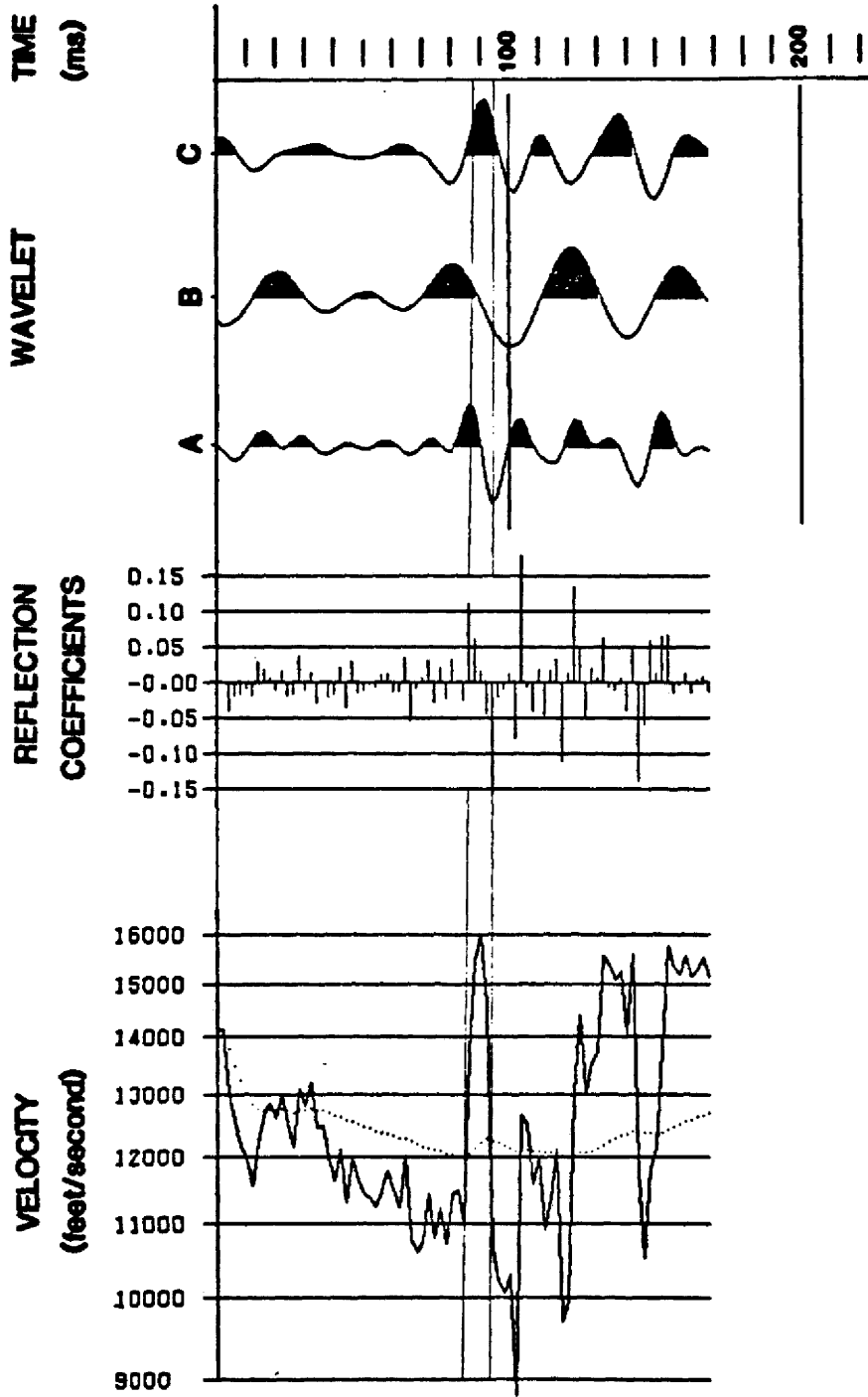
14 T45N R90W

TEXAS PACIFIC OIL #1 USA-D



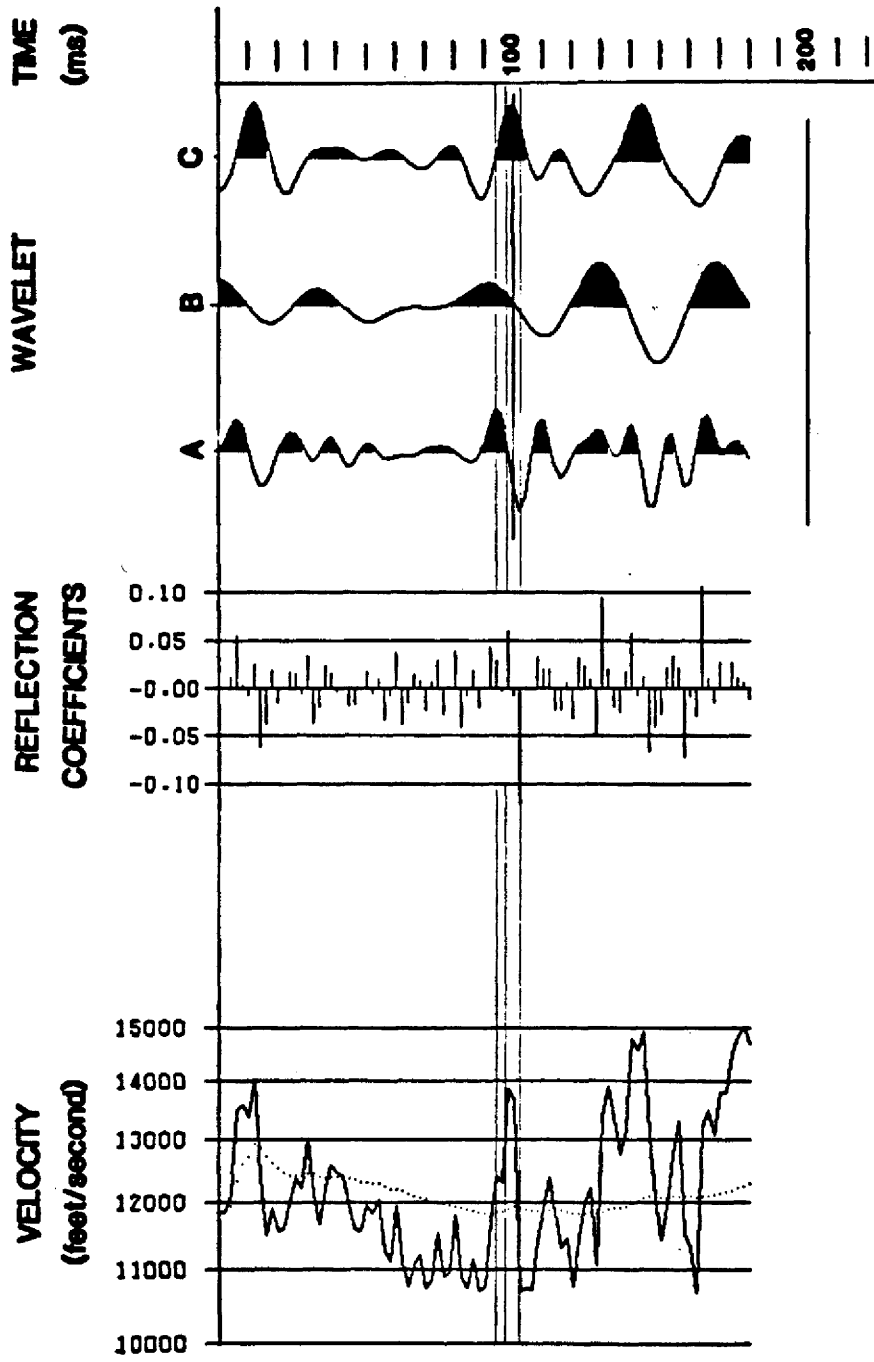
10 T45N R91W

1 AMOCO-USA-OZMAN



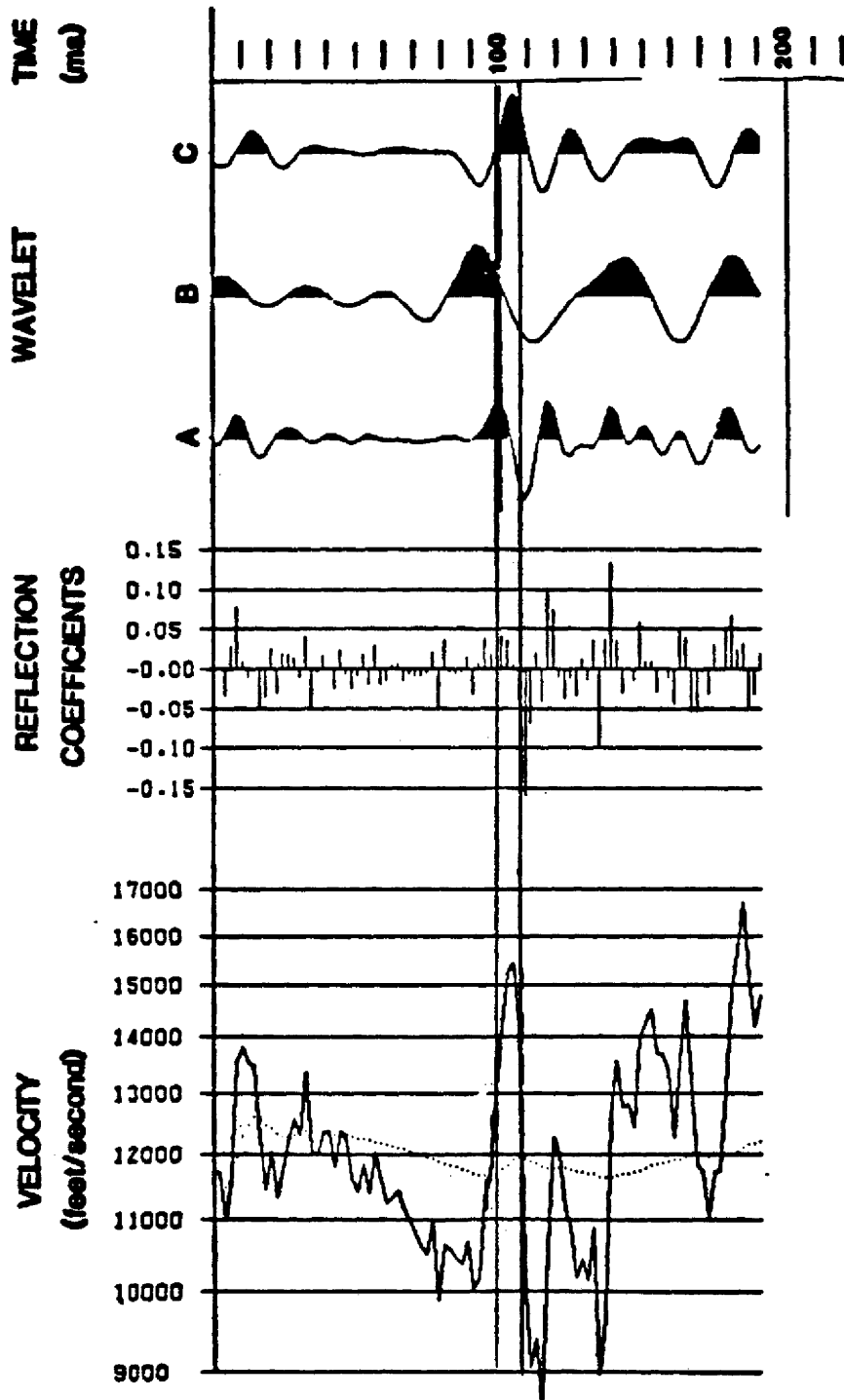
29 T45N R91W

TEXACO #1 GOVT -McGRADY-HAMMOND



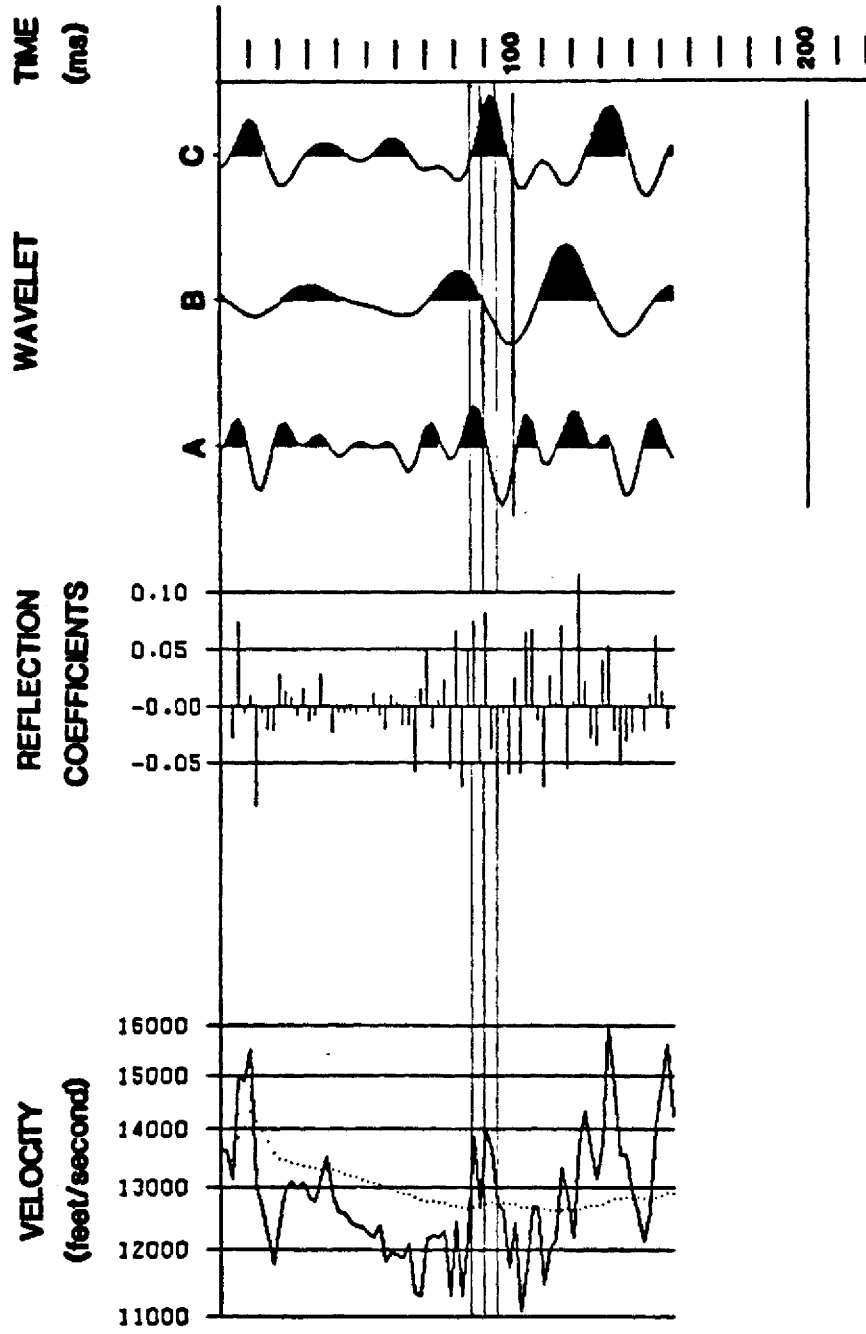
36 T45N R91W

PAN AMERICAN #1 WAGON PRONG UNIT



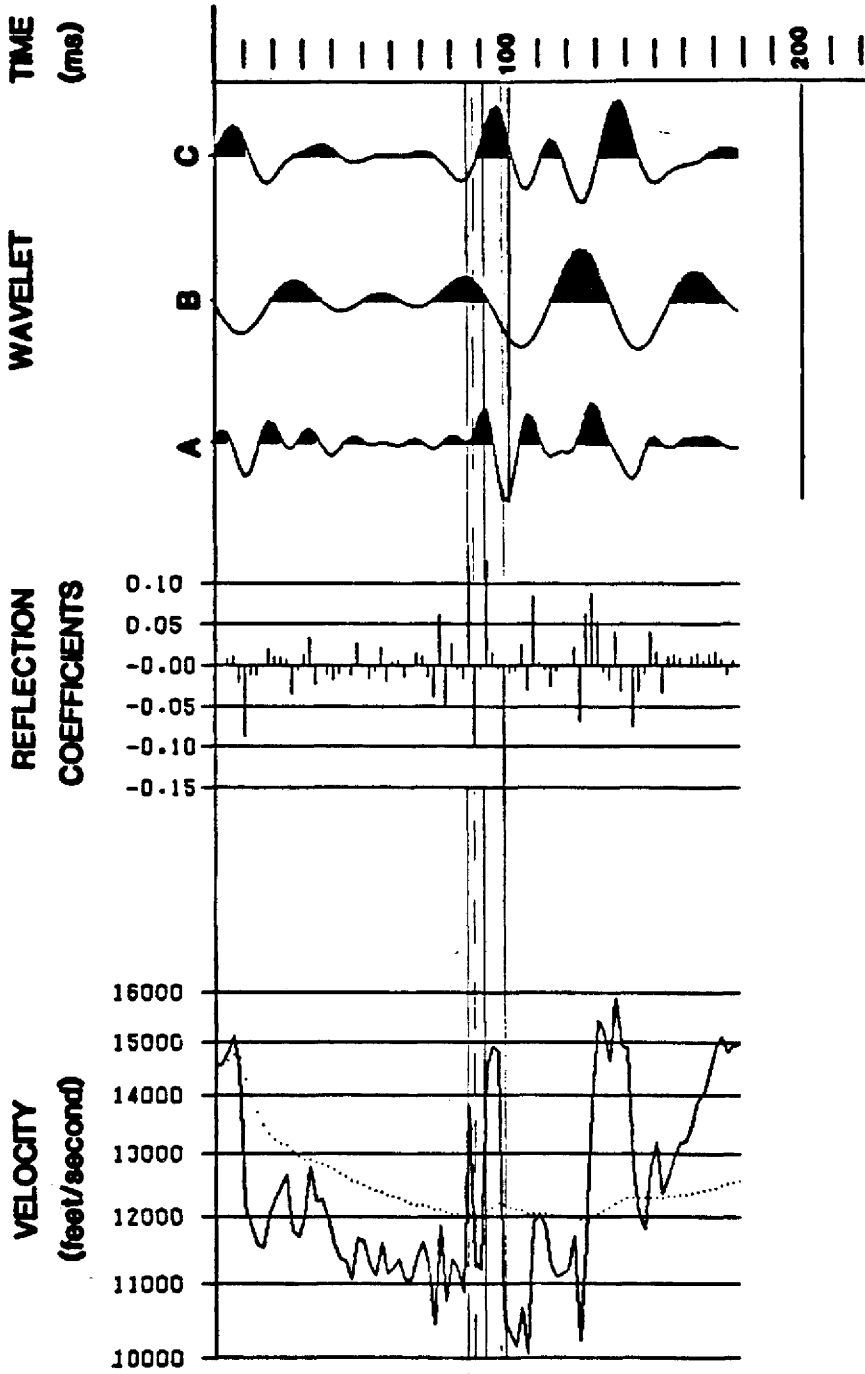
8 T45N R92W

BLACK HAWK #33-8 CHAMBERS FED.



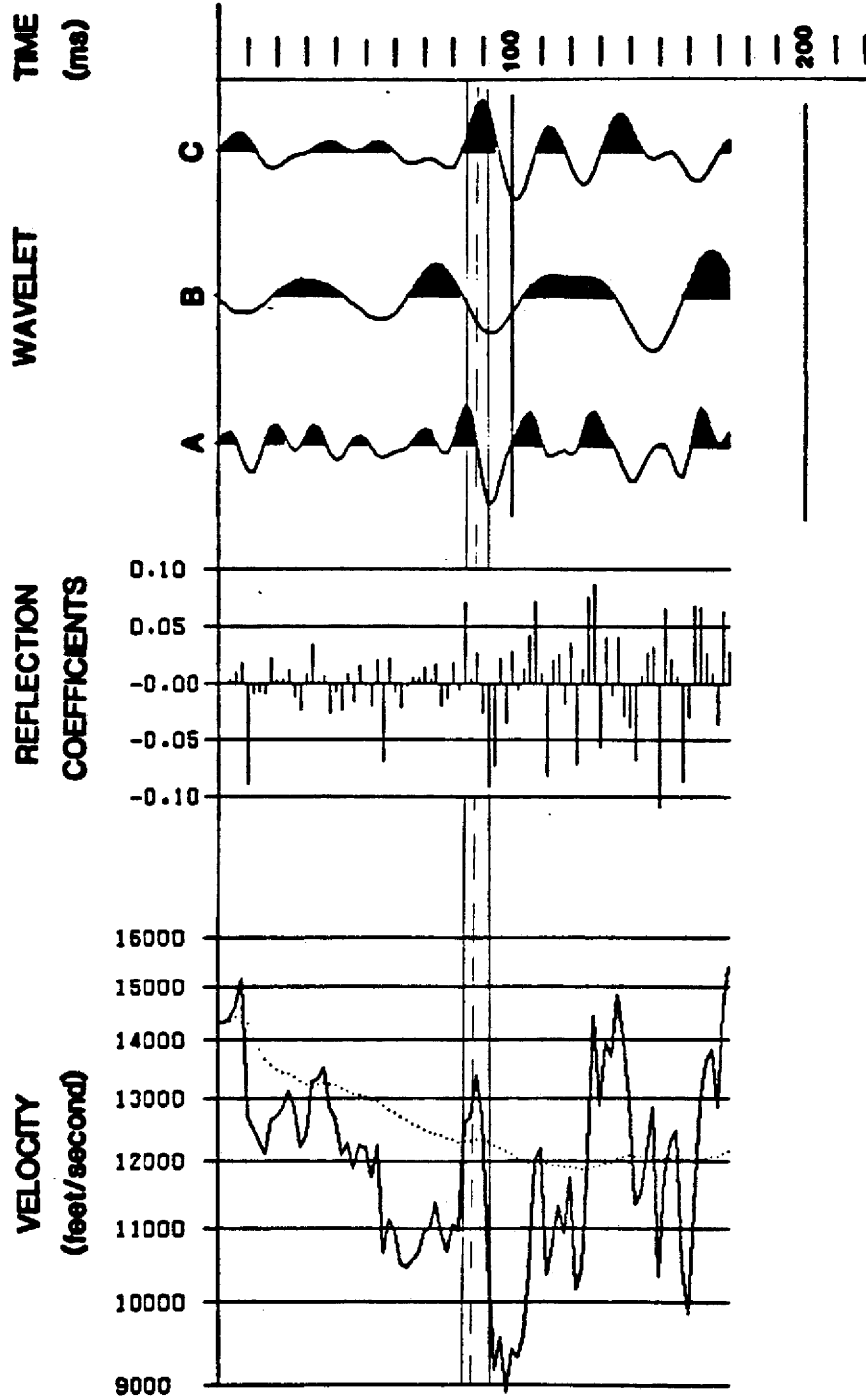
13 T45N R92W

TENNECO #1 TUFFY FEDERAL



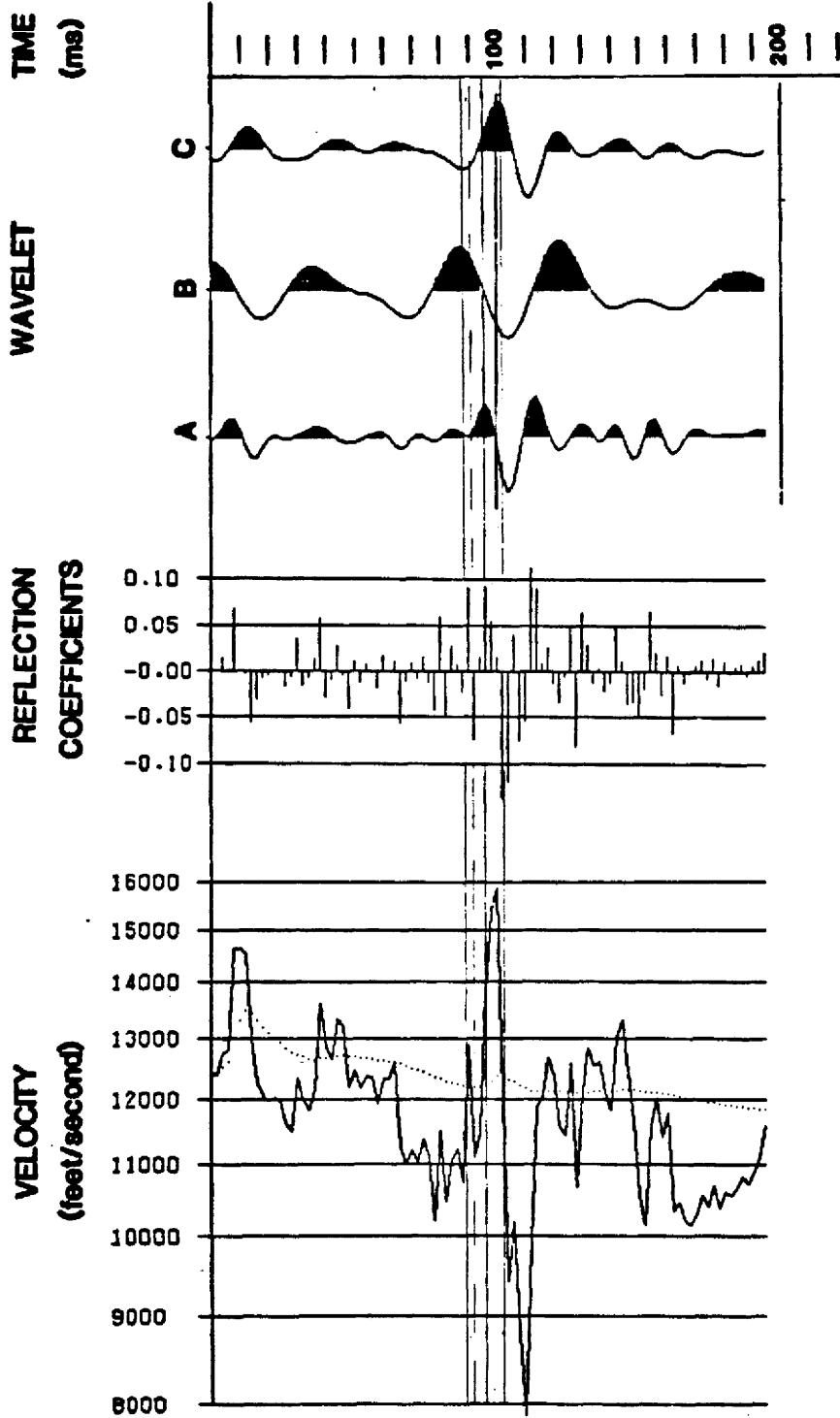
19 T45N R92W

TENNECO OIL #1 NEIBER TWO UNIT



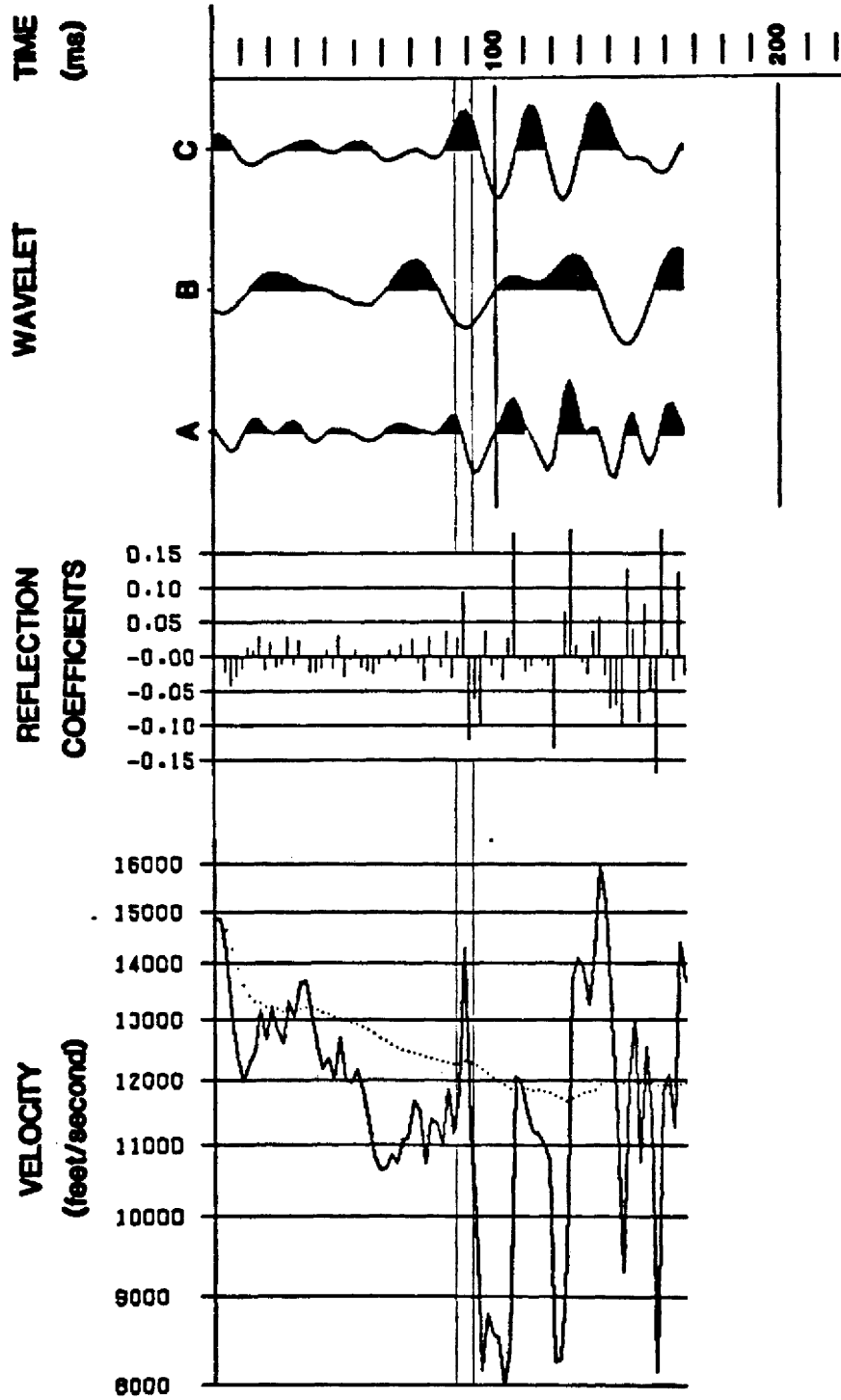
24 T45N R92W

TENNECO #1 FEDERAL



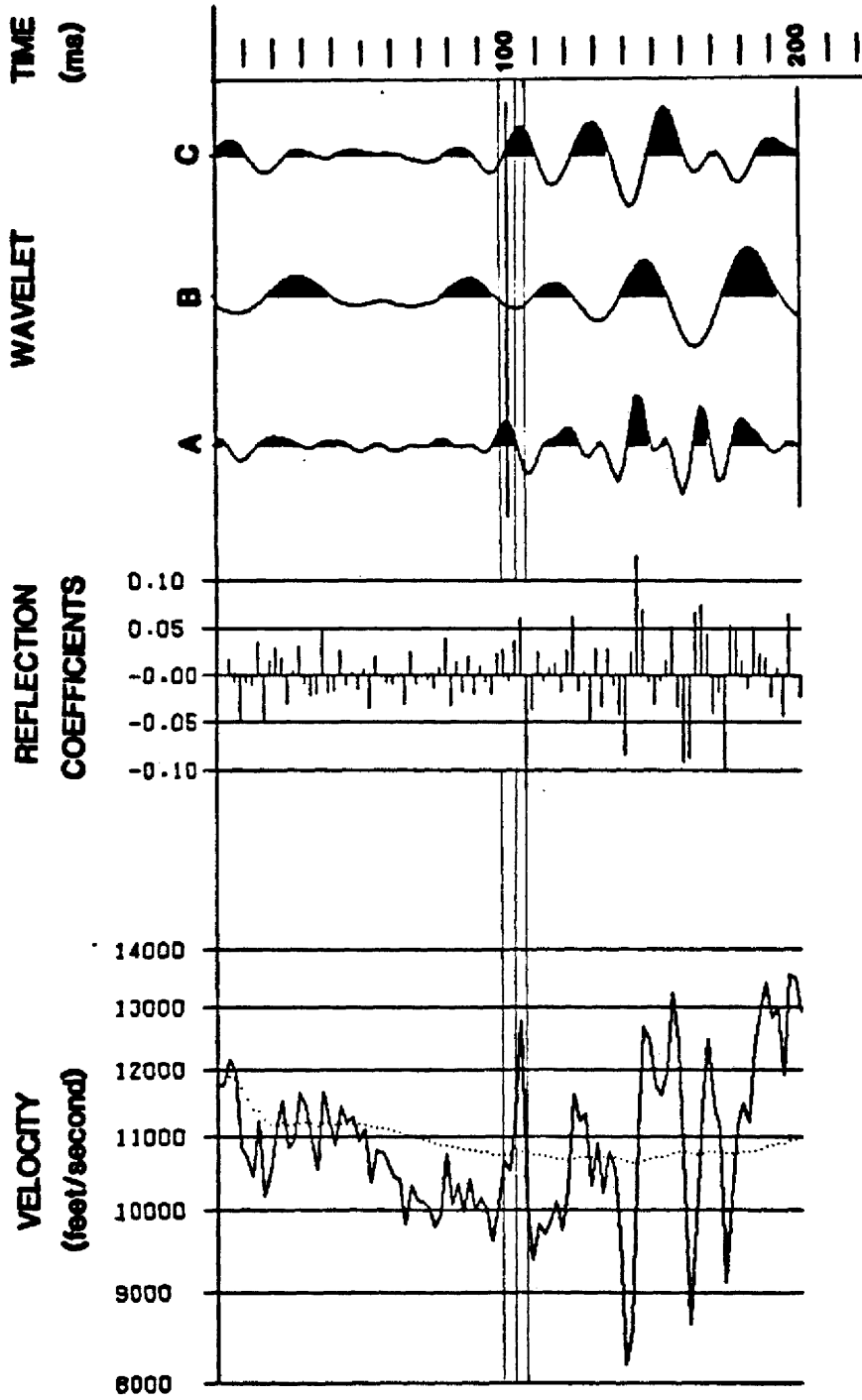
TENNECO OIL #1 DYE FEDERAL

13 T45N R93W



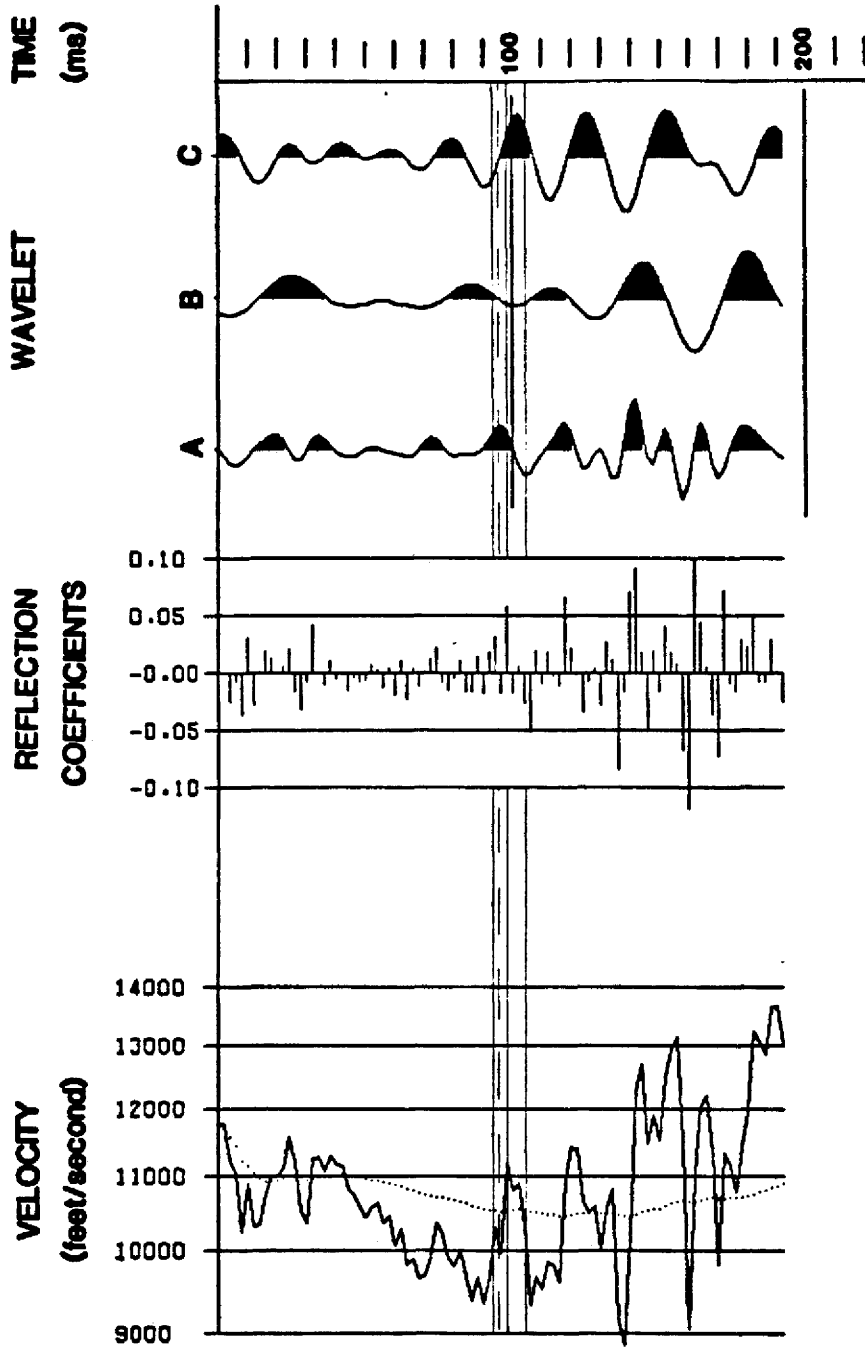
6 T46N R89W

CHORNEY #2 SHOAL UNIT



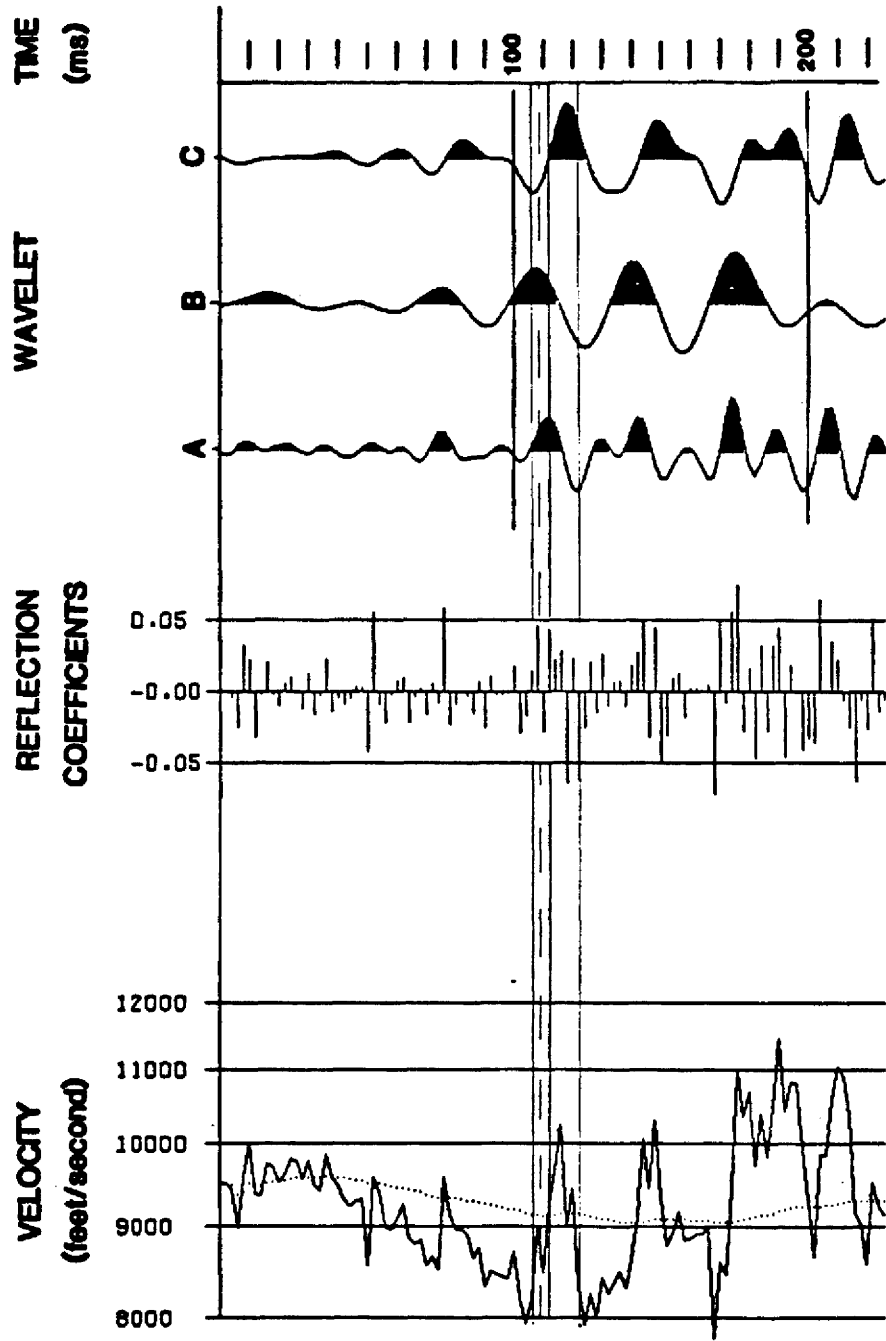
9 T46N R89W

SINCLAIR SHOAL UNIT #1



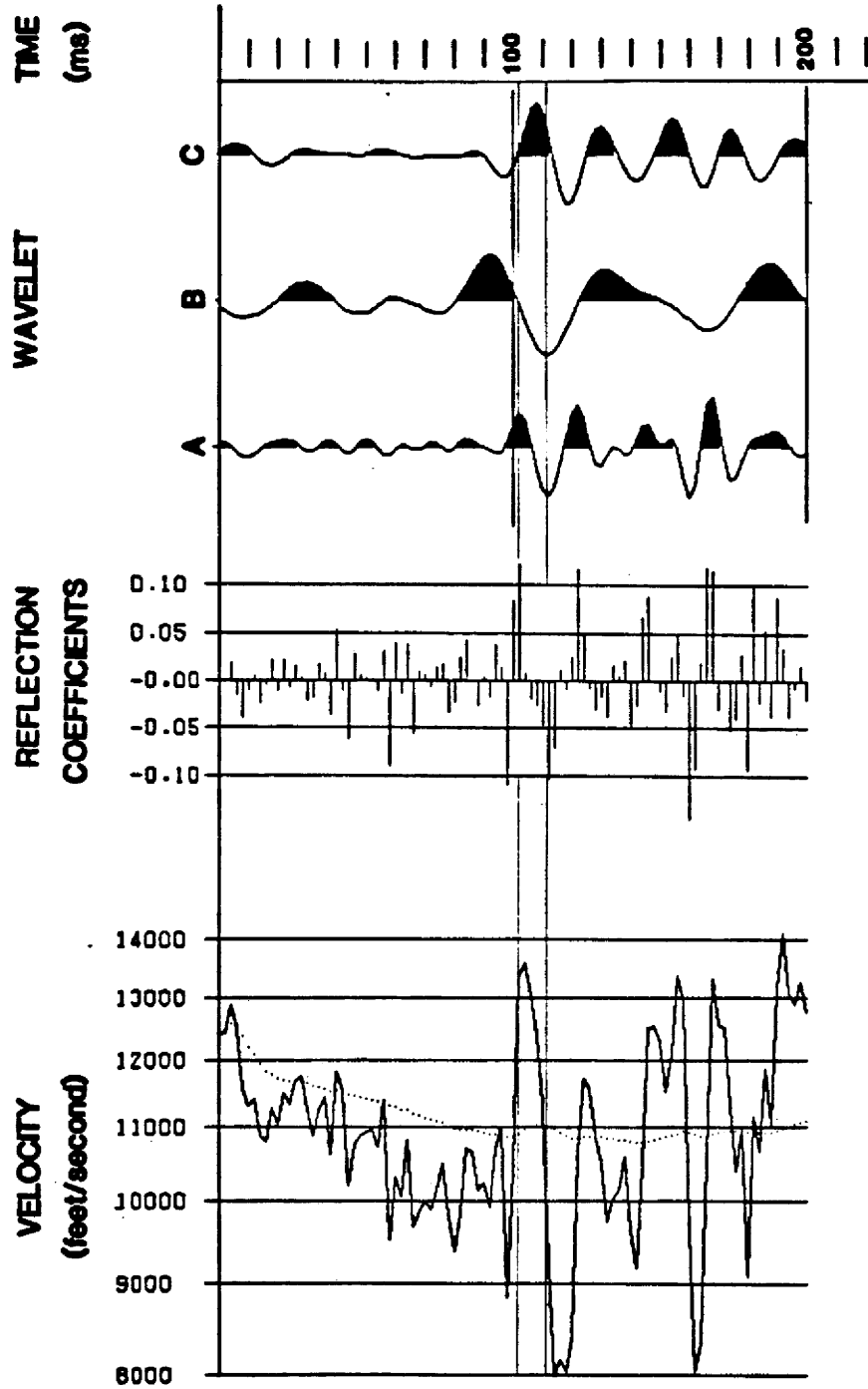
13 T46N R89W

SAMEDAN OIL #1 KELLOGG-FEDERAL



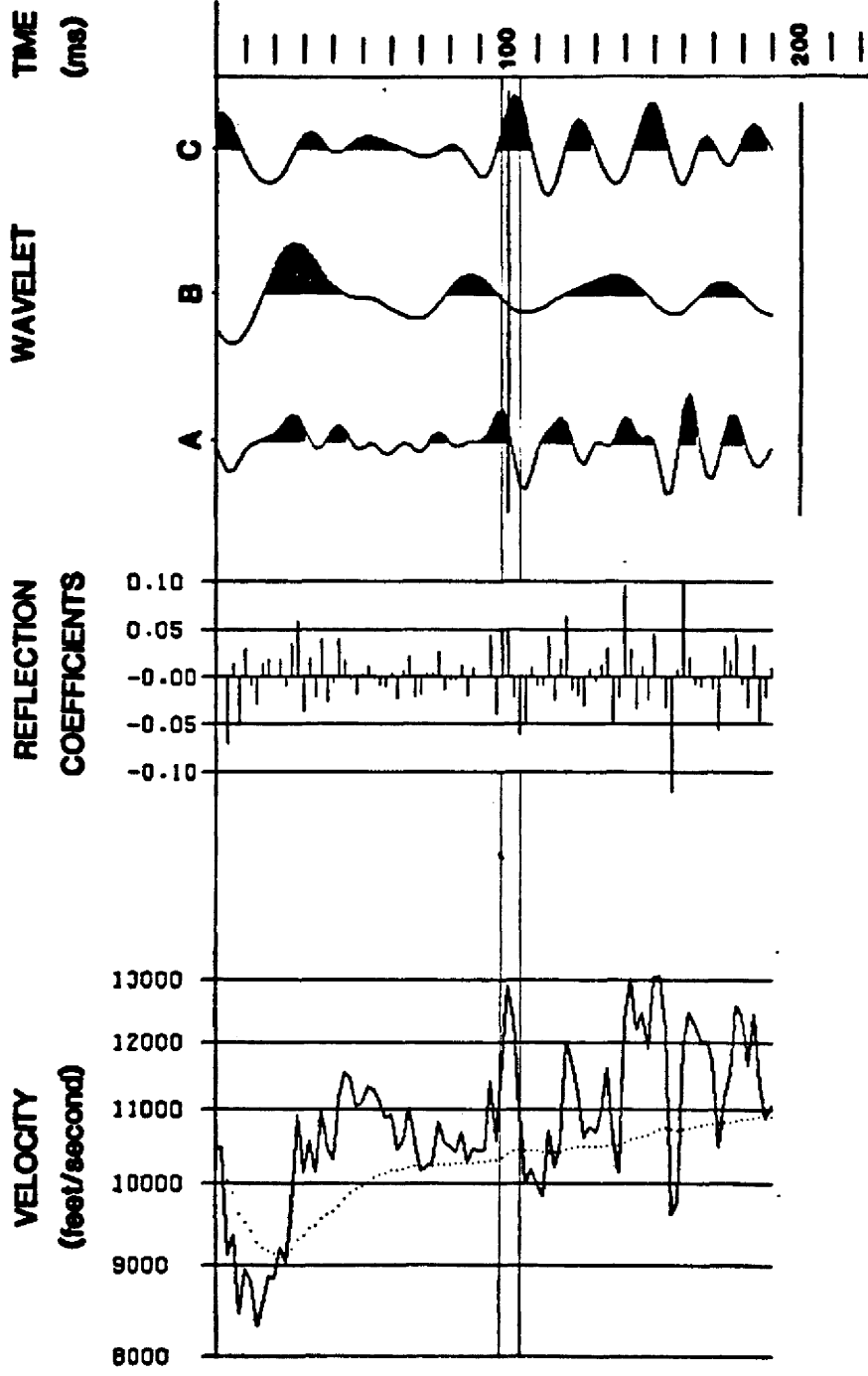
6 T46N R90W

STUARCO OIL #1 SHETTLE SKYLINE-USA



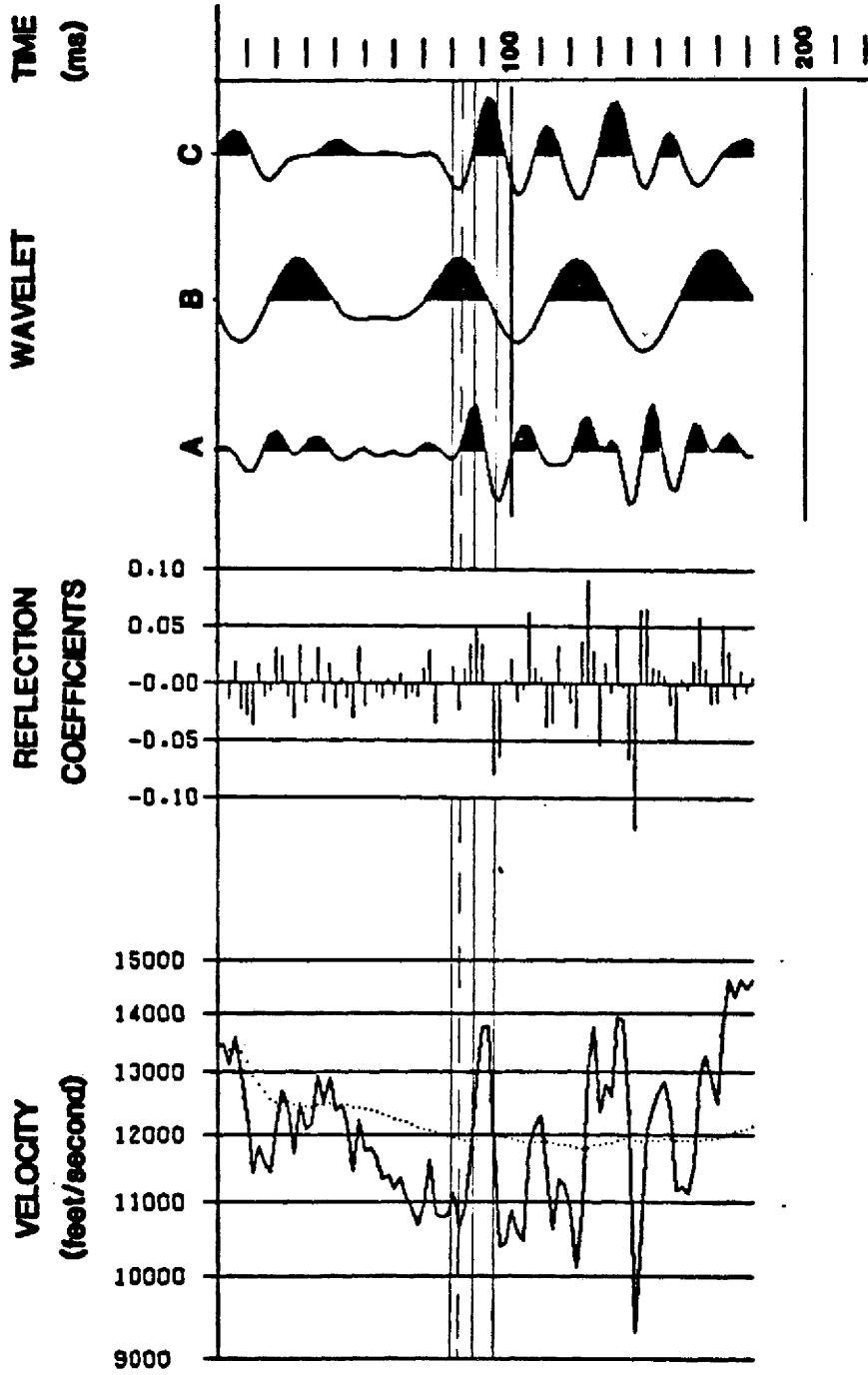
10 T46N R90W

GULF OIL #1 MEYER GULCH FEDERAL



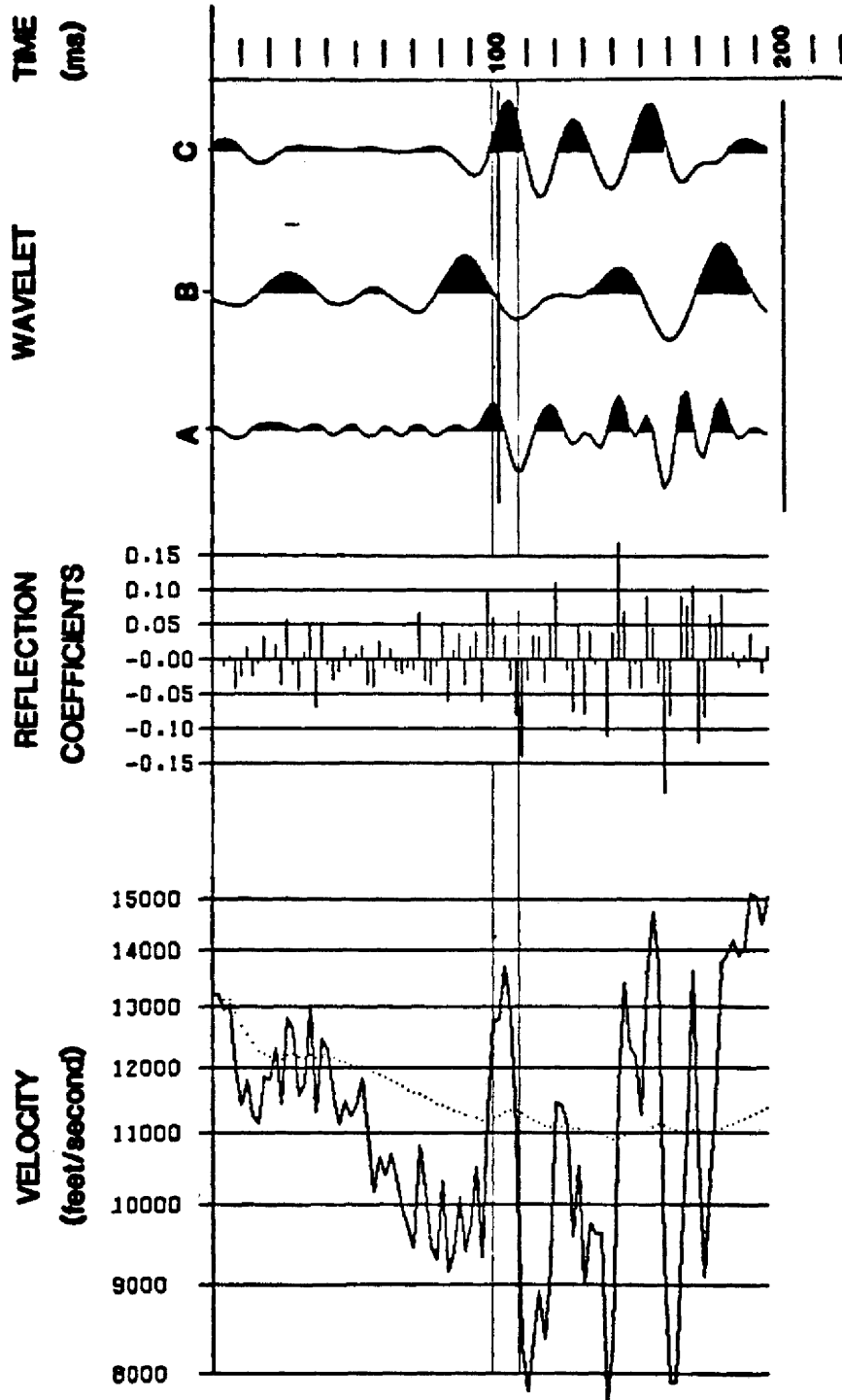
18 T46N R90W

#1 CONOCO FEDERAL-18



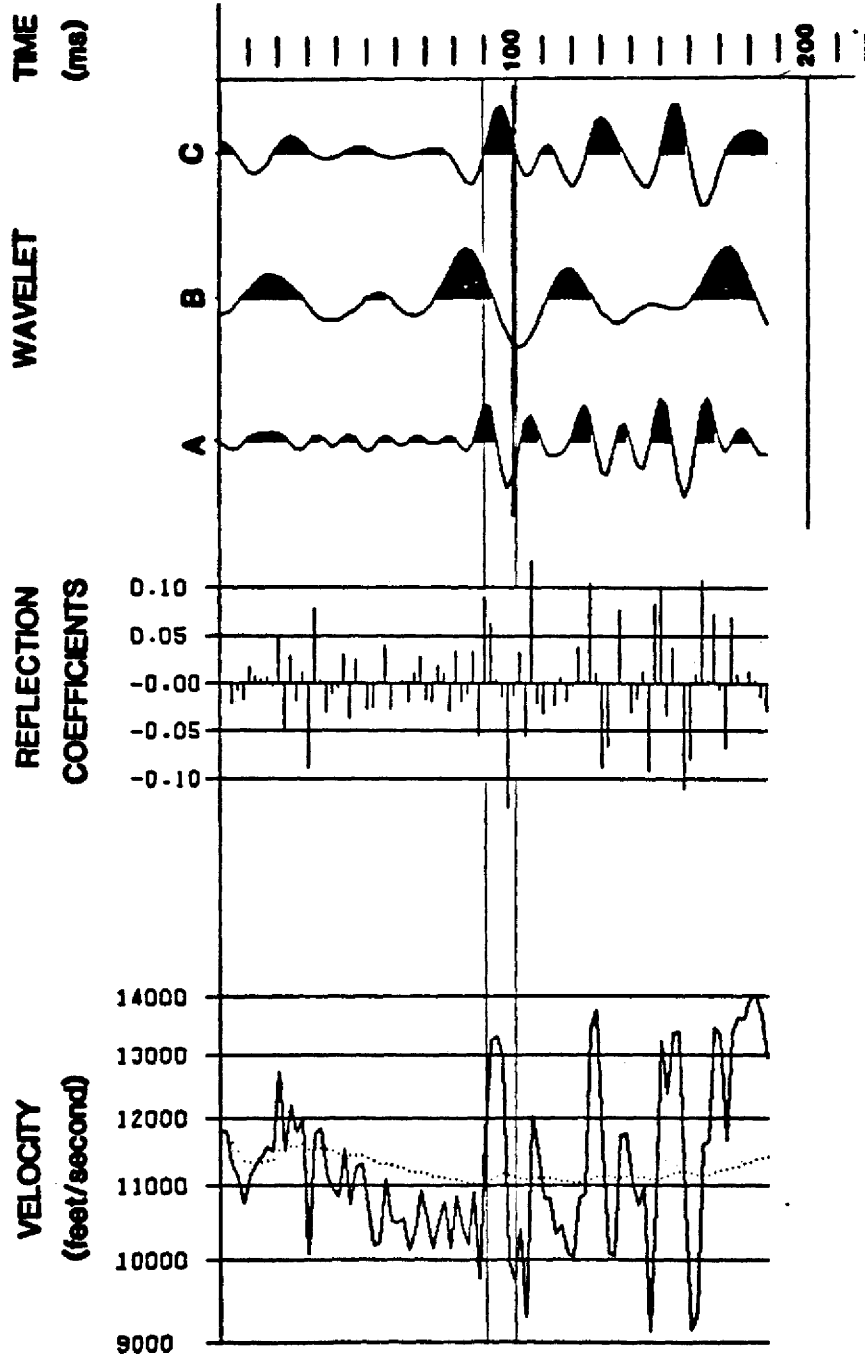
31 T46N R90W

CONTINENTAL OIL #1 GOVT.



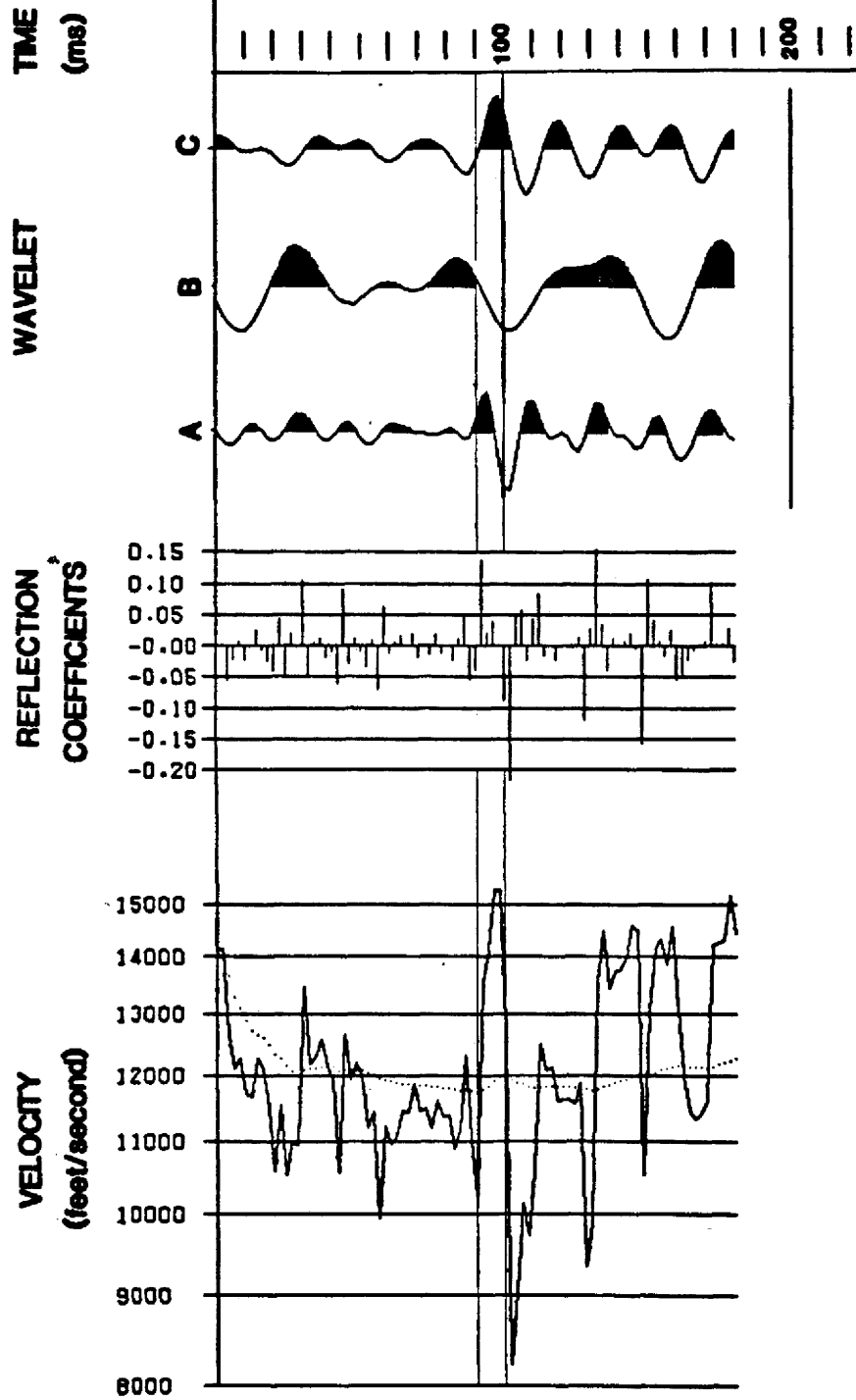
3 T46N R81W

TENNECO OIL #1 USA-SLINGERLAND



6 T46N R91W

TENNECO OIL #2 NO WATER CREEK UNIT



14 T46N R92W

J.M. HUBER #14-1 NO WATER CREEK B

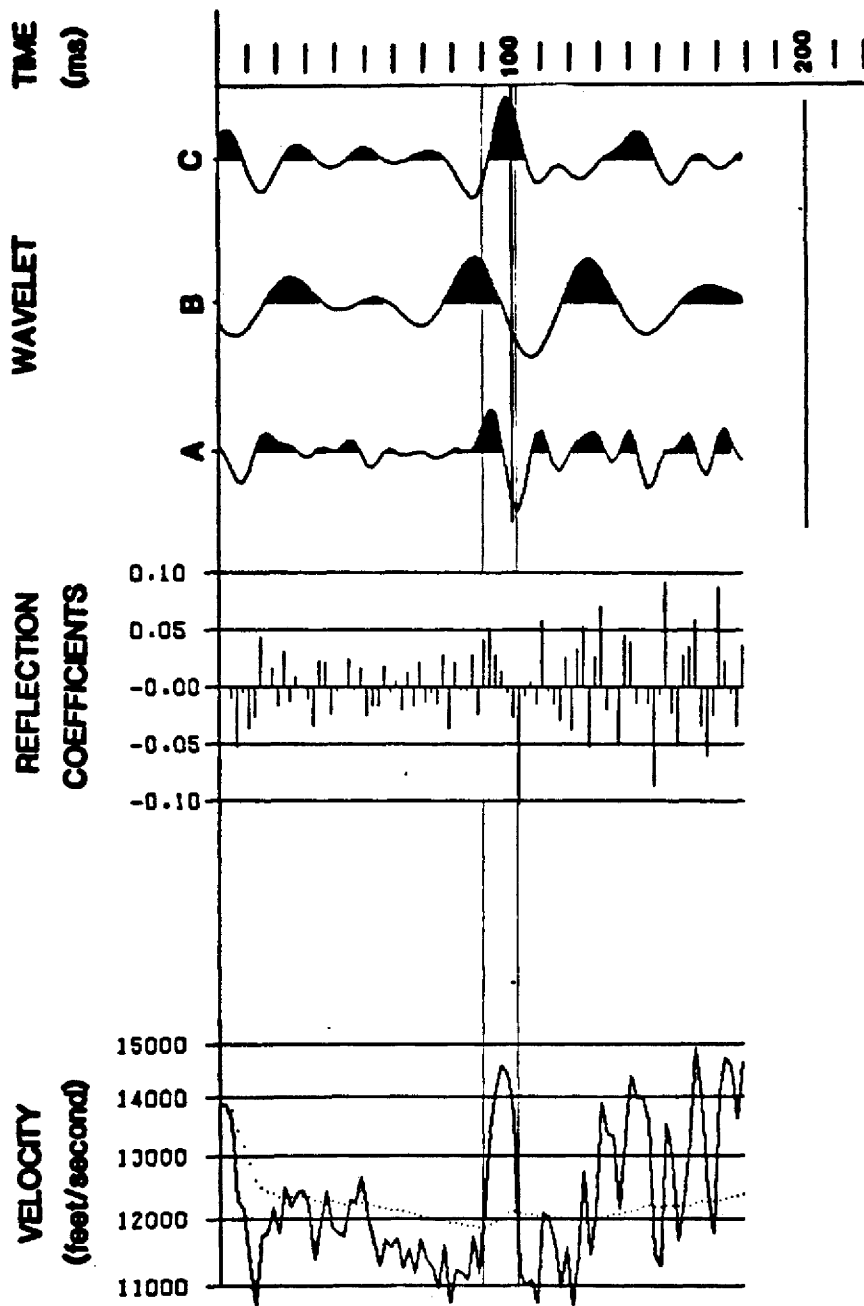
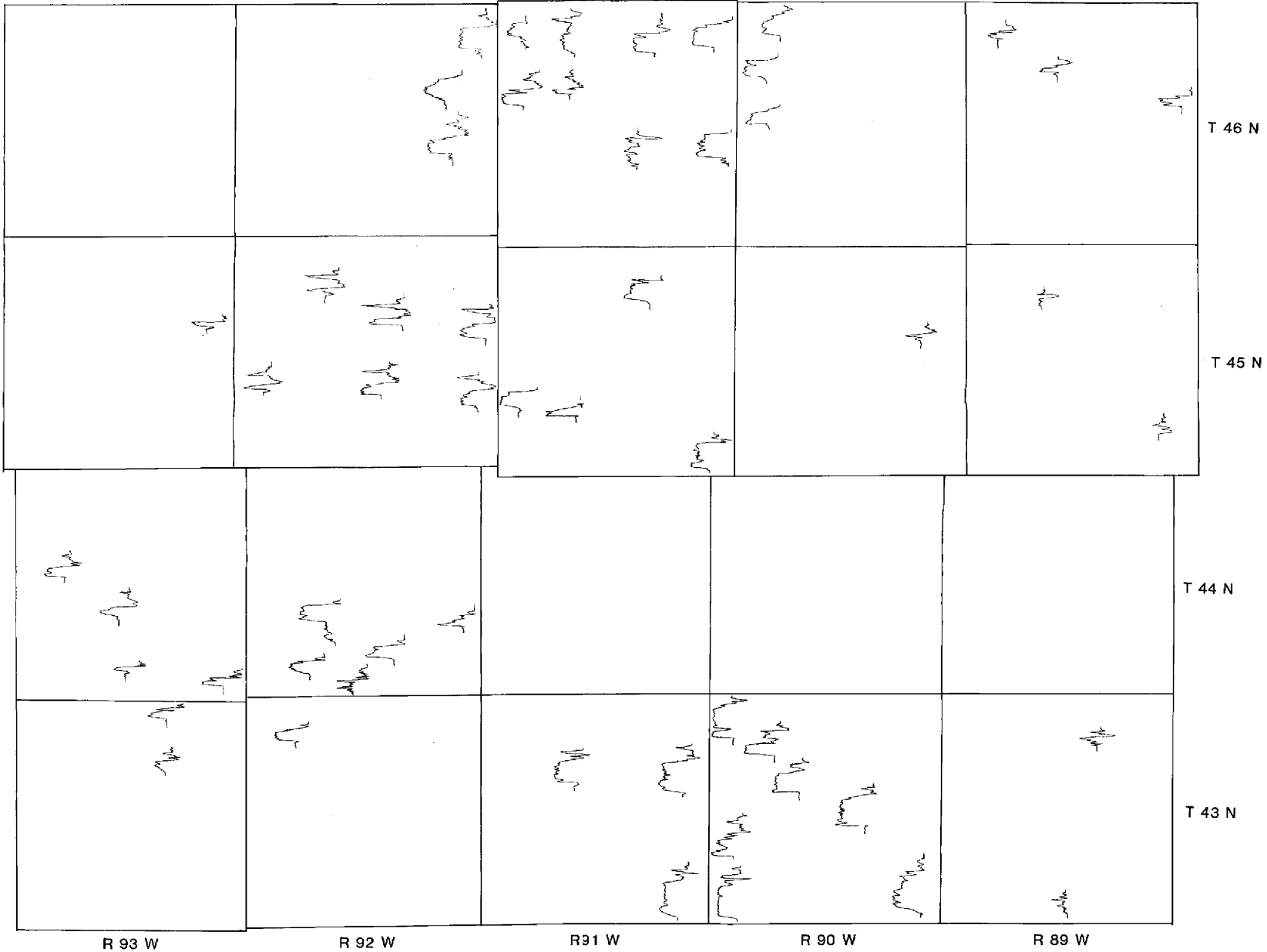


PLATE I

GAMMA RAY RESPONSE OF THE MUDDY INTERVAL

T-2742



Steve E. Milligan

T-2742

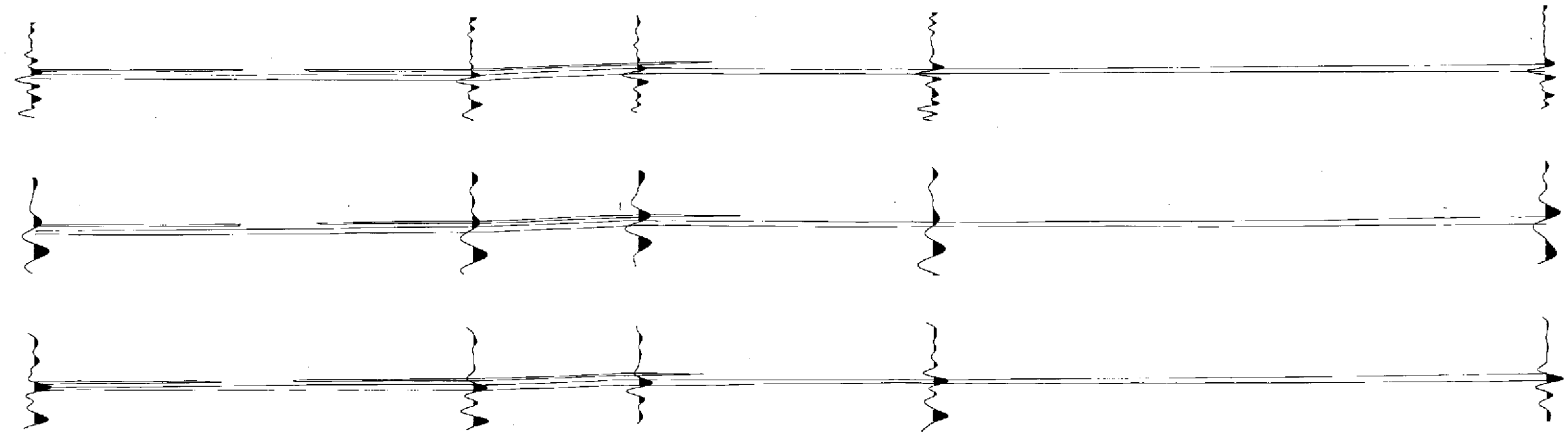
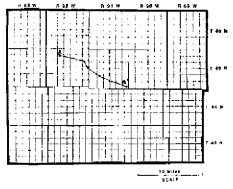
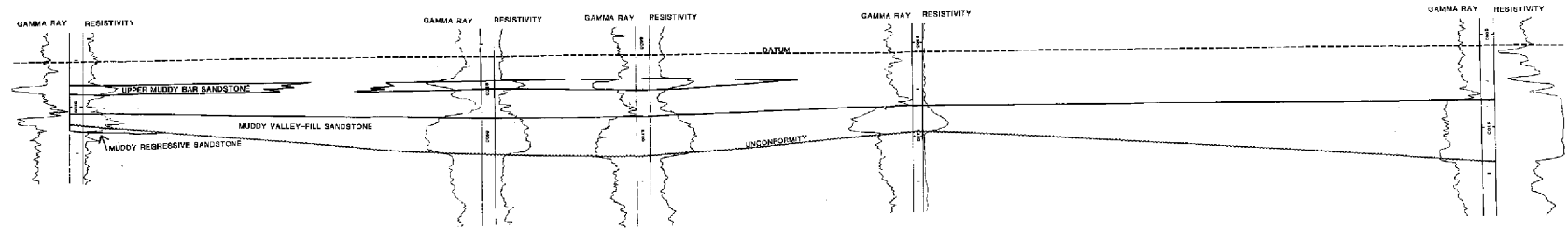


PLATE II

CROSS SECTION THROUGH STUDY AREA

A A'

BLACK HAWK TENNECO TENNECO TEXACO PAN AMERICAN
 #33-8 CHAMBERS FEDERAL #1 TUFFY FEDERAL #1 FEDERAL #1 GOVT McGRADY-HAMMOND #1 WAGON PRONG UNIT
 8 T45N R92W 13 T45N R92W 24 T45N R92W 29 T45N R91W 36 T45N R91W



HIGH RESOLUTION WAVELET

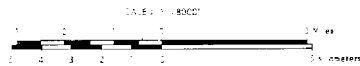
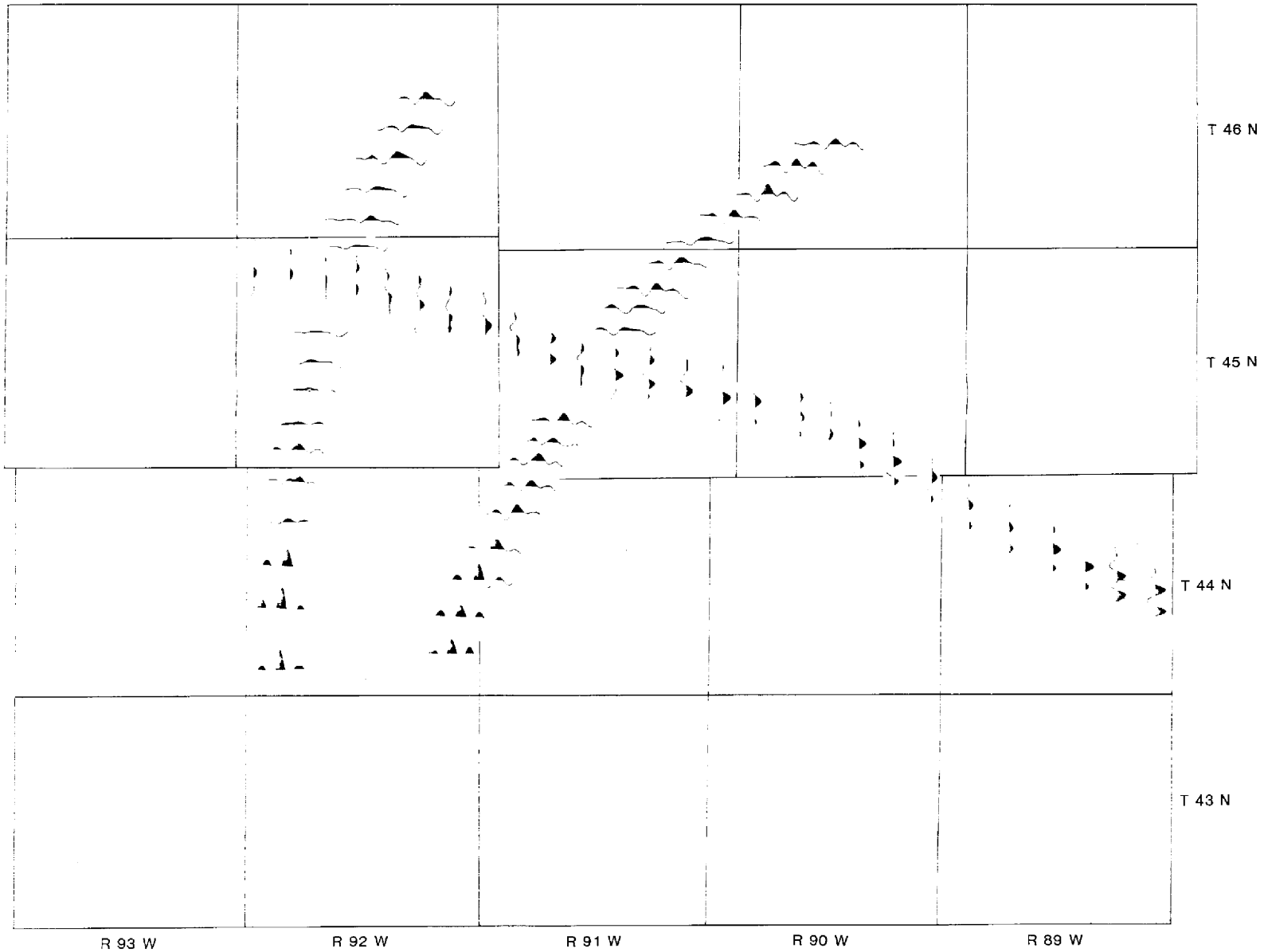
LOW RESOLUTION WAVELET

EXTRACTED WAVELET

PLATE III

MUDDY INTERVAL SEISMIC RESPONSE FROM ACTUAL DATA

U38600064226



Steve E. Milligan

T-2742